Seamless Manipulation of the Varicella-Zoster Virus Genome via Bacterial Artificial Chromosome Engineering

Dissertation

zur Erlangung des Doktorgrades

der Mathematisch-Naturwissenschaftlichen Fakultät

der Christian-Albrechts-Universität

zu Kiel

vorgelegt von

Felix Wussow

Kiel, 2009

Referent:	Prof. Dr. Helmut Fickenscher
Korreferent:	Prof. Dr. Dr. h.c. Thomas C. G. Bosch
Tag der mündlichen Prüfung:	17.12.2009

Meinen Eltern, meiner Schwester

und

meiner Blume

Index

1. Summary 1

2. Zusammenfassung 2

3. Introduction 3

3.1 The varicella-zoster virus 3

3.1.1 Structure of the virus particle 4

3.1.2 Life cycle of the virus 6

3.1.3 Replication of the viral genome 9

3.2 Mutagenesis of herpesvirus genomes 12

3.2.1 Progress in herpesvirus genome manipulation strategies 12

3.2.2 Infectious bacterial artificial chromosomes 13

3.2.3 Progress in varicella-zoster virus research 16

3.3 Manipulation of bacterial artificial chromosomes 16

3.3.1 Red recombination-mediated DNA manipulation 17

3.3.2 Two-step *en passant* mutagenesis 18

4. Results 22

4.1 The BAC-cloned infectious genomes of VZV strains P-Oka and HJO 22

4.2 Mini-F vector self-excision by stabilized genomic duplication 23

4.2.1 Insertion of genomic duplications into the BAC vector sequences 25

4.2.2 Maintenance of the BAC-cloned VZV DNA after insertion of genomic duplications 28

4.2.3 Genome position-dependent BAC vector self-excision by genomic duplication 29

4.2.4 Repair of the VZV genome upon duplication-mediated BAC excision 31

4.2.5 Extension of the genomic duplications within the BAC vector sequences 32

4.2.6 Stable propagation of the VZV BAC after extension of the genomic duplications 33

4.2.7 Duplication-mediated BAC vector excision depends heavily on genome position 33

4.3 Duplication-mediated mini-F vector self-excision from essential genes 34

4.3.1 Red-mediated mini-F vector transposition into VZV essential genes 36

4.3.2 Maintenance of the VZV genome during the mini-F vector transposition 40

4.3.3 Efficient vector excision from essential genes following delayed virus reconstitution 41

4.4 Genome-intrinsic mini-F vector release 43

4.4.1 Mini-F transposition into duplicated genes or the terminal genome junction 43

4.4.2 Preservation of the VZV DNA after BAC transposition into repeated regions 46

4.4.3 Efficient intrinsic BAC vector release from the genomic junction 47
4.4.4 Sequence inversions after insertion of the BAC vector into the terminal junction 48
4.4.5 Seamless intrinsic BAC vector release from the VZV DNA termini 50
4.4.6 Repair of the VZV genome upon vector release from the DNA termini 51
4.4.7 Wild-type virus-like replication kinetics after vector release from the DNA termini 53

5. Discussion 54

5.1 Mini-F vector self-excision by stabilized genomic duplication 54
5.2 Duplication-mediated mini-F vector self-excision from essential genes 58
5.3 Genome-intrinsic mini-F vector release 61

6. Materials and Methods 66

6.1 Molecular biology techniques and bacterial strains 66
6.1.1 DNA preparation 66
6.1.2 Polymerase chain reaction 67
3.1.3 Oligonucleotides 67
6.1.4 Restriction enzyme digestion 68
6.1.5 Agarose-gel electrophoresis 68
6.1.6 Nucleotide sequencing 68
6.1.7 DNA cloning 69
6.1.8 Transformation of bacteria 69
6.1.9 Southern-blot hybridization 70
3.1.10 *En passant* mutagenesis 71
6.2 Cell biology techniques and virus culture 73
6.2.1 Virus and cell culture 73
6.2.2 Virus reconstitution 73
6.2.3 Immunofluorescence 74
6.2.4 Multi-step growth kinetics 74

7. References 76

8. Abbreviations 90

9. Publications and Presentations 92

10. Acknowledgements 93

11. Erklärung 94

1. Summary

The human α-herpesvirus varicella-zoster virus (VZV) causes chickenpox during primary infection and shingles upon reactivation from its latent state in sensory ganglia. Shingles are often associated with severe pain that can persist as postherpetic neuralgia. In order to facilitate the investigation of VZV, we constructed the genomes of the VZV strains P-Oka and HJO as infectious F-factor-derived bacterial artificial chromosomes (BACs). These two VZV BACs (pP-Oka and pHJO) can be seamlessly manipulated by versatile recombination techniques in *Escherichia coli* and subsequently delivered into VZV-permissive eukaryotic cells to allow the reconstitution of infectious mutant virus.

In this work, the two different VZV BACs were engineered in *E. coli* to induce the seamless removal of the bacterial mini-F sequences upon virus reconstitution in VZV-permissive cells via novel replication-based strategies. In pP-Oka-derived virus, the mini-F sequences were efficiently released by homologous recombination of a stabilized inverse genomic duplication inserted into the bacterial vector elements. In contrast, this system was ineffective in virus progeny recovered from pHJO. To increase the efficiency of the vector elimination upon virus reconstitution from the cloned HJO genome, the mini-F sequences were precisely and seamlessly transposed within the viral DNA via a novel synchronous Red-recombination reaction in *E. coli*, whereby six different BAC variants were generated. The insertion of the mini-F sequences directly between the genomic termini resulted in a BAC derivate, of which the vector elements were autonomously and efficiently released during the virus reconstitution even without a genomic duplication. In addition, the derived progeny exhibited genome properties and replication kinetics virtually identical to that of the wild-type virus.

In conclusion, the pP-Oka BAC with an inverse genomic duplication and the BAC variant of pHJO with terminal integrated mini-F vector are two optimized constructs to rapidly generate VZV mutants without leaving behind any operational sequences. Moreover, the mini-F vector transposition reaction eliminates the last hurdle to perform virtually any kind of imaginable targeted and seamless BAC modifications in *E. coli*. Thus, the newly developed manipulation techniques can be useful to optimize, repair, or restructure other established BACs as well, not even for the specific research field of herpesviruses, which may facilitate the development of gene therapy and vaccine vectors.

2. Zusammenfassung

Das menschliche α-Herpesvirus Varicella-Zoster-Virus (VZV) verursacht Windpocken bei der Primärinfektion und Gürtelrose bei der Reaktivierung aus der Latenz in sensorischen Ganglien. Die Gürtelrose ist häufig mit schweren Schmerzen verbunden, die als postherpetische Neuralgie persistieren können. Um die Erforschung von VZV zu erleichtern, klonierten wir die Genome der VZV-Stämme P-Oka und HJO als infektiöse, F-Plasmid-abgeleitete bakterielle artifizielle Chromosomen (BACs). Diese beiden VZV-BACs (pP-Oka und pHJO) können durch vielseitig anwendbare Rekombinationstechniken in *Escherichia coli* nahtlos manipuliert und anschließend in VZV-permissive eukaryote Zellen transfiziert werden, um die Rekonstitution von infektiösen Virusmutanten zu ermöglichen.

In dieser Arbeit wurden die beiden unterschiedlichen VZV-BACs in *E. coli* verändert, um die nahtlose Entfernung der bakteriellen Mini-F-Sequenzen nach der Virusrekonstitution durch neuartige Replikationsstrategien zu induzieren. Bei aus pP-Oka hergestelltem Virus wurden die Mini-F-Elemente durch homologe Rekombination einer inversen stabilisierten genomischen Duplikation im bakteriellen Vektoranteil effizient entfernt. Im Gegensatz dazu war dieses System in Viren hergestellt aus pHJO ineffektive. Um die Effizienz der Vektorelimination nach der Virusrekonstitution aus dem klonierten HJO-Genom zu verstärken, wurden die Mini-F-Sequenzen durch eine neuartige, synchrone Red-Rekombinationsreaktion in *E. coli* innerhalb der viralen DNA transponiert, wodurch sechs verschiedene BAC-Varianten konstruiert wurden. Die Insertion der Mini-F-Sequenzen direkt zwischen die Genomenden resultierte in einer BAC-Variante, von der die Vektorsequenzen autonom und effizient nach der Virusrekonstitution entfernt wurden, auch ohne genomische Duplikation. Zudem zeigten die hergestellten Viren Genomeigenschaften und Replikationskinetiken, die mit denen vom Wildtyp-Virus identisch waren.

Der pP-Oka BAC mit inverser genomischer Duplikation und die BAC-Variante von pHJO mit terminal integriertem Mini-F-Vektor sind somit zwei optimierte Konstrukte zur schnellen Herstellung von Virusmutanten, ohne irgendwelche Fremdsequenzen zu hinterlassen. Zudem eliminiert die Mini-F-Transpositionsreaktion die letzte Hürde um jede vorstellbare, nahtlose BAC-Modifikation in *E. coli* durchzuführen. Die neuentwickelten Manipulationstechniken können somit nützlich sein um auch andere etablierte BACs zu optimieren, reparieren oder restrukturieren, nicht nur für das spezielle Forschungsgebiet der Herpesviren, was die Entwicklung von Gentherapie- oder Impfstoffvektoren erleichtern könnte.

3. Introduction

3.1 The varicella-zoster virus

The neurotropic human α-herpesvirus varicella-zoster virus (VZV) is the etiological agent of varicella and herpes zoster, commonly termed chickenpox and shingles (Garland, 1943; Hope-Simpson, 1954; Steiner, 1875; von Bokay, 1909; Weller et al., 1958). Primary infection with VZV results in varicella, which is most prevalent in childhood and usually characterized by fever and a generalized pruritic dermatomal rash (Grose, 1981). VZV disseminates in a cell-associated viremia throughout the human body, to invade the skin, mucous membranes, and visceral and nervous tissue (Grose, 1981; Jones and Arvin, 2006; Ku et al., 2005; Ku et al., 2004). During primary infection, VZV establishes life-long latency of episomal viral genomes in the nucleus of sensory neurons especially of the dorsal root and trigeminal ganglia (Head et al., 1997; Kennedy et al., 1998; Laguardia et al., 1999). In immunocompromized patients or in elderly people, VZV can be reactivated from its latent state by undefined stimuli and provoke herpes zoster, a dermatomal rash that is largely confined to regions of the skin served by a single sensory nerve. Herpes zoster is associated with acute and often severe, long-lasting pain that can persist as postherpetic neuralgia (Annunziato et al., 2000; Hope-Simpson, 1965; Schmidt et al., 2003).

Infectious cell-free virus particles are released from the human body during varicella and herpes zoster only after lytic replication in the cutaneous epithelium or in respiratory mucous membranes (Chen et al., 2004). Since the respiratory secretions from patients with chicken-pox and shingles allow the airborne transmission of the virus, approximately 95% of the population in temperate climates are latently infected with VZV at the age of 20-29 years (Cohen et al., 2007; Sawyer et al., 1994). The live-attenuated vaccine Oka (V-Oka), which has become publicly recommended for infants and susceptible older children and adults in several countries, including Germany, has greatly reduced the morbidity and fatality rates of VZV infection (Hambleton and Gershon, 2005; Krause and Klinman, 1995; Krause and Klinman, 2000; Takahashi et al., 1974). In addition, a high-dosage vaccine administration strategy has also been shown to reduce the zoster morbidity in latently infected healthy adults of 60 years or older (Oxman and Levin, 2008; Oxman et al., 2005; Sperber et al., 1992).

In the *herpesviridae* family (gr. *herpein*, to creep), VZV is classified as a member of the genus *varicellovirus* within the *alphaherpesvirinae* subfamily (Cohen et al., 2007). VZV and the two closely related herpes-simplex viruses HSV-1 and HSV-2 are the only human-pathogenic members of the α-herpesviruses which share the ability to establish primarily but not

exclusively life-long latency in sensory nerve ganglia. In contrast to HSV, VZV has a narrow host range, restricted to selected cell types of human or simian origin. The genomic arrangement as well as the ability to disseminate widely through the natural host assigns VZV together with pseudorabies virus (PRV), equine herpesvirus type 1 (EHV-1), bovine herpesvirus type 1 (BoHV-1), or simian varicella virus into the genus varicellovirus (Cohen et al., 2007).

3.1.1 Structure of the virus particle

The highly cell-associated replication of VZV *in vivo* as well as *in vitro* has continuously impaired the investigation of the virus, primarily because of the inability to obtain substantial amounts of cell-free intact viral particles in tissue culture (Chen et al., 2004; Harson and Grose, 1995; Weller, 1953). Although it has been demonstrated that the VZV particle comprises the typical components of a mature herpesviral virion, its final structural description has been deduced by analogies mainly to HSV-1 (Figure 1) (Cohen et al., 2007).

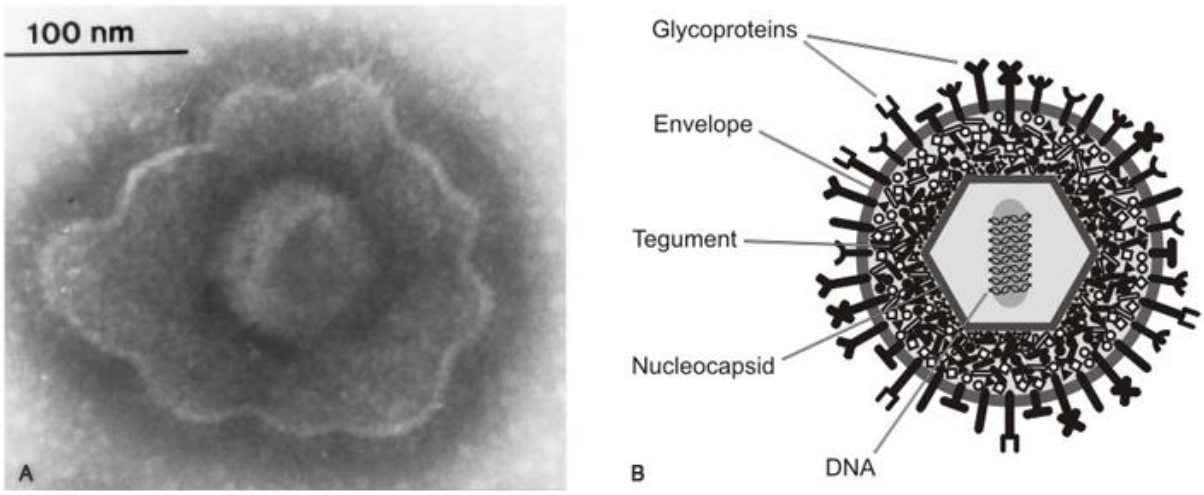

Figure 1. Virion structure of VZV. A) Electron microscopic appearance (Cohen et al., 2007) and **B**) schematic overview of the mature VZ virion particle.

The VZ virion core contains a single copy of the linear double-stranded DNA (dsDNA) genome, which appears to be suspended on a fibrillar protein spindle (Furlong et al., 1972; Puvion-Dutilleul et al., 1987). The particle core is encased by the nucleocapsid, an icosahedron of 12 pentameric and 150 hexameric protein capsomers. The capsid is 80 to 120 nm in diameter (Almeida et al., 1962). An amorphous protein matrix, the tegument, which is unique for the *herpesviridae* family, connects the nucleocapsid with the viral envelope and contains structural components as well as regulatory proteins that immediately take control of the host

environment after infection (Kinchington et al., 1995; Kinchington et al., 1992; Stevenson et al., 1994). The virus envelope consists of a double lipid membrane which is derived from cellular vesicles and decorated with various VZV-specific glycolproteins during the virion maturation process. The mature, spherical infectious VZV particle is pleomorphic and measures 180 to 200 nm in diameter (Figure 1) (Almeida et al., 1962).

The 125,000 bp linear dsDNA genome of VZV can be subdivided into two covalently linked components of varying length, each comprising a unique region flanked by inverted repeats (Figure 2) (Davison and Scott, 1986). The long component (L) consists of a unique long region (UL, 105,000 bp) bracketed by very small repeats (TRL, terminal repeat long; IRL, internal repeat long; 88.5 bp). The short (S) component includes a unique short region (US, 5,232 bp) flanked by very large repeats (IRS, internal repeat short; TRS, terminal repeat short; 7,319.5 bp) (Figure 2) (Davison and Scott, 1986). Five repetitive regions, termed *R1* to *R5*, contain variable numbers of serially repeated short sequences and are distributed over the viral genome in the unique as well as in the repeat regions. The VZV genome has a GC base pair content of 46%, which is higher for the repeat elements in comparison to the unique segments, being 59% for the large S repeats and even 68% for the small L repeats (Davison and Scott, 1986). Both 3'-ends of the linear dsDNA genome terminate with a single unpaired G or C overhanging nucleotide (Davison, 1984). Despite of the extensive repeat sequences and although a number of different VZV genotypes have been identified, the genome shows a high degree of genetic stability upon propagation *in vitro* (Straus et al., 1983).

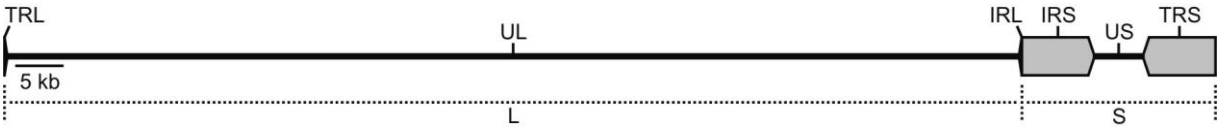

Figure 2. Genome organization of VZV. The genome of VZV consists of a long (L) and a short (S) component (dotted lines), comprising a unique long (UL) or a unique short (US) region flanked by very short (TRL, terminal repeat long; IRL, internal repeat long) or large (IRS, internal repeat short; TRS, terminal repeat short) inverted repeats, respectively.

The VZV DNA is densely packed with open reading frames (ORF) of a least 71 specific genes (Davison and Scott, 1986). Three genes are present twice within the viral DNA, since they are located within the large S repeats, and one ORF (*ORFS/L*) is additionally constituted at the terminal genomic junction of the S and L component upon circularization of the VZV molecule during the viral DNA replication (Davison and Scott, 1986; Kemble et al., 2000). Hybridization and sequence analysis have revealed that the VZV genome shares extensive

colinearity with that of HSV-1, aiding for the prediction of specific gene and DNA element functions by analogy (Davison and Wilkie, 1983; McGeoch et al., 1988; McGeoch et al., 1985; McGeoch et al., 2006). Based on amino acid sequence comparison, 64 genes of VZV have HSV-1 homologs, 4 ORFs have EHV-1 or EHV-4 homologs, and one coding domain has a homolog in the γ-herpesvirus Kaposi's sarcoma-associated herpesvirus. At least 40 genes of VZV, which encode mainly viral enzymes and structural proteins, appear to be conserved throughout the human-pathogenic herpesviruses (Cohen et al., 2007). Although genes spanning the genomic termini have been found in some other herpesvirus genomes, a homolog for the VZV S/L protein has not been determined via the available sequence databases (Kemble et al., 2000).

3.1.2 Life cycle of the virus

As for all other α-herpesviruses, the initial attachment of VZV to the host cell appears to be mediated by non-specific electrostatic interactions between the viral glycoproteins and cellular surface glycosaminoglycans such as heparan sulfate (Jacquet et al., 1998; Zhu et al., 1995). Insulin-degrading enzyme has been identified as a specific cellular receptor for VZV, whereby it has not been clarified whether this interaction triggers the viral entry on the cell surface or in endosomes after virus endocytosis (Figure 3) (Li et al., 2006). In addition, the entry of cell-free virus particles into the cytoplasm seems to be significantly facilitated by the interaction of phosphorylated N-linked oligosaccharides on VZV viral glycoproteins with the cation-independent mannose 6-phospahte receptor (MPR^{ci}) (Chen et al., 2004). It is not yet well investigated for VZV how the de-enveloped capsids are transported after virus entry through the cytoplasm and translocated into the nucleus, and how the genome is released into the nucleoplasm. It has been shown for HSV-1 that the entered capsids are transported along microtubules by dynein/dynactin motor protein complexes through the cytoplasm and bind to nuclear pores, where they are degraded concomitantly with the release of their DNA content into the nucleus (Dohner et al., 2002; Ojala et al., 2000).

All evidence suggests that the VZV transcription program is coordinated similarly to that of HSV-1 (Cohen et al., 2007). Specific regulatory tegument proteins that were released into the cytoplasm after virus entry and transported into the nucleus are assumed to initiate or promote the transcription of the VZV immediate early (IE) genes (Defechereux et al., 1997; Forghani et al., 1990; Kinchington et al., 1995; Kinchington et al., 1992). The resulting IE messenger RNAs (mRNAs) are transported into the cytoplasm, translated, and the synthesized IE

proteins are translocated back into the nucleus to initiate the transcription of the early (E) genes. The derived E proteins then support or enhance the activation of the transcription of the late (L) genes in an analogous way (Figure 3). In this temporally coordinated expression cascade, the IE proteins have mainly regulatory functions, the E products especially constitute the DNA-replication machinery, and the L genes encode nearly exclusively structural components for nucleocapsid and subsequent virion assembly (Cohen et al., 2007). Unlike HSV-1 latency, where only one type of non-translated transcripts is detectable, protein products of six genes are expressed during the latent state of the VZV genome (Croen et al., 1988; Mahalingam et al., 1993; Mahalingam et al., 1990).

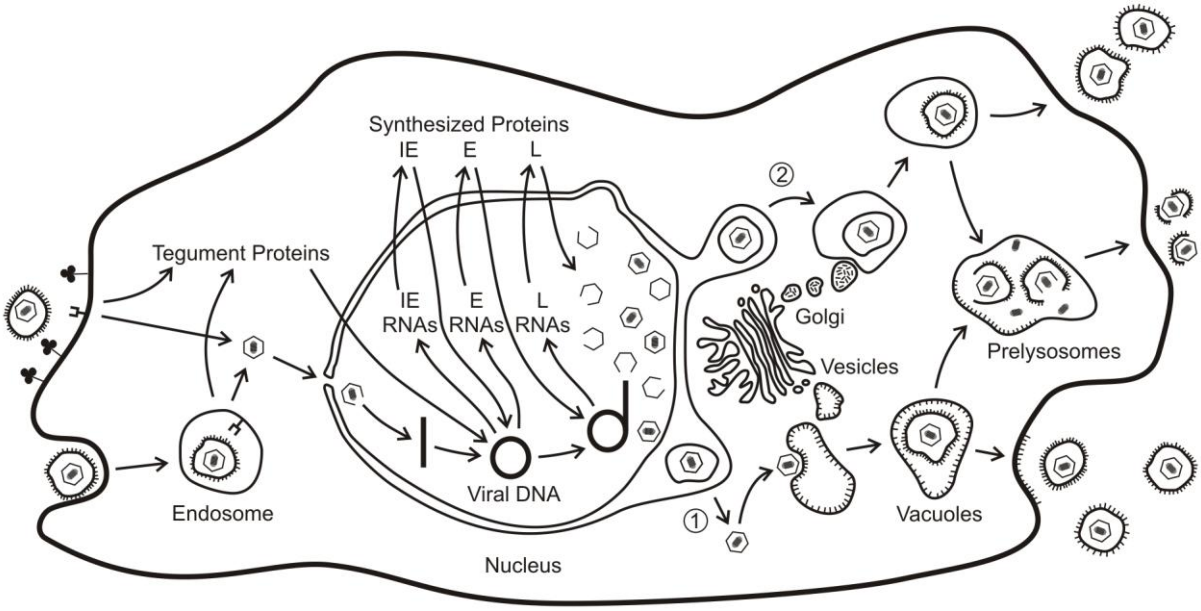

Figure 3. Replication cycle of VZV. The model of the VZV replication cycle is adapted to a scheme from Cohen et al. (Cohen et al., 2007). First, the virion attaches to the host cell. Following that, the nucleocapsid together with the tegument proteins is released into the cytoplasm upon receptor-mediated membrane fusion on the cell surface or within endosomes after internalization of the virus particle. The nucleocapsid and specific tegument proteins are transported into the nucleus, where the viral genome is released. Immediate-early (IE), early (E), and late (L) mRNAs and proteins are synthesized and the viral DNA is packaged into pre-assembled nucleocapsids. The capsids are enveloped and de-enveloped as they traverse the nuclear membranes and then re-enveloped and decorated with glycoproteins as they bud into membrane vesicles from the *trans*-Golgi network (1). In an alternative model, the capsids are enveloped as they bud into the perinuclear space, transported through the cytoplasm in vesicles budded from cisternae of the rough endoplasmic reticulum and decorated with glycoproteins after membrane fusion of the virus-laden vesicles with glycoprotein-laden microvesicles from the *trans*-Golgi network (2). In both pathways, the particles are either diverted in vesicles to prelysosomes and subjected to degradation, or transported to the cell surface and released from the cell as mature virions.

Two competing pathways for VZV assembly and egress have been favoured from studies with VZV-infected human tissues and cells in culture that illustrate the virus tegumentation, envelopement process, degradation and release *in vivo* and *in vitro* (Cook and Stevens, 1968; Gabel et al., 1989; Gershon et al., 1973; Gershon et al., 1994; Harson and Grose, 1995; Jones

and Grose, 1988). One model postulates that VZV capsids acquire the tegument in the nucleus, are enveloped during the transit through the inner nuclear membrane, and traverse the cytoplasm in vesicles budded from cisternae of the rough endoplasmic reticulum (Figure 3). Microvesicles born from the *trans*-Golgi network (TGN) subsequently release their content upon membrane fusion into the virus-laden vesicles and the available VZV-specific glycoproteins decorate the viral envelope. The evolving particles are then transported in large cytoplasmic vesicles to the cell surface and released by exocytosis into the extracellular environment (Figure 3) (Harson and Grose, 1995; Jones and Grose, 1988). In the second model, the nucleocapsids receive an initial tegument layer within the nucleus and acquire and lose an envelope as they transit through the inner and outer nuclear membrane into the cytoplasm (Figure 3). The de-enveloped capsids interact via additional tegument proteins with cytoplasmic tails of VZV-specific glycoproteins exposed on membranes of TGN cisternae, and are then re-enveloped by invagination into TGN-budded vesicles. The derived particles with glycoprotein-decorated envelopes are then transported in vacuoles to the cell surface and released by exocytosis as mature virions into the extracellular space (Figure 3) (Gershon et al., 1973; Gershon et al., 1994).

VZV remains tightly associated with cells in culture, as most of the viral particles undergo degradation in the cytoplasm before they are assembled and released as infectious mature virions (Grose, 1990; Taylor-Robinson, 1959; Weller, 1953). The majority of the cytoplasmic particles in cell culture develop deformed dense cores and fragmented membranes, and virions harvested from supernatants often have incomplete envelopes and teguments, or even empty nucleocapsids (Caunt and Taylor-Robinson, 1964; Cook and Stevens, 1968; Grose, 1990; Harson and Grose, 1995). Recently, it has been demonstrated that on average 40,000 VZV particles from culture supernatants are required to generate one infection in monolayers of permissive cells, whereas only 10 units are sufficient to support HSV-1 propagation *in vitro* (Carpenter et al., 2009). Primary cells or cell lines are not available for yielding substantial amounts of cell-free intact VZV in culture (Grose et al., 1979; Harper et al., 1998; Harson and Grose, 1995). Consequently, VZV is usually propagated *in vitro* by dispersing infected cell monolayers and passaging them onto uninfected cells (Cohen et al., 2007).

Considering the highly cell-associated nature in cell culture and the efficient release of mature particles from infected individuals, it has to be envisaged that VZV has different growth properties *in vitro* and *in vivo* at least in concern of certain cell-types of the human body. Cell culture studies demonstrated that VZV assembly usually ends up in MPR^{ci}-receptor-dependent diversion of the virus-laden vesicles into prelysosomes, where the viral particles

are subjected to enzymatic degradation (Figure 3) (Chen et al., 2004; Gabel et al., 1989; Gershon et al., 1994). MPR^{ci}-receptor-deficient cells release cell-free intact VZV virions much more efficiently than their non-mutated progenitors. Moreover, it was found that superficial epidermal cells in fact lack the MPR^{ci}-receptor, which may account for the high amount of infectious cell-free VZV particles in vesicular fluids (Chen et al., 2004).

3.1.3 Replication of the viral genome

A model for the mechanisms and intermediates of the VZV DNA replication and maturation process has been predominantly deduced from the sequence, the different arrangements, and especially from the structure of the termini of the viral genome (Davison, 1984; Davison and Scott, 1986; Ecker and Hyman, 1982; Kinchington et al., 1985). Immediately after release into the nucleus, the linear dsDNA genome of VZV circularizes, which is assumed to be mediated or supported by the ligation of the single 3'-overhanging nucleotides at the viral DNA ends (Garber et al., 1993; Kinchington et al., 1985; Nagaike et al., 2004). Initially, the resulting covalently closed genome is thought to be bidirectionally replicated from one or both origins of DNA replication within the large S repeats into circular catenated molecules (Boehmer and Villani, 2003; Stow and Davison, 1986). After a short period, the derived catenated genomes are replicated presumable via a rolling-circle mechanism into linear and branched concatemeric DNA molecules of serially and covalently linked genomic units (Davison, 1984). These high-molecular weight molecules have not been explicitly described for VZV, but can be deduced from the generally proposed herpesviral DNA replication intermediates and, specifically, from concatemers of herperviruses with similar genome arrangements, such as EHV-1 and BoHV-1 (Ben-Porat and Tokazewski, 1977; Boehmer and Lehman, 1997; Boehmer and Nimonkar, 2003; Jacob et al., 1979; Schynts et al., 2003; Slobedman and Simmons, 1997).

The concatemeric genome multimers are cleaved precisely at the junctions of the genomic termini by a terminase complex and the derived linear unit-length monomers are packed through a portal vortex by a head-full sensing mechanism into preformed nucleocapsids (Boehmer and Lehman, 1997; Boehmer and Nimonkar, 2003; Davison, 1984). Two highly conserved *cis*-acting DNA packaging signals, termed *pac1* and *pac2*, and an additional *pac2*-associated GC-motif that are located near the herpesviral genomic termini, were identified to be critical for the DNA maturation and encapsidation process (Deiss et al., 1986; Stow et al., 1983). In the linear VZV genome, the *pac2* signal and its associated GC-motif are situated

within the small L repeats and the *pac1* element is present within the large S repeats, whereby these two packaging signals are found at the opposite genomic termini and next to each other at the internal S/L junction (Figure 4) (Davison and Scott, 1986).

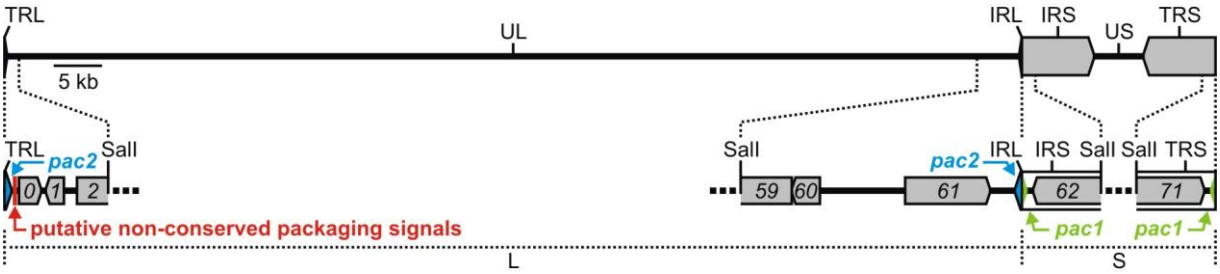

Figure 4. Structure of the genomic termini and the internal S/L junction of VZV. A detailed overview of the SalI fragments at the genomic termini or at the internal S/L junction of the VZV genome is shown. Herpesvirus-conserved DNA packaging signals (*pac1* and *pac2*, blue and green) are located at both opposite genomic termini and at the internal S/L junction. Additional non-conserved *cis*-acting DNA packaging signals (red) are assumed to be present only at the *ORF0* end of the UL region.

Despite of the very small L repeats, both unique regions of VZV are thought to undergo frequent inversion by homologous recombination of the repeat elements during the viral DNA replication, creating presumably all four possible genomic isomers directly adjacent and tandemly in significant amounts in the concatemeric intermediates (Figure 5) (Davison, 1984; Kinchington et al., 1985; Schynts et al., 2003; Slobedman and Simmons, 1997). In regard of the genome arrangement of VZV after circularization of the viral DNA, it is assumed that the large S repeats promote, at least in part, in addition to the inversion of the US region, also the inversion of the UL segment (Davison, 1984). Highly frequent inter- and intramolecular homologous recombination seems to be an inherent mechanism of the herpesvirus DNA replication machinery, whereby inversions and deletions can be generated by inversely or directly repeated elements, which can be even ectopic or extrinsic sequences (McVoy and Ramnarain, 2000; Mocarski et al., 1980; Severini et al., 1996; Slobedman et al., 1999; Thiry et al., 2005; Umene, 1999).

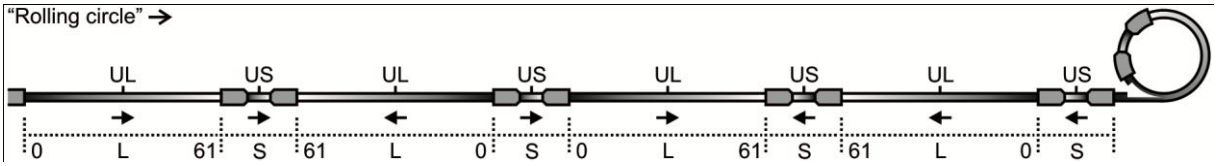

Figure 5. Rolling-circle mechanism. The displayed model describes VZV DNA replication via the hypothetical rolling-circle mechanism. The VZV DNA replicates into concatemeric genome multimers from a "rolling" circular template intermediate. Both unique regions (US and UL) are thought to undergo frequent inversion during DNA replication. The direction of UL and US (small arrows and black to white gradient) and the extent of L and S components (dotted lines) including the positions of *ORF0* and *ORF61* L termini are indicated.

Predominantly, two isomers are detectable in equimolar amounts in VZ virion DNA, since the US region occurs equally frequent in both orientations, whereas the UL segment is found almost in one orientation, only. As a consequence, to 95% the *ORF0* and to 5% the *ORF61* end of the UL region is exposed at the L terminus in an encapsidated linear genome (Figure 6) (Davison, 1984; Ecker and Hyman, 1982; Straus et al., 1981). This "fixed" orientation of the UL region in VZV particle DNA is proposed to be maintained by a selective genome packaging process, which is initiated within S/L transitions on concatemeric DNA termini, mostly at the *ORF0* end (S/L0) and only occasionally at the *ORF61* end (S/L61) of the L component (Figure 5) (Davison, 1984). Further unconserved *cis*-acting packaging sequences are thought to be uniquely present near the duplicated *pac2* and GC-rich signals of the small L repeats at the *ORF0* end of the UL region and are believed to be the main reason for the selective VZV genome packaging into capsids (Figure 4) (McVoy et al., 2000; Wang et al., 2008). The situation, where two of four possible isomers predominate by inversion of a S component relative to a "fixed" L segment in DNA of virions, but where inverted UL regions occur frequently in concatemeric DNA, is characteristic for herpesvirus class D genomes, which all have large S repeats and only very small, imperfect or even no L-repeats (Schynts et al., 2003; Slobedman and Simmons, 1997). In contrast, the herpesvirus class E genome of HSV-1, which is organized into two unique regions that are both flanked by large inverted repeats, exists equimolarly in all four possible isomers in virion DNA (Hayward et al., 1975; Mocarski and Roizman, 1982).

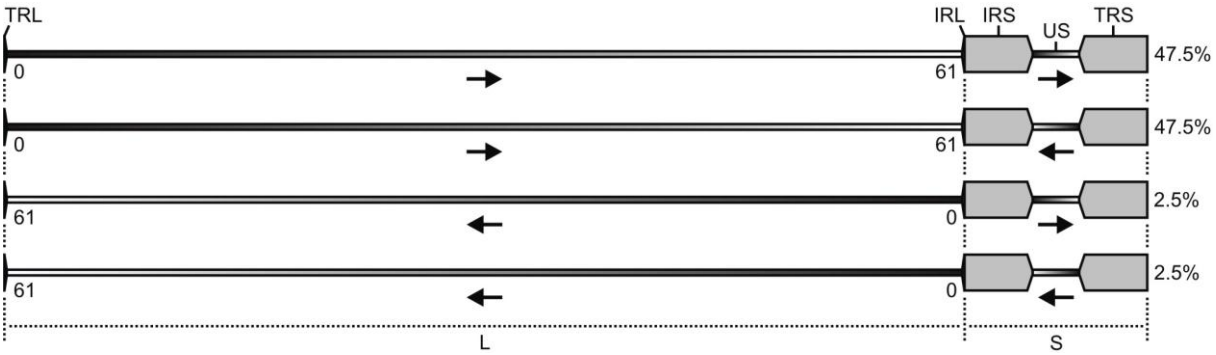

Figure 6. Genome isomers of VZV. Schematic illustration of the four possible isomers of the linear VZV genome. In 47.5%, each of the two isomers with *ORF0*, and in 2.5%, each of the isomers with *ORF61* at the L terminus is found in VZ virion DNA.

3.2 Mutagenesis of herpesvirus genomes

Herpesvirus genomes range from 100-300 kb and are organized into different unique and repetitive regions that contain densely packed, sometimes overlapping ORFs of approximately 70-220 genes (Davison, 2002; McGeoch et al., 2006; Wang et al., 2007). The intimately arranged genes commonly comprise regulatory elements within adjacent coding domains, are often encoded via polycistronic transcription units, and in few cases even expressed into different splice variants (Davison et al., 2002; Davison and Scott, 1986; Kemble et al., 2000; Krause et al., 1988; Roizman et al., 1988; Visalli et al., 2007). Moreover, also microRNAs are encoded by herpesvirus DNA (Pfeffer et al., 2005; Pfeffer et al., 2004). In order to maintain the integrity of these evolutionarily optimized genomes and to avoid collateral or spurious side-effects on the virus viability, minimal and precise sequence modifications are required in herpesviral functional investigations. The establishment of such mutagenesis studies has been a constant challenging research field for herpesvirologists.

3.2.1 Progress in herpesvirus genome manipulation strategies

In the classical approach to analyze herpesvirus genetics, which was introduced almost 40 years ago, temperature-sensitive mutants with conditionally expressible genes were generated by random mutagenesis using chemical compounds (Schaffer, 1975a; Schaffer, 1975b; Schaffer et al., 1984). This method was straightforward since it allowed the temperature-dependent expression of the mutated gene and, therefore, the investigation of even essential domains. However, mapping the location of the randomly introduced alteration is time-consuming and, although the experimental conditions can be well adjusted, second-site mutations are difficult to exclude. Nevertheless, mutants generated by this manipulation strategy have in some cases still relevance for herpesvirus investigations, since they enable the identification and characterization of virus replication-relevant proteins (Adler et al., 2003; Brune et al., 2000; McGregor and Schleiss, 2001; Wagner et al., 2002).

The progress in molecular biology has provided several innovations to study isolated functional genetic domains, but accessing the large herpesvirus genomes directly by standard techniques remains limited to the rarely occurring unique endonuclease recognition sites. Targeted mutagenesis has been established by introducing a selection marker together with the desired genetic alteration into the viral genome via homologous recombination during the virus propagation in cultured eukaryotic cells (Manning and Mocarski, 1988; Mocarski et al., 1980; Post and Roizman, 1981; Smiley, 1980; Spaete and Mocarski, 1987). However,

purification of the rarely generated mutant progeny from the over-represented wild-type virus can be a laborious procedure and often leads to heterogeneous virus populations. Moreover, the investigation of essential genomic regions is logically not feasible with this procedure, since the mutant progeny resulting from the rare events of homologous recombination is immediately lost in presence of the fully replication-competent wild-type virus (Adler et al., 2003; Brune et al., 2000; McGregor and Schleiss, 2001; Wagner et al., 2002).

The disadvantages of the replication-dependent site-directed mutagenesis were considerably reduced by cloning large fragments of herpesvirus genomes as sets of overlapping cosmids in *E. coli* (Zijl et al., 1988). The cloned viral DNA can be manipulated precisely by molecular biology techniques or bacterial genetics and afterwards transferred as cosmid vector-free linear molecules into virus-permissive eukaryotic cells to allow the reconstitution of mutant progeny. This procedure involves the possibility to investigate even essential sites of the viral genome, since replication-deficient progeny can be identified by providing the deleted essential sequence on vector vehicles in *trans* or by *trans*-complementing cell lines. However, the genome repair from the overlapping viral DNA fragments in eukaryotic cells is often associated with illegitimate events of homologous recombination or unwanted second-site mutations (Adler et al., 2003; Brune et al., 2000; McGregor and Schleiss, 2001; Wagner et al., 2002).

3.2.2 Infectious bacterial artificial chromosomes

In the past years, the large DNA genomes of numerous herpesviruses, including that of VZV, and of some poxviruses as well as some large RNA virus genomes have been constructed as infectious bacterial artificial chromosomes (BACs) (Almazan et al., 2006; Almazan et al., 2000; Borst et al., 1999; Cottingham et al., 2008; Delecluse et al., 1998; Domi and Moss, 2002; Horsburgh et al., 1999; Messerle et al., 1997; Nagaike et al., 2004; Schumacher et al., 2000; Smith and Enquist, 2000; Stavropoulos and Strathdee, 1998; Zhou et al., 2002). Full-length viral DNA can be maintained and manipulated in *E. coli* and subsequently delivered into virus-permissive eukaryotic cells to immediately allow the reconstitution of mutant progeny that will represent a uniform and homogenous virus population. Infectious recombinant progeny is, thus, recovered from mutated viral DNA in a controlled manner without the requirement for any additional homologous recombination events to restore the genome integrity, as it would be the case when the virus is reconstituted from overlapping cosmid fragments. The BAC technology has been proven to be a safe, fast, and effective approach to get insight into herpesvirus biology and is predicted to facilitate the development of thera-

peutic gene and vaccine vectors (Adler et al., 2003; Brune et al., 2000; McGregor and Schleiss, 2001; Messerle et al., 1997; Wagner et al., 2002).

BACs are single-copy bacterial F-factor-derived replicon units and have enabled the stable cloning of DNA molecules up to 300 kb in recombination-deficient *E. coli* strains (Shizuya et al., 1992). Regulatory elements of the mini-F replicon strictly maintain the BAC in one or maximally two copies per bacterial cell, thus, minimizing the potential for inter- and intra-molecular homologous recombination between repeated or duplicated sequences (Shizuya et al., 1992; Shizuya and Kouros-Mehr, 2001). Yeast artificial chromosomes (YACs) can propagate larger inserts than BACs, but often appear to have chimeric inserts, sequence rearrangements or contaminations with genomic DNA after purification from the host cell (Ramsay, 1994; Schalkwyk et al., 1995). Mini-F replicons even confer a higher degree of stability to the cloned insert sequences in *E. coli* than cosmid-based plasmids, which are only suitable to maintain DNA fragments up to 50 kb in bacteria (Kim et al., 1992). Therefore BACs, or the similarly constructed bacteriophage P1 based replicons (PACs) with comparable attributes, have become the vehicles of choice for cloning large and complex genomes in *E. coli* (Ioannou et al., 1994; Shizuya et al., 1992). In addition to the generation of infectious viral DNA clones, mini-F replicons are widely used in sequencing projects and functional genomics of diverse organisms, and for the construction of targeting and gene therapy vectors (Copeland et al., 2001; Ristevski, 2005; Shizuya and Kouros-Mehr, 2001; Sparwasser and Eberl, 2007; Yang and Gong, 2005).

Herpesvirus BACs are usually generated by the insertion of a mini-F vector into a non-essential genomic region via homologous recombination during the virus propagation in eukaryotic cells and subsequent transfer of circular replication intermediates of selected recombinant progeny into *E. coli* (Figure 7) (Messerle et al., 1997). In an alternative strategy, the mini-F sequences are inserted via recombination in *E. coli* into the viral DNA cloned as infectious overlapping cosmids, which are afterwards delivered into virus-permissive cells, and circular replication intermediates of reconstituted progeny are transferred back into bacteria (Figure 7) (Tischer et al., 2007). To generate substantial amounts of recombinant circular replication intermediates for the transfer into *E. coli* and, moreover, to reconstitute progeny from the BAC that has attributes comparable to the wild-type virus, the mini-F replicon has to be inserted into or instead of a well-defined non-essential genomic region. Once the viral genome is established as a single infectious BAC clone in *E. coli* and virus can be reconstituted from the cloned DNA in eukaryotic cells that is virtually indistinguishable

from wild-type virus, the door is wide open for mutagenesis studies (Figure 7) (Adler et al., 2003; Brune et al., 2000; McGregor and Schleiss, 2001; Wagner et al., 2002).

Although the mini-F sequences were inserted into a genomic region that is dispensible for the virus propagation, they can still interfere with specific viral functions especially in further *in vivo* experiments (Adler et al., 2001; Chang and Barry, 2003; Strive et al., 2006; Strive et al., 2007; Tanaka et al., 2003; Wagner et al., 1999; Zhao et al., 2008). In addition, the current localization limits the versatility of an established BAC for specific manipulation procedures and minor detrimental effects on the viral replication are not immediately conceivable, which can be even more complicated in concern of vaccine and therapeutic vector development. Therefore, the bacterial vector elements of herpesvirus BACs are often flanked by *loxP* or *FRT* sites to enable their excision after virus reconstitution by site-specific recombinases, which leave behind only one small residual recognition sequence (Adler et al., 2001; Chang and Barry, 2003; Smith and Enquist, 2000; Tanaka et al., 2003; Zhao et al., 2008). Complete removal of the mini-F sequences by homologous recombination has been limited to laborious co-transfection experiments or to BAC constructs with restricted stability in bacteria (Strive et al., 2007; Wagner et al., 1999).

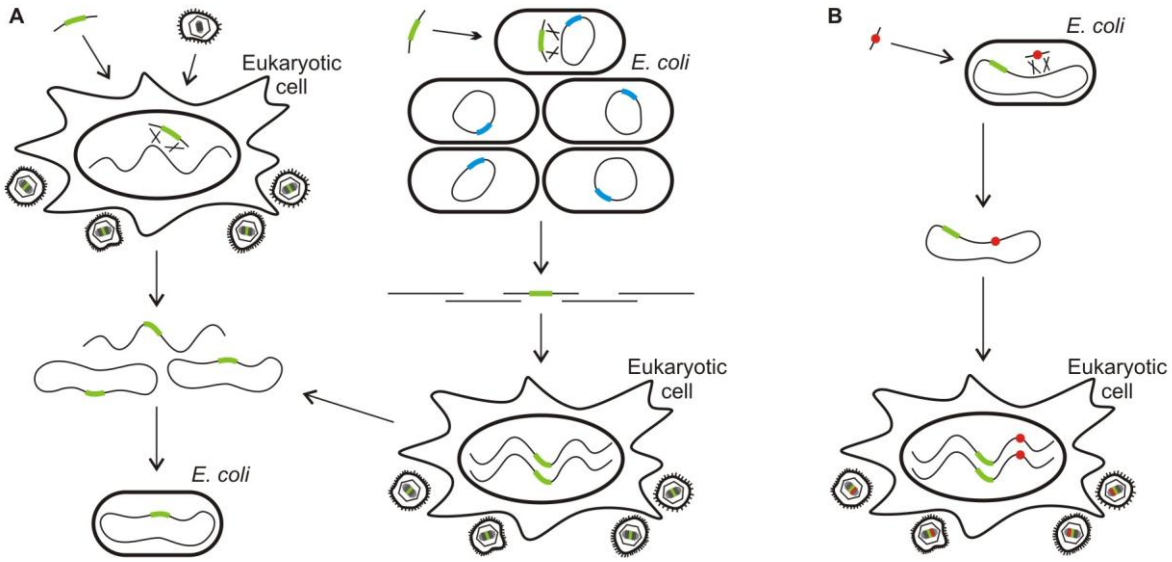

Figure 7. Generation and mutagenesis of herpesvirus BACs. A) Cloning a herpesviral genome as bacterial artificial chromosome (BAC). A mini-F plasmid (green) is inserted into the viral DNA via homologous recombination (crossed lines) during the virus propagation in infected eukaryotic cells. Circular replication intermediates are isolated and transferred into *E. coli* to establish an infectious BAC. Alternatively, the mini-F plasmid is first inserted into the viral DNA cloned as overlapping fragments in cosmid vectors (cyan) in *E. coli*. The overlapping fragments are purified and linearized, and subsequently transferred as cosmid vector-free DNA into virus-permissive cells. Circular DNA intermediates of recovered virus are then isolated and transformed into *E. coli*. **B)** Herpesvirus BAC technology. The herpesviral BAC is maintained in *E. coli* and a mutation is introduced into the viral DNA by homologous recombination. The manipulated BAC is isolated and transfected into virus-permissive eukaryotic cells, where mutant progeny is reconstituted.

3.2.3 Progress in varicella-zoster virus research

Considerable progress in understanding VZV has been made by the determination of the genomic sequences of several wild-type isolates and by the functional analysis using infectious DNA cosmids (Cohen and Seidel, 1993; Davison and Scott, 1986; Mallory et al., 1997). Further insights in VZV biology have been gained by the development, usage, and investigation of effective antiviral agents or live-attenuated vaccines that ameliorate or prevent varicella and herpes zoster (Oxman and Levin, 2008; Oxman et al., 2005; Pickering, 2008; Pickering and Orenstein, 2002; Takahashi et al., 2008; Takahashi et al., 1974; Tan et al., 1996; Whitley, 1999; Whitley, 2008). However, in contrast to other human herpesviruses, there is a huge accumulated demand for VZV investigation because of the impaired handling of the virus in cell culture and its replication discrepancies *in vivo* and *in vitro*. For example, nucleotide polymorphisms of the vaccine strain Oka (V-Oka) in comparison to parental Oka (P-Oka) or to other wild-type VZV strains have been intensively characterized and have been located predominantly within the transactivator *ORF62/71* gene of the large S repeats, but which point mutations actually cause the attenuated phenotype of V-Oka is not yet known (Gomi et al., 2002; Yamanishi, 2008). Recently, the genome of a vaccine strain has been constructed as infectious BAC to facilitate the investigation of the attenuated phenotype of VZV (Nagaike et al., 2004; Yoshii et al., 2007).

Our research group demonstrated that primary wild-type VZV isolates, such as HJO, but not the vaccine strain V-Oka, induce sensitivity to adrenergic stimulation of sensory neurons *in vitro*, which corresponds with *in vivo* observations on neuropathic alterations associated with herpes zoster, but the molecular background for this observation remains to be elucidated (Kress and Fickenscher, 2001; Schmidt et al., 2003). In addition, the wild-type isolate HJO has not been passaged extensively in culture, in contrast to laboratory and Oka strains. The VZV strain HJO can therefore be accepted as an ideal candidate to get further insight into the neuronal alterations associated with herpes zoster and VZV infection. Therefore, we previously constructed the genome of the HJO strain as infectious BAC.

3.3 Manipulation of bacterial artificial chromosomes

Site-directed manipulation of DNA sequences in *E. coli* by homologous recombination has been established for a number of conditional or transient expressible systems. One of the most commonly exploited techniques for the rapid and targeted DNA mutagenesis in bacteria are based on Red recombination or RecET cloning (Lee et al., 2001; Murphy, 1998; Muyrers et

al., 2004; Muyrers et al., 2000; Yu et al., 2000; Zhang et al., 1998). Recombination-mediated genetic engineering (recombineering) relying on Red and RecET manipulation procedures have enabled the generation of almost unlimited modifications of large BAC-cloned DNA sequences in *E. coli* and are, thus, widely used methods in functional genomics of diverse organisms (Copeland et al., 2001; Muyrers et al., 2001; Sawitzke et al., 2007; Sharan et al., 2009; Thomason et al., 2007).

3.3.1 Red recombination-mediated DNA manipulation

The bacteriophage λ recombination system Red consists of the 5'-3'-exonuclease Exo and the single-strand DNA (ssDNA) binding protein Beta. These two proteins mediate in *E. coli* the recombination between dsDNA ends and homologous target sequences on replicating molecules, and are naturally involved in the integration of the phage λ DNA into the bacterial host chromosome (Carter and Radding, 1971). Exo acts processively on the dsDNA ends to generate 3'-ssDNA overhangs (Little, 1967). Beta subsequently recognizes the recessed ends and invades them by its capability to anneal complementary ssDNA into preformed replication forks for their recombination with the homologous sequence (Kmiec and Holloman, 1981; Muniyappa and Radding, 1986).

For efficient DNA manipulation in bacteria, the *red* genes are expressed together with the λ *gam* gene under tight control of a temperature-inducible promoter (Murphy, 1998; Yu et al., 2000). Gam is an inhibitor of the *E. coli* RecBCD exonuclease, which rapidly degrades dsDNA invading into the bacterial host (Karu et al., 1975; Murphy, 1991; Murphy, 2007). Expressing the Red recombination system, a linear fragment bearing only 40-50 bp homologous extensions can be inserted into to a target sequence of interest by the action of Exo and Beta, while Gam inhibits the RecBCD enzyme from attacking the dsDNA ends. The Red system does not require the support of the *E. coli* recA protein, which is naturally the main mediator for homologous recombination in bacteria (Murphy, 1998; Yu et al., 2000). Thus, Red recombination can be used to easily manipulate plasmids or the bacterial host DNA in an recombination-deficient background (*recA*$^{-}$) by polymerase chain-reaction (PCR) products that were generated with primers comprising short target sequence homologous nucleotides at their 5'-termini (Copeland et al., 2001; Oppenheim et al., 2004; Yu et al., 2000).

Red-mediated DNA manipulation was adapted for BAC mutagenesis by expressing the *red* genes and *gam* from a defective prophage integrated into *E. coli* host genome, which obviates the maintenance of an additional expression plasmid (Lee et al., 2001). The λ prophage

system is 50 to 100-fold more efficient than recombineering by expressing the Red functions from a plasmid construct transformed into the *E. coli* cells (Lee et al., 2001; Yu et al., 2000). In addition, the expression of the Red proteins is much more tightly controlled under the temperature-inducible promoter in the prophage system than in the plasmid strategy, which also reduces the risk of unwanted recombination during the bacterial replication.

For the selection of *E. coli* cells harbouring recombinant DNA, the desired mutation is inserted into the target sequence of interest together with a resistance gene. To minimize side-effects on the function of the manipulated region, the selection marker is usually integrated into the DNA with flanking *loxP* or *FRT* sites to enable its excision from the recombinants in bacteria by the expression of the recombinases Cre or FLP (Lee et al., 2001; Yu et al., 2000). However, the persistence of at least one copy of the *FRT* or *loxP* sites limits the repeatability of this procedure and may also interfere with the viral gene expression in some circumstances.

3.3.2 Two-step *en passant* mutagenesis

Recently, a few straightforward recombination systems have been introduced for engineering BAC DNA in *E. coli* without retaining any operational sequences (Sawitzke et al., 2007; Sharan et al., 2009; Thomason et al., 2007; Tischer et al., 2009; Tischer et al., 2006; Warming et al., 2005). Two-step *en passant* mutagenesis is a versatile and highly efficient markerless BAC manipulation technique, combining Red recombination with the cleavage of the homing endonuclease I-SceI (Tischer et al., 2009; Tischer et al., 2006). The non-symmetrical 18 bp I-SceI recognition site can be introduced into *E. coli* and cleaved after expression of the homing enzyme with a high degree of sequence specificity to generate dsDNA ends accessible for homologous recombination (Jamsai et al., 2003). In the *en passant* procedure, large primers are designed to generate a PCR product for the insertion by Red recombination of a selection marker together with an I-SceI recognition site flanked by a 50 bp direct sequence duplication into the target sequence. After selection of recombinants, a double-strand break can be initiated at the I-SceI recognition site to seamlessly excise the positive selection marker by a second Red-mediated homologous recombination utilizing the short duplicated sequences. Using corresponding available plasmid tools and bacterial strains, *en passant* mutagenesis can be applied to rapidly generate point-mutations, substitutions, or large deletions, to insert large sequences or expression cassettes, or to include epitope-tagged or autofluorescent fusion proteins (Figure 8) (Tischer et al., 2009; Tischer et al., 2006).

To generate point mutations in BAC clones using *en passant* mutagenesis, a cassette comprising a positive selection marker (*psm*) and an I-SceI recognition site is PCR-amplified with primers adding extensions of 60-80 bp to the *psm*-I-SceI cassette (Figure 8A). The outer 40-50 bp of the primers and the derived PCR products are homologous to the target locus in the BAC DNA. Both primers are also constructed in such a way that they contain approximately 40-50 bp of the mutated target sequence, which are reverse complementary to each other (Figure 8A). In the first Red recombination, the PCR product containing the positive selection marker flanked by the appropriate sequence duplication and modification is inserted into the locus of interest. In a second step, following the cleavage induction at the I-SceI site, Red recombination between the duplicated sequences results in the excision of the positive selection marker and the generation of the markerless point mutation (Figure 8A). Large deletions are introduced via a similar strategy except that the primers used to amplify the *psm*-I-SceI cassette contain correspondingly arranged 5'-extensions homologous to the regions up- and downstream of the sequence to delete (Figure 8C).

Large sequences of interest can be seamlessly inserted into a target region by *en passant* mutagenesis via PCR amplification of correspondingly prepared transfer constructs. Therefore, a construct is cloned that contains the sequence of interest with an inserted positive selection marker, an adjoining I-SceI site, and a duplication of a 40-50 bp short stretch of the sequence of interest. This construct is generated by PCR amplification of a *psm*-I-SceI cassette with a forward primer containing an approximately 50 bp DNA duplication of nucleotides present in the sequences of interest (Figure 8B). In addition, both the forward and reverse primers contain restriction sites to allow the cloning of the PCR product in the correct orientation into a unique restriction site within the sequences of interest. The unique restriction site is chosen in such a way that it is located immediately upstream of the approximately 50 bp sequence duplicated within the forward primer (Figure 8B).

The transfer construct is then used to insert the sequence of interest precisely into the desired target region present in the BAC. First, the transfer construct is amplified by PCR with primers possessing approximately 50 bp of homology to the respective target (Figure 8B). The resulting linear DNA fragment is then inserted into the target BAC clone by Red recombination. Recombinants are selected and the resistance marker is seamlessly removed in the second *en passant* step via recombination of the engineered 50 bp duplication of the inserted sequence of interest (Figure 8B).

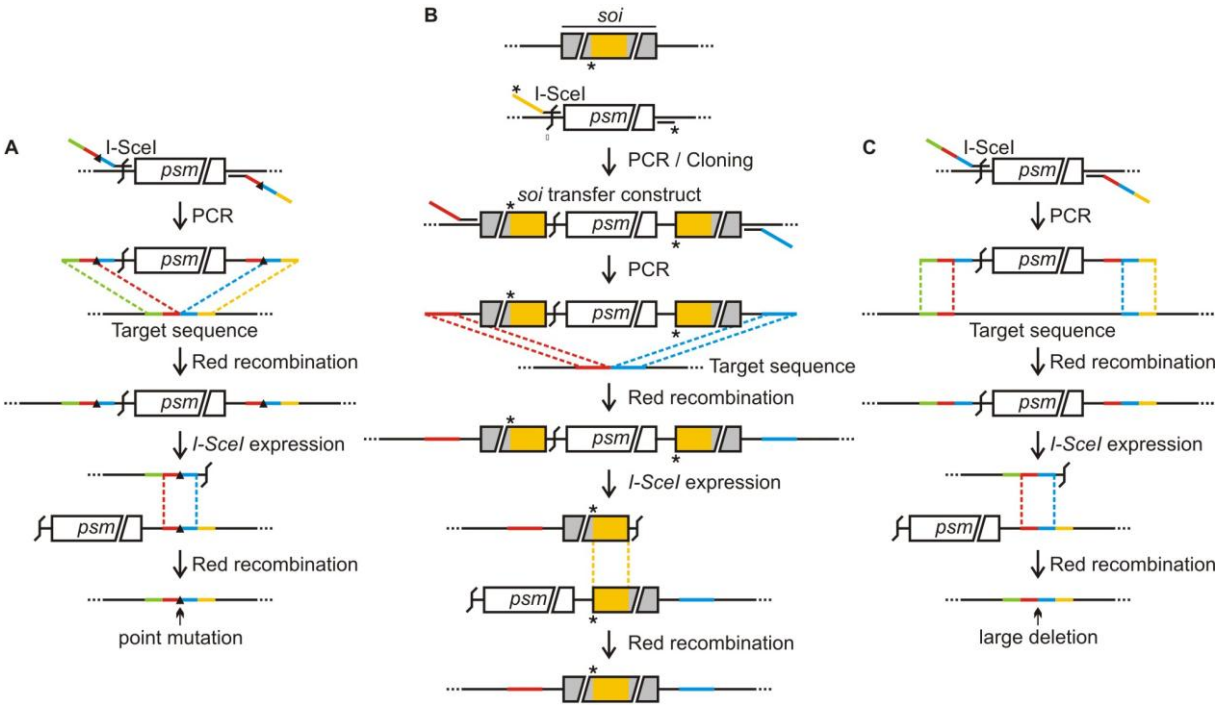

Figure 8. The *en passant* mutagenesis. The shown scheme is adapted from Tischer et al. (Tischer et al., 2006) **A)** Generation of point mutations. First, a positive selection marker (*psm*) and an I-SceI site are amplified via PCR with primers bearing 60-80 bp homologous extensions (coloured elements). Approximately 40-50 bp around the target core sequence (red and blue) of both primers are reverse complementary and contain the mutation (rectangles). The PCR product is inserted via Red recombination into the target sequence. After initiation of a double-strand break at the I-SceI site, *psm* is excised via Red recombination of the duplication, leaving behind only the point mutation. **B)** Insertion of large sequences. First, a *psm*-I-SceI cassette is amplified with primers, of which one provides a 40-50 bp duplication (yellow), and inserted into a restriction site (asterisks*) of a cloned sequence of interest (*soi*). Subsequently, the *soi* transfer construct is PCR-amplified with primers comprising 40-50 bp extensions (red and blue), and inserted into the target region via Red recombination. Upon expression of *I-sceI* and *red*, *psm* is excised from *soi* by recombination of the short duplication. **C)** Generation of large deletion. A *psm*-I-SceI element is amplified with primers, each having 5'-ends that are homologous to sequences located adjacent to the region to delete (coloured elements). The resulting product is used to delete the region of interest by Red recombination. The following steps are the same as in A.

3.4 Objectives of the thesis

A long-term objective of our group is the definition of the sequence variations responsible for the attenuated vaccine phenotype and for the pain induction during herpes zoster and VZV infection. In order to facilitate these approaches, we previously constructed the genomes of the VZV strains parental Oka (P-Oka) and HJO as infectious BACs in *E. coli* to rapidly generate appropriate VZV mutants for functional investigations.

During this thesis project, the two established VZV BACs should be modified by the highly versatile and markerless *en passant* mutagenesis, to provide the efficient and seamless excision of the bacterial vector sequences after virus reconstitution. The engineered BAC variants should allow on one hand the stable propagation of the cloned VZV genomes in Red-recombination-competent *E. coli* and on the other hand the rapid release of the vector elements

during viral DNA replication in eukaryotic cells. Such infectious BAC clones would facilitate the generation of recombinant VZV with seamlessly manipulated viral DNA and, thus, allow the precise interpretation of the derived mutant phenotype.

4. Results

4.1 The BAC-cloned infectious genomes of VZV strains P-Oka and HJO

The infectious BACs of the full-length VZV genomes P-Oka and HJO, termed pP-Oka and pHJO, were previously generated via cosmid vector-based strategies by Tischer et al. and Schmidt et al. (Figure 7) (Schmidt and Fickenscher, 2009; Tischer et al., 2007). For the construction of pP-Oka, a shortened derivative of the pBeloBAC11 vector, comprising the essential mini-F replicon elements *oriS*, *repE*, *sopA*, *sopB* and *sopC*, and the chloramphenicol (Cm) resistance gene *cat* as a positive selection marker, but not the *loxP* and *cos* sequences, was placed directly between the poly-A signals of *ORF64* and *ORF65* of the P-Oka VZV genome (Figure 9). This mini-F vector insertion position is located within the IRS region of the large S repeats approximately 200 bp distant to the UL region. The pHJO BAC construct was generated via the insertion of the complete pBeloBAC11 sequences into the unique AvrII site of the US region between the *ORF65* and *ORF66* of the VZV HJO genome (Figure 9). With respect to the defined VZV prototype genome organization (Figure 2 and 4), the unique regions of pHJO are inversely oriented to each other in the circular BAC arrangement.

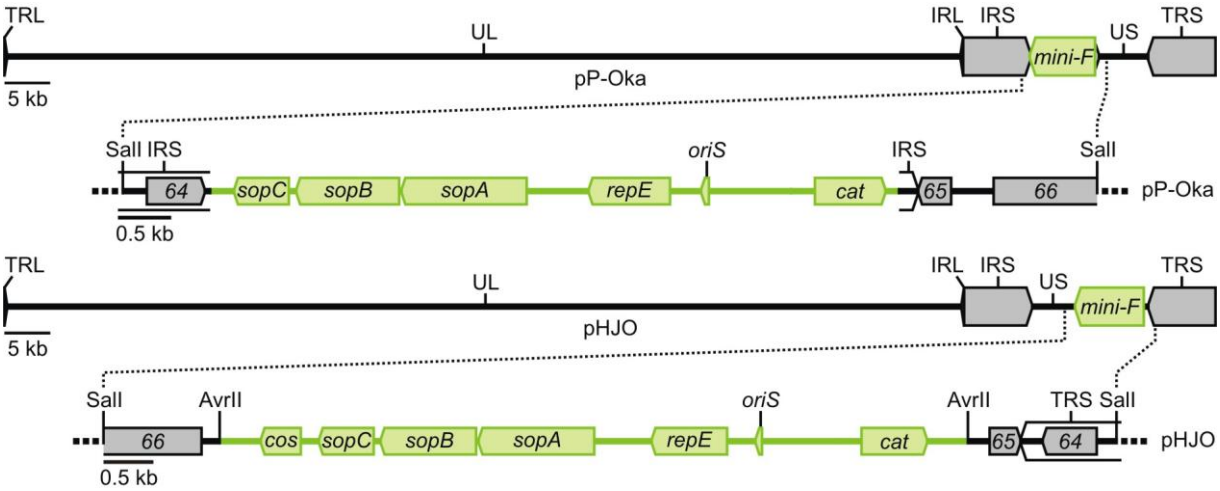

Figure 9. The infectious BACs pP-Oka and pHJO. For the generation of pP-Oka, a shortened derivate of pBeloBAC11 sequences without *loxP* and *cos* sequences, was placed between the poly-A signals of *ORF64* and *ORF65* of the IRS region of the P-Oka VZV genome. To establish pHJO, the mini-F sequences were inserted into the unique AvrII site of the VZV US region between the *ORF65* and *ORF66* of the HJO genome.

The circular VZV genomes of the BACs with directly or reversely oriented unique regions can be the result of one of the major and one of the minor linear isomers (Figure 6). Therefore, it is only possible to determine the terminal and internal genomic junction as well as the terminal and internal repeats with a probability of 95%. Despite of this complication, the

repeated elements of the circular VZV genomes are usually defined according to their designation in the two predominantly occurring genomic isomers (Kemble et al., 2000; Nagaike et al., 2004; Tischer et al., 2007; Yoshii et al., 2007). The three duplicated ORFs within the large S repeats are commonly defined according to their relative position to the orientation of the US region of the VZV prototype isomer (Figures 2 and 4). Consequently, the *ORF62*, *ORF63*, and *ORF64* are located within pP-Oka in the IRS region and are repeated as *ORF71*, *ORF70*, and *ORF69* in the TRS region, whereas vice versa in pHJO (Figure 9).

Both pP-Oka and pHJO could be stably propagated in *E. coli*, and allowed upon delivery into VZV-permissive eukaryotic cells the reconstitution of recombinant progeny that exhibited replication kinetics comparable to that of the wild-type viruses P-Oka or HJO (Schmidt and Fickenscher, 2009; Tischer et al., 2007). In addition, the two BACs have been successfully used to manipulate the viral genomes via Red recombination in bacteria and to recover and characterize mutant virus progeny *in vitro* (Schmidt and Fickenscher, 2009; Tischer et al., 2007). Thus, pP-Oka and pHJO are two valuable tools to rapidly generate mutant virus progeny for functional investigations. However, to prevent any side-effects of the bacterial vector elements with virus functions or adjacent viral sequences, especially in regard of further *in vivo* experiments, I should optimize the two infectious BACs for the efficient and seamless self-excision of the mini-F sequences from the VZV genomes upon virus reconstitution in eukaryotic cells. In addition to the recently introduced markerless DNA manipulation techniques in *E. coli*, such BACs would enable the rapid generation of mutant virus without any secondary genome alterations or operational sequences.

4.2 Mini-F vector self-excision by stabilized genomic duplication

Seamless excision of the mini-F sequences from the viral DNA by homologous recombination after virus reconstitution from an infectious herpesvirus BAC has been first introduced by flanking the bacterial vector elements with directly oriented 0.5 kb genomic duplications (Wagner et al., 1999). Since only one recombination event of such an arranged duplication leads to the complete deletion of the mini-F vector from the viral genome, this BAC construct has restricted stability during the F-factor mediated replication also in *E. coli* cells which harbour an expression cassette for the recombineering proteins on a defective prophage integrated into the host chromosome. We assumed that the vector elements can also be released from the viral DNA in eukaryotic cells and additionally stabilized within the cloned genome in *E. coli* when a genomic duplication of viral sequences flanking the mini-F

insertion site is introduced in forward or even in reverse direction between the bacterial origin of replication and the resistance gene of the BAC vector (Figure 10).

If such a genomic duplication was introduced in forward orientation into the vector sequences of the viral BAC, any single recombination should separate the mini-F replicon from the resistance gene (Figure 10A). Therefore, we supposed that the growth of bacteria harbouring such deletion constructs can be prevented by steady selection with antibiotics, since both the mini-F replicon and the resistance gene are then required for the survival of the *E. coli* cells. In addition, if a corresponding genomic duplication was inserted in inverse orientation between the replicon unit and the selection marker, an antiparallel recombination event followed by a successive parallel recombination should be necessary for the complete excision of the bacterial vector elements from the viral DNA (Figure 10B). However, we assumed that such a successively induced recombination reaction is unlikely in *E. coli* regarding the reduced potential for homologous recombination during the strictly controlled F-factor-mediated replication (Shizuya et al., 1992; Shizuya and Kouros-Mehr, 2001). Taken together, we concluded that a herpesvirus BAC with forward or reverse genomic duplication, regardless of whether it contains inversely or directly repeated regions of the cloned viral DNA, inserted between the replicon unit and the resistance gene, should be stabilized in *E. coli* by the reduced potential of homologous recombination provided by the low-copy mini-F replicon and additionally by antibiotic selection.

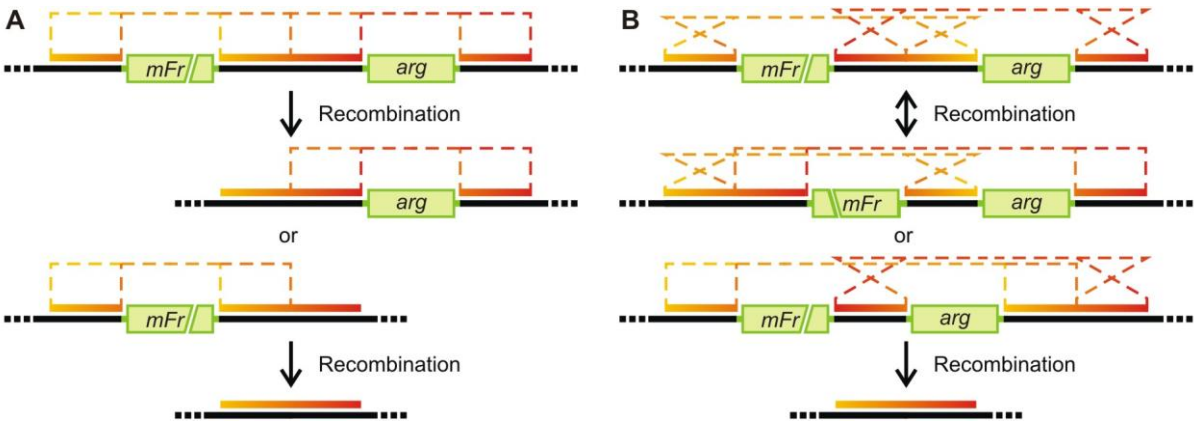

Figure 10. Self-excision of BAC sequences by stabilized genomic duplication. **A)** BAC vector (green) self-excision from the viral DNA (black) by a forward genomic duplication (yellow to red gradient bars) inserted between the mini-F replicon (*mFr*) and the antibiotic resistance gene (*arg*). Two independent recombination events are necessary to release the mini-F replicon or the resistance gene from the viral DNA. **B)** Self-excision of the BAC sequences from the viral DNA by a genomic duplication inserted in inverse orientation into the vector elements. Here, two successive events of recombination are required for the complete excision of the BAC sequences from the viral DNA.

In contrast to the propagation in *E. coli*, parallel and antiparallel inter- and intramolecular homologous recombination is frequently mediated during the herpesviral DNA replication and a maintenance mechanism for the bacterial vector elements is not active in eukaryotic cells (McVoy and Ramnarain, 2000; Mocarski et al., 1980; Severini et al., 1996; Slobedman et al., 1999; Thiry et al., 2005; Umene, 1999). For this reason, we assumed that a genomic duplication inserted into the vector elements of a herpesviral BAC, independently of its orientation, can rapidly induce the seamless self-excision of the complete vector sequences upon virus reconstitution in permissive cells. In the first task of my thesis, I planned to engineer corresponding genomic duplications between the *oriS* origin of replication and the *cat* gene or the pBeloBAC11 sequences of the two established VZV BACs pP-Oka and pHJO. To evaluate which arrangement can mediate more efficiently the mini-F sequence self-excision after virus reconstitution, the duplication should be introduced into the vector elements in reverse as well as in forward orientation.

4.2.1 Insertion of genomic duplications into the BAC vector sequences

For the insertion of the forward and reverse genomic duplications into the pBeloBAC11 sequences of pP-Oka and pHJO, I used the plasmids pEP-P-Oka-DXfw-in, pEP-P-Oka-DX-in, pEP-HJO-DXfw-in, and pEP-HJO-DX-in (Figure 11). These plasmids were provided by Dr. Tischer and derived from the universal transfer vector pEP*MCS*-in-Belo (Figure 11), which is ready for *en passant* mutagenesis. The transfer construct of pEP*MCS*-in-Belo consists of the kanamycin resistance gene *aphAI*, an I-SceI homing endonuclease restriction site, a short 50 bp directly oriented duplication of pBeloBAC11 sequences that flank the *aphAI*-I-SceI fragment, a multiple cloning site (*MCS*), and 0.7 kb pBeloBAC11 sequences flanking the entire *aphAI*-I-SceI-*MCS* cassette and homologous to regions of the *oriS* of the mini-F replicon or to the *cat* gene (Figure 11). To release the transfer construct from the vector backbone, it was placed between the two I-CeuI sites of the plasmid pCeu2 (Figure 11) (Tischer et al., 2007). The pCeu2 plasmid contains a *MCS* between two 19 bp I-CeuI homing endonuclease recognition sites and, thus, allows the cloning and subsequent release of very large sequences from the vector backbone without taking the risk to cleave the inserted DNA. Consequently, pEP*MCS*-in-Belo can be easily applied to insert large sequences via the *MCS* of the transfer construct into the pBeloBAC11 elements between the *oriS* and the *cat* gene and to seamlessly release the *aphAI* selection marker afterwards by two-step Red-mediated *en passant* mutagenesis. For the construction of the provided plasmids pEP-P-Oka-DXfw-in and pEP-P-Oka-DX-in, a 1.6 kb P-Oka genomic region of 0.5 kb and 1.1 kb sequences adjoining

the poly-A signals of *ORF64* and *ORF65* were PCR amplified with the primers A and B (Table 1), afterwards digested with SpeI and inserted in forward or reverse direction into the AvrII site between the Belo fragments of the universal transfer construct of pEP*MCS*-in-Belo (Figure 11). To construct pEP-HJO-DX-in and pEP-HJO-DXfw-in, 1.4 kb HJO wild-type sequences of 0.7 kb regions that are located adjacent to the unique AvrII site of the VZV US region were amplified by PCR with the primers C and D (Table 1) and cloned analogously into the *MCS* of the pEP*MCS*-in-Belo transfer construct (Figure 11).

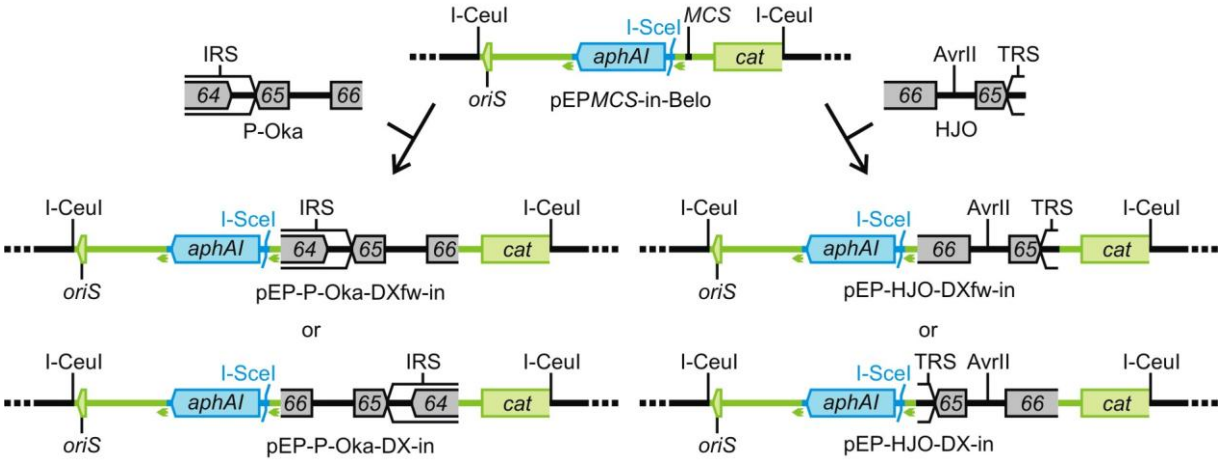

Figure 11. Generation of the plasmids pEP-P-Oka-DXfw-in, pEP-P-Oka-DX-in, pEP-HJO-DXfw-in, and pEP-HJO-DX-in. To generate the plasmids, 1.6 kb P-Oka or 1.4 kb HJO wild-type sequences found at either sites of the poly-A signals of *ORF64* and *ORF65*, or the unique AvrII site of the VZV US region, were introduced in forward or inverse orientation into the *MCS* of the universal transfer construct of plasmid pEP*MCS*-in-Belo. The transfer construct consists of an *aphAI*-I-SceI cassette (cyan), a 50 bp pBeloBAC11 duplication (small green arrows), a multiple cloning site (*MCS*) and 0.7 kb pBeloBAC11 elements (green). The whole construct was placed in the *MCS* between the two I-CeuI sites of the vector pCeu2.

Using the transfer constructs, the corresponding duplications of P-Oka and HJO were inserted by *en passant* mutagenesis in *E. coli* GS1783 into the pBeloBAC11 vector of the BACs pP-Oka and pHJO. *E. coli* GS1783 cells were used for the *en passant* manipulation procedure because they harbour an expression cassette integrated into the host chromosome for the homing endonuclease I-SceI and the Red recombination proteins (Tischer et al., 2009). With this bacteria strain, introduction and temporary maintenance of an additional plasmid for *I-sceI* expression in *E. coli* was not necessary during the *en passant* procedure. Since the plasmid pEP-P-Oka-DXfw-in contained a double-insert of the viral sequences within the *MCS*, a duplication was not inserted additionally in forward orientation into the pBeloBAC11 vector of pP-Oka. In the first step of the *en passant* mutagenesis, the transfer constructs of pEP-P-Oka-DX-in, pEP-HJO-DX-in, and pEP-HJO-DXfw-in were released from the plasmid backbone by I-CeuI digestion and used to introduce via Red recombination the 1.6 kb or 1.4

kb viral sequence duplications together with the *aphAI*-I-SceI cassette flanked by the direct 50 bp pBeloBAC11 duplication in inverse or forward orientation between the *oriS* and the *cat* gene of pP-Oka or pHJO (Figure 12A). After selection of recombinants, the *aphAI* resistance gene was seamlessly excised from the vector backbone of the BACs in the second *en passant* step by I-SceI double-strand break-promoted and Red-mediated homologous recombination of the 50 bp pBeloBAC11 duplication (Figure 12A).

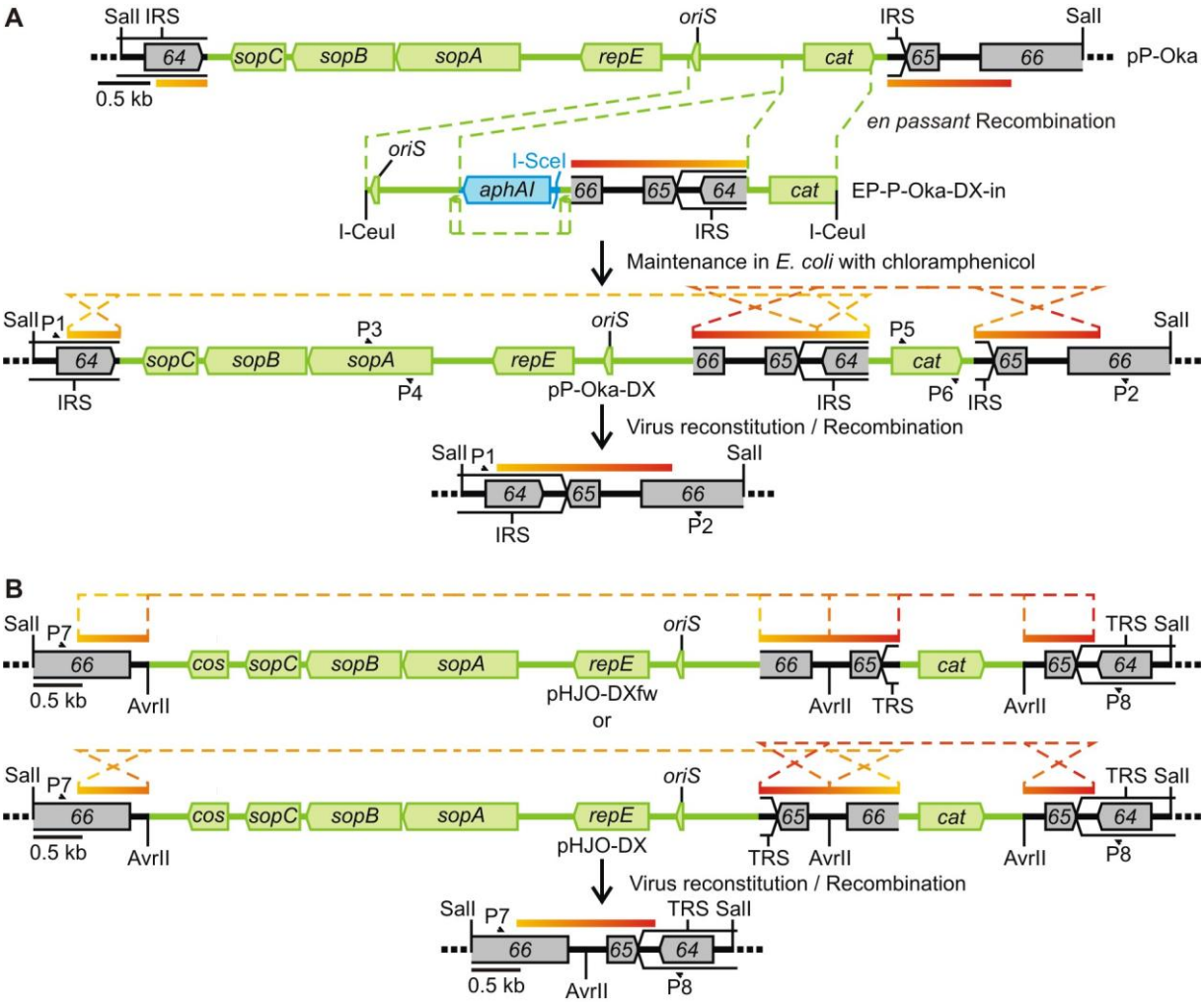

Figure 12. Construction of pP-Oka-DX, pHJO-DXfw, and pHJO-DX. A) Generation of pP-Oka-DX. The transfer construct EP-P-Oka-DX-in was used to insert 1.6 kb P-Oka sequences adjoining the mini-F insertion site (yellow to red gradient bars) between the *oriS* and the *cat* gene of the pBeloBAC11 vector (green) of pP-Oka and to remove afterwards the selection marker *aphAI* (cyan) by two-step *en passant* Red recombination (green lines), resulting in pP-Oka-DX. Upon virus reconstitution, the mini-F sequences were released by two events of homologous recombination (yellow to red dotted lines). Primers P1 and P2 were used to analyze the vector excision and primers P3 and P4 or P5 and P6 were used to determine the persistence of *sopA* and *cat* sequences **B)** Construction of pHJO-DXfw and pHJO-DX. In this constructs, 1.4 kb genomic duplication (yellow to red gradient bars) were engineered in forward or reverse orientation within the pBeloBAC11 elements of pHJO. Primers P7 and P8 were used to investigate the excision of the vector elements by homologous recombination (yellow to red dotted lines) upon virus reconstitution from the two pHJO-DX clones.

The resulting self-excisable BACs with reversely (DX) or forwardly (DXfw) inserted duplication in the pBeloBAC11 sequences were termed pP-Oka-DX and pHJO-DX, or pHJO-DXfw, respectively (Figure 12). These BACs allowed the stable propagation of the P-Oka or HJO genome in *E. coli* grown in presence of Cm and the seamless excision of the pBeloBAC11 elements from the viral DNA by two events of homologous recombination after virus reconstitution in VZV-permissive eukaryotic cells (Figure 12).

4.2.2 Maintenance of the BAC-cloned VZV DNA after insertion of genomic duplications

To verify the maintenance of the BAC-cloned HJO genome and the insertion of the genomic duplications, I prepared the original pHJO BAC and both pHJO-DX constructs from *E. coli* GS1783 cells, digested the BAC DNAs with XhoI, SacI, or SwaI and compared the resulting restriction fragment length polymorphism (RFLP) pattern. The observed fragment rearrangements of pHJO-DXfw and pHJO-DX in relation to the original pHJO BAC were confirmed to correspond to the insertion of the forward or reverse genomic duplication into the pBeloBAC11 elements (Figure 13). For example, the 7.6 kb SacI fragment of pHJO which comprises the vector sequences appeared in pHJO-DXfw and pHJO-DX due to the presence of the 1.4 kb genomic duplications within the vector as a 9 kb SacI fragment (Figure 13).

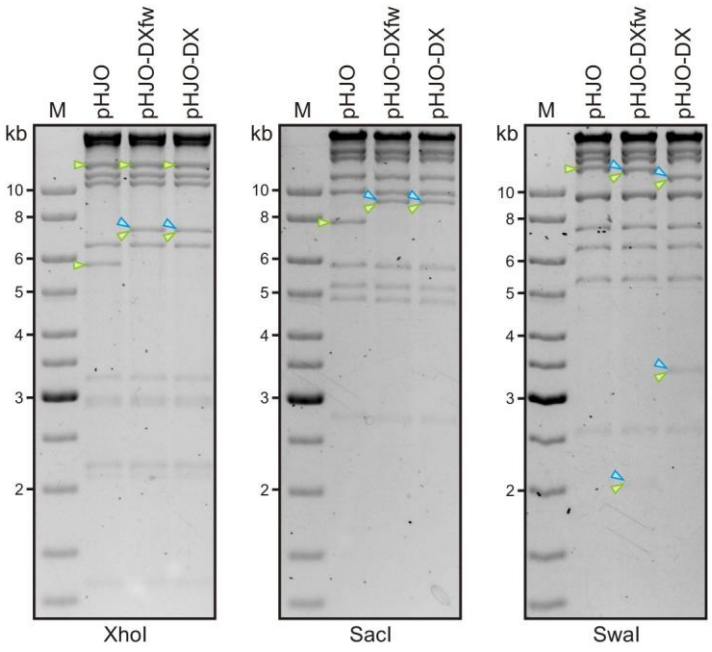

Figure 13. RFLP analysis of pHJO-DXfw and pHJO-DX. B) RFLP analysis of XhoI, SacI, or SwaI digested pHJO-DXfw of pHJO-DX BAC DNA in comparison to original pHJO. DNA fragments containing the pBeloBAC11 vector sequences (green arrows) or sequences of the genomic duplications (blue arrows) are marked. All fragment rearrangements of the engineered BACs correspond to the insertion of the genomic duplication into the vector elements.

The restriction fragment patterns of pP-Oka-DX were investigated via Southern-blot hybridization (see section 4.2.4) and the detected fragment shifts in comparison to the original pP-Oka-DX clone correlated also with the expected fragments sizes according to the insertion of the reverse genomic duplication into the pBeloBAC11 vector sequences. In addition, the presence of the corresponding reverse or forward genomic duplications in the pP-Oka-DX and pHJO-DX or pHJO-DXfw BAC DNA was confirmed via PCR (data not shown). Since unexpected rearrangements were not detected in the derived restriction fragment patterns, these results demonstrated that the three engineered VZV BAC can be stably propagated by the mini-F replicon in Red-recombination-proficient *E. coli* cells, independently in which direction the duplicated sequences were introduced into the pBeloBAC11 vector elements.

4.2.3 Genome position-dependent BAC vector self-excision by genomic duplication

For the investigation of the mini-F vector excision after virus reconstitution from pP-Oka-DX, pHJO-DXfw, or pHJO-DX, I purified the BAC DNAs from *E. coli* and transfected them into the eukaryotic VZV-permissive melanoma cell line MeWo. In contrast to primary cells that promote the propagation of VZV *in vitro*, such as human forskin fibroblast (HFF), MeWo cells are highly receptive for DNA by transfection (Cohen and Seidel, 1993). In addition, the unlimited and dense growth of the MeWo cells allows the viral progeny to pass a high number of replication cycles in each virus passage and, thus, the efficient propagation of VZV in cell culture. However, as with all other cell lines permissive for VZV, MeWo cells do not release substantial amounts of cell-free intact infectious virus particle into the supernatant (Cohen et al., 2007; Harson and Grose, 1995). For this reason, whole cell-lysates are usually prepared for the investigation of VZV *in vitro*.

Virus reconstitution from the three BACs transfected into the MeWo cells was detected by the formation of the local, VZV-typical cytopathic effects (CPEs) four to five days post transfection, which corresponded to the time period required for the virus reconstitution from the original BACs pP-Oka and pHJO. In consequence of the highly cell-associated growth of VZV, the derived recombinant progenies were propagated by the co-cultivation of infected cells with uninfected cells. To eventually analyze the elimination of the mini-F sequences by the two proposed homologous recombination events of the genomic duplications (Figure 12), the DNA of the MeWo cells infected with the recombinant progenies of the different virus passages was prepared for PCR analysis. For the determination of the complete excision of the pBeloBAC11 elements from the viral DNA in pP-Oka-DX-derived virus or in the

progenies generated from the two pHJO-DX clones, I utilized the primers P1 and P2 or P7 and P8 (Table 1) that annealed within the viral DNA flanking the mini-F insertion site and outside of the respective duplicated sequences (Figure 12). To analyze the persistence of the two pBeloBAC11 vector fragments separated by the genomic duplication, I applied the primers P3 and P4 or P5 and P6 (Table 1) in the PCR, which are specific for the *sopA* mini-F replicon element or the *cat* gene (Figure 12). In all three recombinant viruses, the removal of the mini-F sequences was immediately detectable in a portion of the viral genomes after virus reconstitution and not in the corresponding BAC DNA used for the transfection of the MeWo cells (Figure 14). In addition, the genomic wild-type sequence was restored between the poly-A signals at *ORF64* to *ORF65* in pP-Oka-DX-derived virus and at the unique AvrII site of the US region in the two pHJO-DX-derived viruses (data not shown).

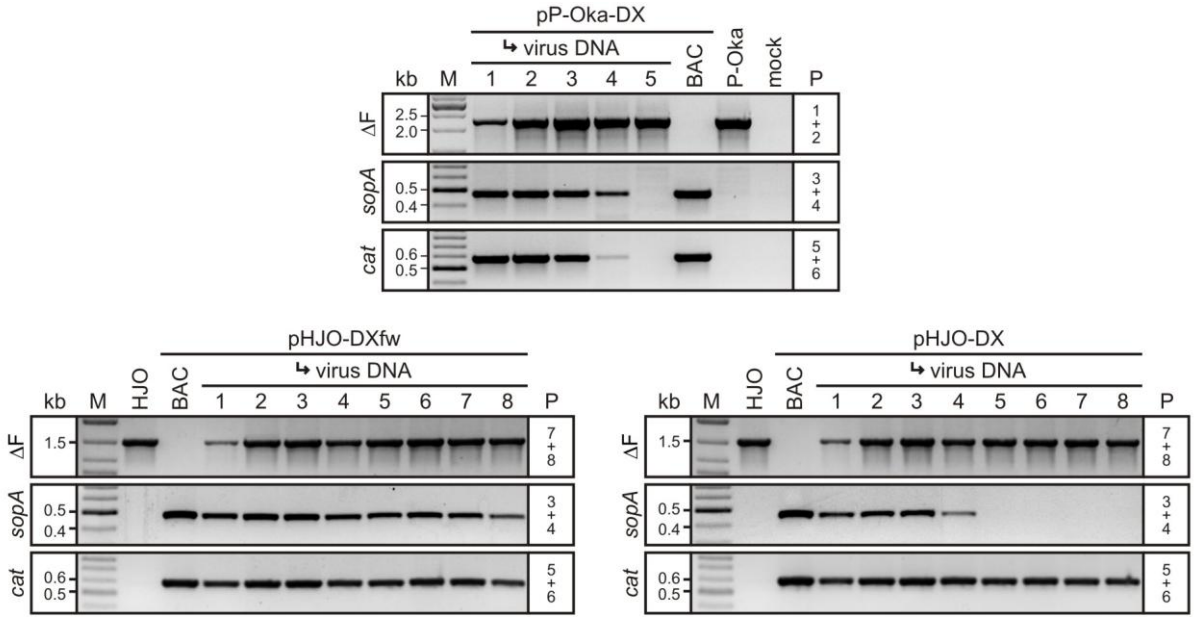

Figure 14. PCR anaylsis of the mini-F vector excision upon virus reconstitution from pP-Oka-DX, pHJO-DXfw, or pHJO-DX. A) PCR analysis of the pBeloBAC11 excision (ΔF) or the persistence of *sopA* or *cat* sequences in DNA of MeWo cells infected with pP-Oka-DX-, pHJO-DX-, or pHJO-DXfw-derived progeny of virus passages 1-5 or 1-8 using the indicated primers (P). BAC DNA as well as DNA of wild-type P-Oka or HJO infected cells or uninfected cells were analyzed for control.

In the pP-Oka-DX- and pHJO-DX-derived progeny, the *sopA* sequences were detectable only until virus passage 4. In contrast, the *sopA* element was traceable in progeny reconstituted from pP-HJO-DXfw until virus passage 8 and beyond (Figure 14). Remaining sequences of the *cat* gene were confirmed to be present in progeny recovered from pP-Oka-DX also until virus passage 4, only. However, in both pP-HJO-DX- and pP-Oka-DXfw-derived viruses, the *cat* gene was detected at least until virus passage 8 (Figure 14). Thus, the pBeloBAC11

sequences were efficiently and seamlessly released by the reverse genomic duplication upon virus reconstitution from pP-Oka-DX during four rounds of passaging the generated viral progeny. In the virus progenies generated from the two pHJO-DX variants, the pBeloBAC11 sequences were also seamlessly released, but only the *sopA* vector part was efficiently removed when the genomic duplication was present in inverse orientation within the vector.

4.2.4 Repair of the VZV genome upon duplication-mediated BAC excision

Since the mini-F vector self-excision in pP-Oka-DX-derived virus was highly efficient, I investigated the DNA of the viral progeny devoid of the two vector parts, termed rP-Oka-F$^-$, via Southern-blot, to confirm the correct repair of the P-Oka genome organization. Therefore, I prepared total DNA from MeWo cells infected with HJO wild-type virus or rP-Oka-F$^-$ as well as BAC DNA of original pP-Oka or pP-Oka-DX from *E. coli* GS1783, digested the DNAs with BamHI, NcoI, or SphI, and analyzed the resulting restriction fragment patterns by a Southern-blot probe specific for pP-Oka fragments or for the pBeloBAC11 vector (Figure 15).

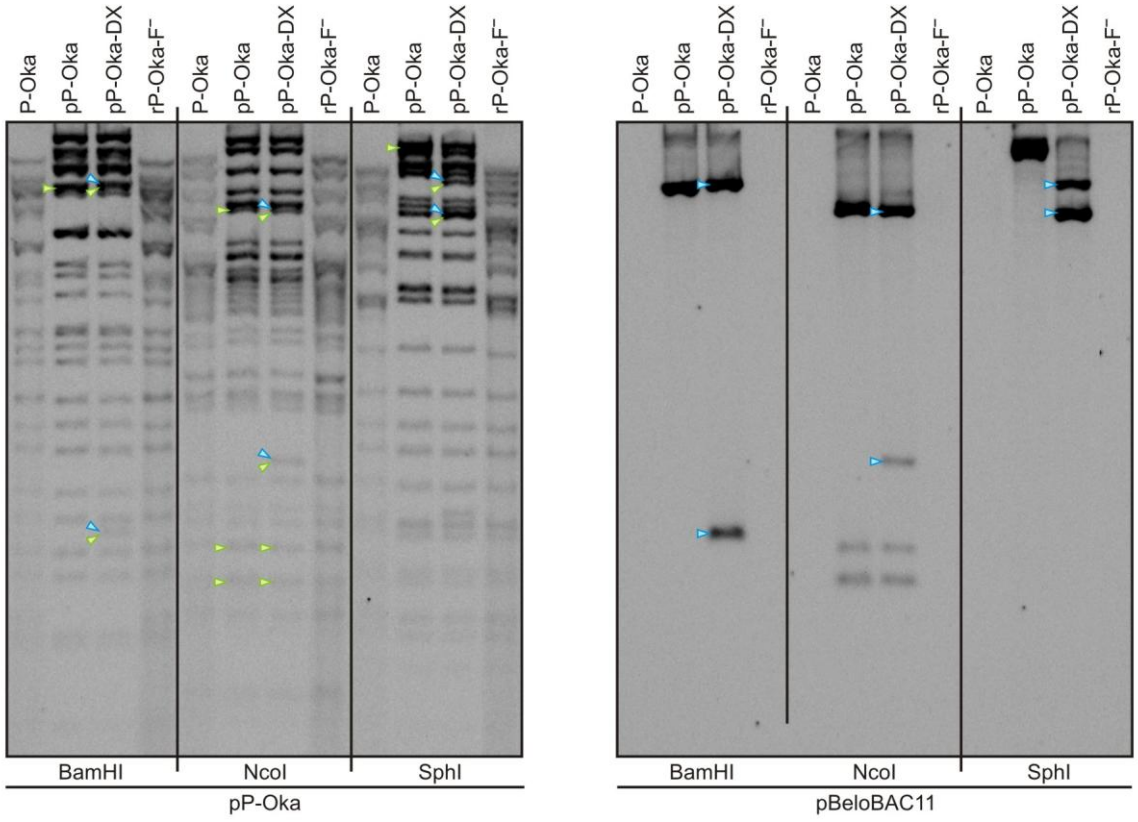

Figure 15. Southern-blot analysis of pP-Oka-DX-derived rP-Oka-F$^-$. Southern-blot analysis for detection of pP-Oka or pBeloBAC11 vector-specific fragments in BamHI, NcoI, or SphI digested DNA from MeWo cells infected with wild-type P-Oka or recombinant rP-Oka-F$^-$, or in BAC DNA of original pP-Oka and engineered pP-Oka-DX. Fragments containing sequences of the pBeloBAC11 vector (green arrows) or of the reverse genomic duplication (blue arrows) are marked.

The obtained genomic restriction fragment patterns of rP-Oka-F⁻ were comparable to that of wild-type P-Oka DNA (Figure 15). In addition, pBeloBAC11 sequences were only detected in the RFLP pattern of pP-Oka and pP-Oka-DX and not in that of the virus DNA (Figure 15). These results demonstrated that the reverse genomic duplication, although it contained sequences of the large S repeats (Figure 12A), mediated the required homologous recombination events for the repair of the P-Oka genome upon virus reconstitution from pP-Oka-DX. Thus, pP-Oka-DX allowed the reconstitution of virus progeny that exhibited genome properties virtually identical to the wild-type virus P-Oka.

4.2.5 Extension of the genomic duplications within the BAC vector sequences

In order to increase the efficacy of the elimination of the *cat* gene vector part from the unique AvrII site, I engineered larger genomic duplications within the pBeloBAC11 sequences of pHJO. Therefore, 3 kb viral sequences of 1.5 kb regions that span the unique AvrII site of the VZV US region of HJO were amplified with primers E and F (Table 1) and inserted after SpeI digestion in forward or reverse direction into the *MCS* AvrII site between the I-CeuI sites of the universal transfer vector pBelo*MCS*-in-Belo (Figure 11), resulting in pEP-HJO-DX3fw-in or pEP-HJO-DX3-in. As described before (Figure 12), the I-CeuI fragments of the generated transfer vectors were released and used to insert the viral sequences via *en passant* mutagenesis in *E. coli* GS1783 cells between the mini-F replicon and the *cat* resistance gene of pHJO. The obtained BAC derivates of pHJO with inverse of forward oriented 3 kb genomic duplications within the pBeloBAC11 sequences were termed pHJO-DX3 and pHJO-DX3fw (Figure 16).

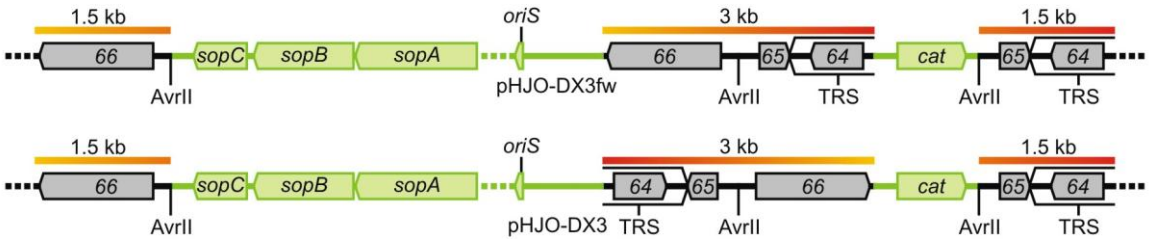

Figure 16. Construction of pHJO-DX3fw and pHJO-DX3. For the construction of pHJO-DX3fw and pHJO-DX3, 3 kb genomic duplication of 1.5 kb viral sequences (yellow to red gradient bars) flanking the mini-F insertion site were engineered within the pBeloBAC11 vector elements (green) of pHJO.

4.2.6 Stable propagation of the VZV BAC after extension of the genomic duplications

To confirm the full preservation of the HJO genome after insertion of the 3 kb genomic duplication into the vector elements, I prepared pHJO-DX3fw and pHJO-DX and original pHJO from the GS1783 *E. coli* cells and compared the XhoI, SacI, and SwaI RFLP pattern of the isolated BACs. In relation to the pHJO BAC, only the expected fragment rearrangements that correspond with the presence of the 3 kb forward or inverse genomic duplication within the pBeloBAC11 vector were detected in the two engineered BACs (Figure 17). For instance, the 5.6 kb XhoI fragment of pHJO which comprises sequences from the *oriS* to the *cat* gene of the pBeloBAC11 vector is found in the pHJO-DX3fw and pHJO-DX restriction fragment pattern as an 8.8 kb XhoI fragment due to the insertion of the 3 kb genomic duplications (Figure 17). The presence of the corresponding forward or reverse genomic duplication between the mini-F replicon and the *cat* gene was also verified via PCR (data not shown). These results indicated that even the insertion of the 3 kb genomic duplication into the vector elements of pHJO did not have a destabilizing effect on the genome organization during the mini-F replication in Red-recombination-competent *E. coli* cells.

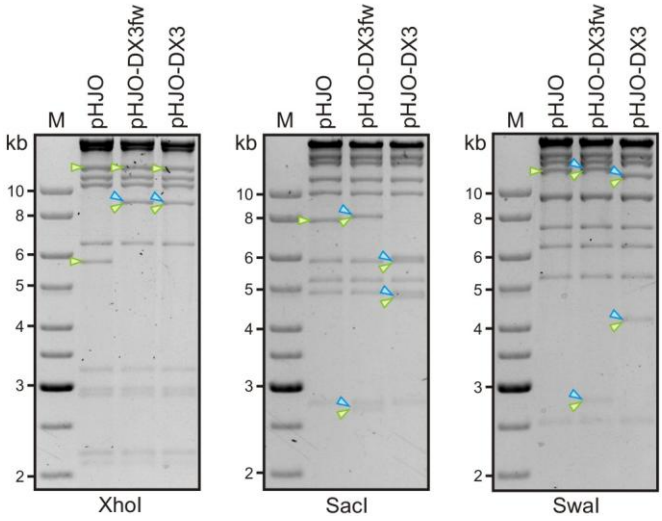

Figure 17. Restriction fragment pattern of pHJO-DX3 and pHJODX3fw. RFLP analysis of XhoI, SacI or SwaI digested BAC DNA of the two pHJO-DX constructs in comparison to original pHJO. DNA fragments containing vector elements (green arrows) or sequences of the 3 kb genomic duplication (cyan arrow) are marked.

4.2.7 Duplication-mediated BAC vector excision depends heavily on genome position

In order to investigate the excision of the *cat* gene fragment by homologous recombination of the introduced 3 kb genomic duplications during the viral DNA replication, I transfected pHJO-DX3fw and pHJO-DX3 BAC DNA into VZV-permissive MeWo cells. Virus recovery

by observation of the VZV-typical CPEs was detected in the cell cultures after four to five days post transfection. The derived recombinant progenies were propagated as described before and cell lysates of the different virus passages were analyzed by PCR using the *cat* specific primers P5 and P6 (Figure 12). In both pHJO-DX3fw- and pHJO-DX3-derived viruses, the *cat* sequences were still detectable until passage 8 and beyond that (Figure 18). Thus, even 3 kb genomic duplications within the vector elements did not significantly increase the efficacy of the vector elimination from the unique AvrII site of the VZV US region upon virus reconstitution from the pHJO-cloned VZV genome. These results demonstrated that the efficiency of the novel duplication-mediated self-excision strategy apparently depends heavily on the BAC vector insertion site within the viral genome.

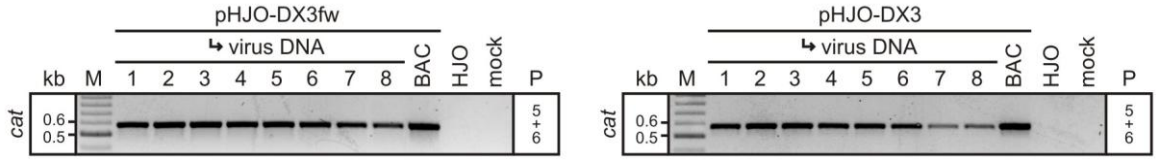

Figure 18. PCR anaylsis of the persistence the vector elements in pHJO-DXfw-, or pHJO-DX-derived virus progeny. PCR analysis of the persistence of *cat* sequences in DNA of MeWo cells infected with pHJO-DXfw-, or pHJO-DX-derived progeny of virus passages 1-8 using the indicated primers (P). BAC DNA as well as DNA of wild-type P-Oka or HJO infected cells or uninfected cells were analyzed for control.

4.3 Duplication-mediated mini-F vector self-excision from essential genes

Since the duplication-mediated vector release from the unique AvrII site of the US region appeared to be significantly impaired, different BAC constructs of the HJO genome were required that allow the efficient excision of the mini-F sequences after virus reconstitution. We assumed that the elimination of the vector sequences can be significantly increased due to a highly detrimental effect on the virus propagation, if they are engineered with corresponding genomic duplications in ORFs which are essential for the efficient growth of VZV. However, to maintain a potential for homologous recombination of the genomic duplication and, thus, the repair of the gene function, the self-excisable vector elements had to be generated in ORFs that are not involved in the viral DNA replication.

The HSV-1 homologs of the VZV *ORF22* large tegument protein and of the *ORF54* capsid portal protein were known to be essential for proper particle assembly or DNA packaging into capsids (Batterson et al., 1983; Desai, 2000; Knipe et al., 1981; Lamberti and Weller, 1996; Newcomb et al., 2001; Patel et al., 1996). Furthermore, the HSV-1 homolog of the VZV *ORF50* membrane glycoprotein M had been determined to be dispensible for the virus propa-

gation, but appeared to be required for the efficient cell-to-cell spread of the viral particles *in vitro* (Baines and Roizman, 1993; Browne et al., 2004; MacLean et al., 1993). In addition, the glycoprotein M of the avian α-herpesvirus Marek's disease virus, which replicates similarly to VZV in a highly cell-associated nature *in vitro* as well as *in vivo*, was even known to be essential for the virus cell-to-cell spread in cell culture (Tischer et al., 2002). Therefore, we assumed that the large tegument protein, the glycoprotein M, and the capsid portal protein are essential for the VZV propagation *in vitro*, whereas not involved in the viral DNA replication. Consequently, I planned to engineer BAC variants of HJO that encompass self-excisable mini-F sequences with corresponding genomic duplications in *ORF22*, *ORF50*, and *ORF54*, to induce the rapid pBeloBAC11 excision upon recovery of progeny in eukaryotic cells. To ensure the complete disruption of the gene function and, thus, the efficient vector release, the pBeloBAC11 elements should be placed into 5'-end positions of the chosen ORFs. Since a genomic duplication in reverse orientation apparently mediates the vector excision during the viral DNA replication more efficiently than in forward orientation (Figure 14), the viral sequences should be inserted only in inverse direction into the vector sequences of the engineered BAC constructs.

The only possibility for the targeted generation of HJO BACs with mini-F sequences in essential viral genes was given by shifting the pBeloBAC11 sequences of pHJO within the cloned VZV genome into these positions via homologous recombination in *E. coli*. For this mini-F transposition, a second pBeloBAC11 vector hat to be inserted into the considered essential gene, while removing the pre-existing mini-F replicon from the unique AvrII site of the US region of the BAC-cloned HJO DNA. However, to prevent the uneven segregation or disruption of putative intermediates with two mini-F replicons during the stringently coordinated chromosomal-like separation upon bacterial cell division and, thus, the loss of BAC or viral sequences, the mini-F vector insertion and removal reaction had be performed in an immediately successive reaction (Shizuya et al., 1992; Shizuya and Kouros-Mehr, 2001). In addition, the second pBeloBAC11 elements should be inserted in inverse orientation with respect to the pre-existing vector fragment to avoid the degradation of the BAC DNA by intramolecular homologous recombination. Therefore, we developed a novel mini-F sequence transposition protocol, which allows the targeted insertion of the novel pBeloBAC11 vector into a different position of the viral genome by Red recombination, simultaneously with the seamless removal of the primary mini-F vector from the unique AvrII site of the US region via *en passant* mutagenesis.

4.3.1 Red-mediated mini-F vector transposition into VZV essential genes

For the insertion of the pBeloBAC11 sequences into the 5‘-end positions of *ORF22*, *ORF50*, or *ORF54* via Red recombination, I generated the plasmids pBelo-HJO22-in, pBelo-HJO50-in, and pBelo-HJO54-in as follows. First, to allow the eventual cloning of the mini-F sequences into SphI or BamHI sites and to remove redundant sequences, such as the *loxP* site and the *cos* element, the commercially available pBeloBAC11 vector was digested with SalI and the derived 6.4 kb fragment was ligated with the XhoI-treated hybrid of the oligonucleotides G and H or I and J (Table 1), resulting in the BAC vectors pBeloBamHI or pBeloSphI, respectively. Subsequently, 1.4 kb viral sequences of 0.7 kb regions flanking 5’-end positioned SphI or BamHI sites of *ORF22*, *ORF50*, or *ORF54*, were PCR amplified with the primers K and L, M and N, or O and P (Table 1), cleaved with SpeI, and cloned into the XbaI site of the *MCS* of the pCeu2 plasmid. Then, the mini-F plasmid pBeloSphI was cleaved with SphI and inserted into the SphI site of the pCeu2-cloned fragment of *ORF22* or *ORF54* to generate pBelo-HJO22-in or pBelo-HJO54-in. In an analogous reaction, the BAC vector pBeloBamHI was digested with BamHI and inserted in forward orientation into the BamHI site of the pCeu2-cloned *ORF50* fragment, resulting in pBelo-HJO50-in (Figure 19).

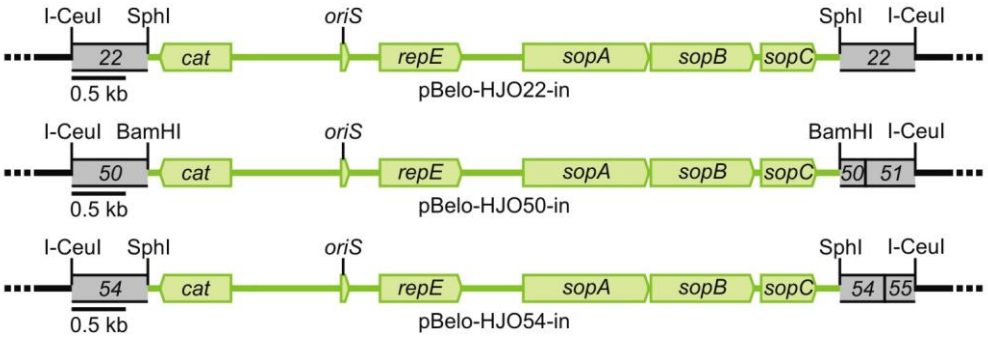

Figure 19. Mini-F vector transfer plasmids pBelo-HJO22-in, pBelo-HJO50-in, and pBelo-HJO54-in. For the construction of pBelo-HJO22-in, pBelo-HJO50-in, and pBelo-HJO54-in, the pBeloBAC11 sequences were inserted in the SphI or BamHI sites of the pCeu2-cloned fragments of *ORF22*, *ORF50*, or *ORF54.*

In the first step of the *en passant* mutagenesis, the original pHJO BAC clone was prepared for the subsequent synchronous insertion and excision reaction of the pBeloBAC11 elements. Therefore, the kanamycin resistance gene *aphAI* and the I-SceI recognition site of the plasmid pEPkan-S (Tischer et al., 2006) were amplified by PCR with the primers Q and R (Table 1), whereby the latter provided a 50 bp duplication of viral sequences found adjacent at the left vector end of pHJO, and used to substitute the *cat* gene at the right pBeloBAC11 vector terminus in pHJO via Red recombination in *E. coli* GS1783 (Figure 20). The resulting BAC con-

struct, termed pHJOF*ep*, with *aphAI*-I-SceI linked pBeloBAC11 mini-F replicon flanked by a 50 bp genomic sequence duplication was ready for the integration of the second pBeloBAC11 vector by selecting for Cm resistance, and for the seamless mini-F vector excision from the US unique AvrII site by the second *en passant* mutagenesis step (Figure 20).

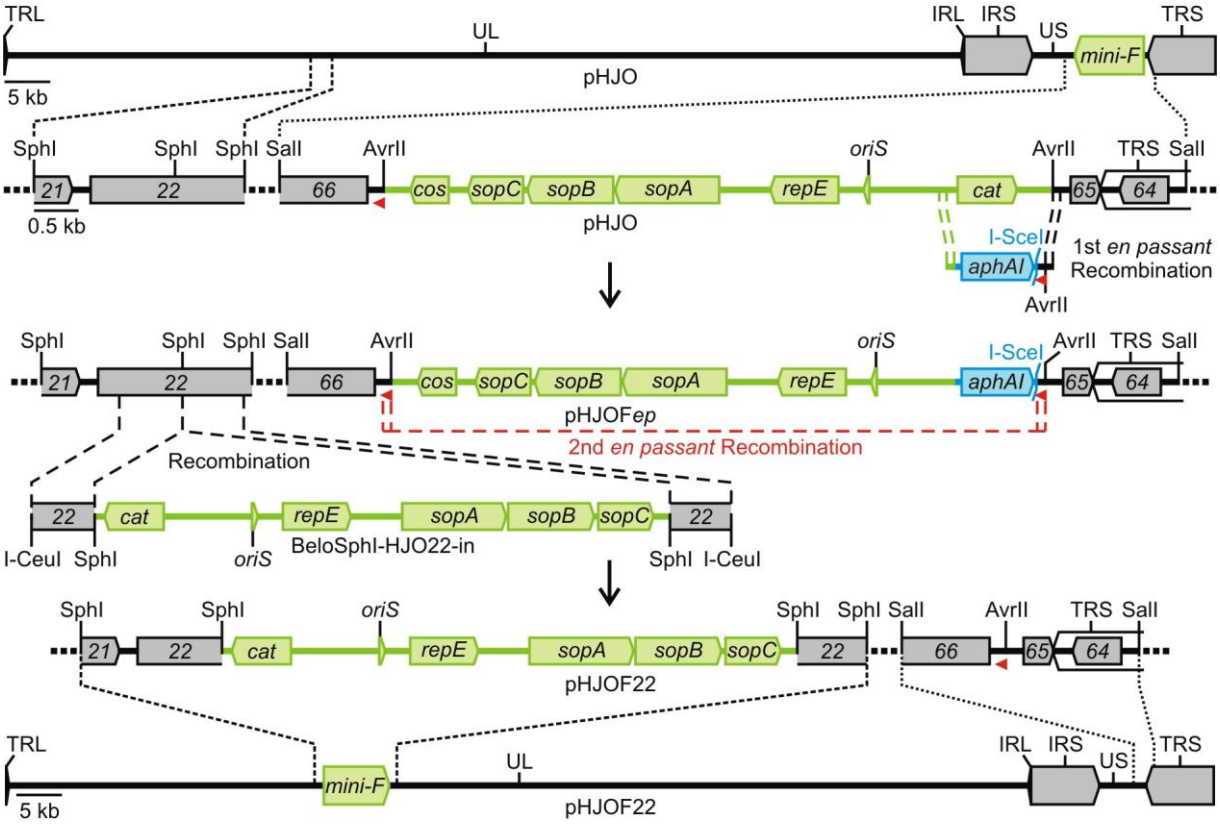

Figure 20. Mini-F vector transposition. Scheme of the transposition of the mini-F vector exemplified by the insertion into *ORF22*. First, the resistance gene *cat* of the pBeloBAC11 mini-F vector (green) of pHJO within the unique AvrII site of the US region was replaced by an *aphAI*-I-SceI cassette (blue) and a 50 bp direct viral sequence duplication (red arrows) via Red recombination (green and black dashed lines, first *en passant* step) resulting in pHJOF*ep*. Second, the BAC vector pBeloSphI was inserted into *ORF22* of pHJOF*ep* via Red recombination (black dashed lines) using the transfer construct BeloSphI-HJO22-in and the present vector was removed from the unique US AvrII site via I-SceI induced double-strand break and Red-mediated recombination (red dashed lines, second *en passant* step) of the short duplications, to yield pHJOF22.

In the mini-F vector transposition reaction, the pBeloBAC11 elements were inserted into *ORF22*, *ORF50*, or *ORF54*, and simultaneously removed from the US AvrII site by two successively induced Red recombinations combined with an interposed I-SceI double-strand break. For this procedure, the I-CeuI transfer constructs were released from the plasmids pBelo-HJO22-in, pBelo-HJO50-in, and pBelo-HJO54-in, and applied to introduce by Red recombination in GS1783 cells the pBeloSphI and pBeloBamHI BAC vector in inverse orientation with respect to the present *aphAI*-I-SceI-associated mini-F fragment into the 5'-end positions of *ORF22*, *ORF50*, or *ORF54* within the cloned VZV genome of pHJOF*ep*

(Figure 20). Upon induction of a double-strand break at the I-SceI recognition site, the *aphAI*-I-SceI-linked pBeloBAC11 mini-F fragment was immediately removed in the second *en passant* step from the unique AvrII site of the US region by Red-mediated recombination of the short 50 bp genomic duplication adjoining the vector insertion site (Figure 20). The resulting BAC derivates of pHJO comprising pBeloBAC11 sequences in *ORF22*, *ORF50*, or *ORF54* were termed pHJOF22, pHJOF50, or pHJOF54, respectively (Figure 20).

Finally, I generated the transfer plasmids pEP-HJO22-DX-in, pEP-HJO22-DX-in, and pEP-HJO22-DX-in to introduce corresponding genomic duplications into the pBeloBAC11 sequences of the derived pHJO variants. For this purpose, I used the 1.4 kb PCR products of the 0.7 kb regions adjoining the 5'-end positioned SphI or BamHI sites of *ORF22*, *ORF50*, or *ORF54* that were generated with the primers K and L, M and N, or O and P (Table 1) and afterwards digested with SpeI for the generation of the mini-F vector transfer plasmids. These PCR products were cloned here in reverse orientation with respect to the pBeloBAC11 sequences in pHJOF22, pHJOF50, or pHJOF54 into the AvrII site between the Belo fragments of the pEP*MCS*-in-Belo vector (Figure 11). The resulting plasmids were termed pEP-HJO22-DX-in, pEP-HJO22-DX-in, or pEP-HJO22-DX-in, respectively (Figure 21).

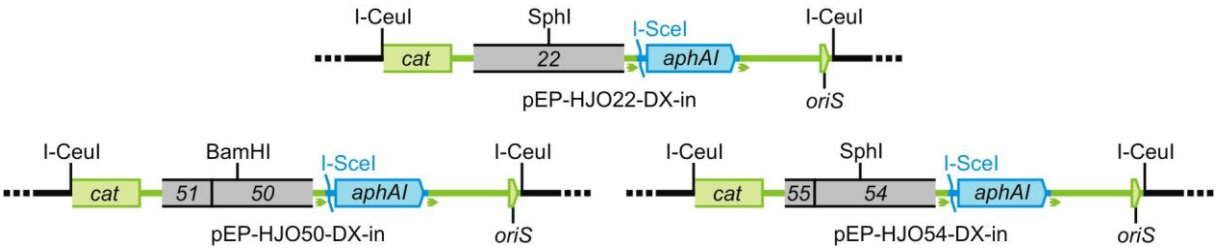

Figure 21. Plasmids pEP-HJO22-DX-in, **pEP-HJO22-DX-in, and pEP-HJO22-DX-in.** For the construction of the plasmids pEP-HJO22-DX-in, pEP-HJO50-DX-in, or pEP-HJO22-DX-in, the 1,4 kb HJO sequences spanning the 5'-end positioned SphI or BamHI site of *ORF22*, *ORF50*, or *ORF54* were inserted into the universal transfer construct (green and blue) of plamid pEP*MCS*-in-Belo (Figure 11)**.**

Using the released I-CeuI fragments of the plasmids pEP-HJO22-DX-in, pEP-HJO50-DX-in, or pEP-HJO54-DX-in, the genomic duplications were introduced by *en passant* mutagenesis in GS1783 *E. coli* cells as described above (Figure 12) between the *oriS* and the *cat* gene of the pBeloBAC11 vector of pHJOF22, pHJOF50, or pHJOF54, resulting accordingly in the self-excisable constructs pHJOF22-DX, pHJOF50-DX, or pHJOF54-DX (Figure 22). Also these constructs could stably be propagated in *E. coli* GS1783 and enabled the mini-F vector removal and repair of the disrupted gene function by the two assumed events of homologous recombination in eukaryotic VZV-permissive cells (Figure 22).

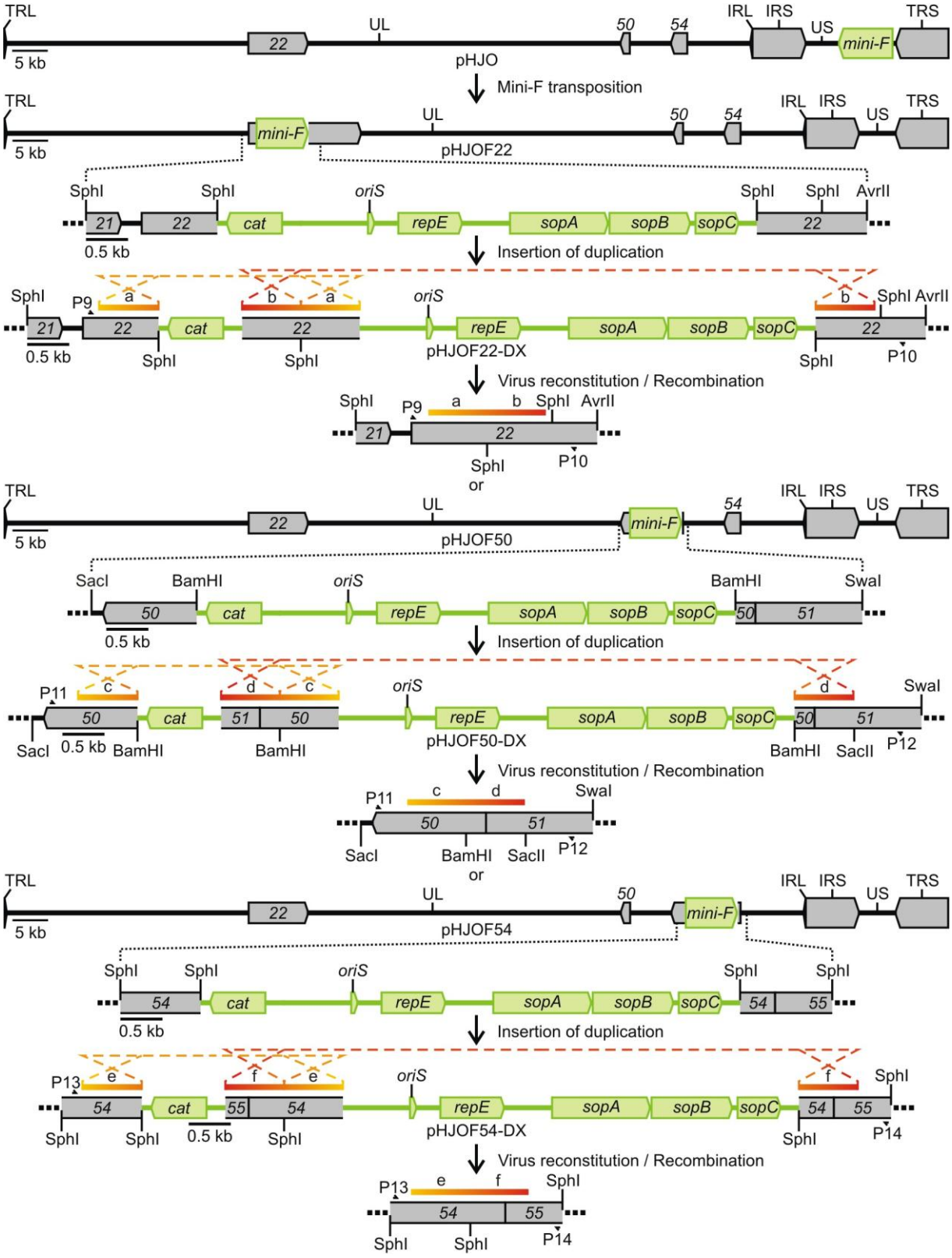

Figure 22. Construction of pHJOF22-DX, pHJOF50-DX, and pHJOF54-DX. Upon mini-F transposition, the pBeloBAC11 elements were removed from the pHJO-cloned VZV genome and inserted into 5'-end positions of *ORF22*, *ORF50*, or *ORF54*, resulting in pHJOF22, pHJOF50, or pHJOF54. Then, corresponding 1.4 kb genomic duplications of 0.7 kb viral sequences flanking the mini-F insertion site (a, b; c, d; e, f; yellow to red gradient bars) were inserted in inverse orientation into the pBeloBAC11 sequences, to generate pHJOF22-DX, pHJOF50-DX, or pHJOF54-DX. Homologous recombination of the genomic duplications led to the excision of the vector sequences during the virus reconstitution in transfected eukaryotic cells. Primers P9 and P10, P11 and P12, or P13 and P14 were used to investigate the vector excision in virus progeny derived from pHJOF22-DX, pHJOF50-DX, or pHJOF54-DX, respectively.

4.3.2 Maintenance of the VZV genome during the mini-F vector transposition

To confirm the integrity of the HJO genome organization, the transposition of the mini-F sequences and the insertion of the reverse genomic duplications, I prepared pHJO and pHJOF*ep* as well as the three engineered pHJO variants and pHJO-DX constructs from the GS1783 *E. coli* cells, treated the BACs with HindIII, SalI, or BamHI, and compared the resulting RFLP pattern. All observed fragment rearrangements in pHJOF22, pHJOF50, or pHJOF54 in comparison to pHJOF*ep* and pHJO were confirmed to correspond with the transposition of the pBeloBAC11 elements into *ORF22*, *ORF50*, or *ORF54* and with the vector excision from the unique AvrII site of the VZV US region (Figure 23). Also the observed band shifts in pHJOF22-DX, pHJOF50-DX, or pHJOF54-DX in relation to pHJOF22, pHJOF50, or pHJOF54 correlated to the expected rearrangements by the insertion of the respective reverse genomic duplications into the pBeloBAC11 sequences (Figure 23).

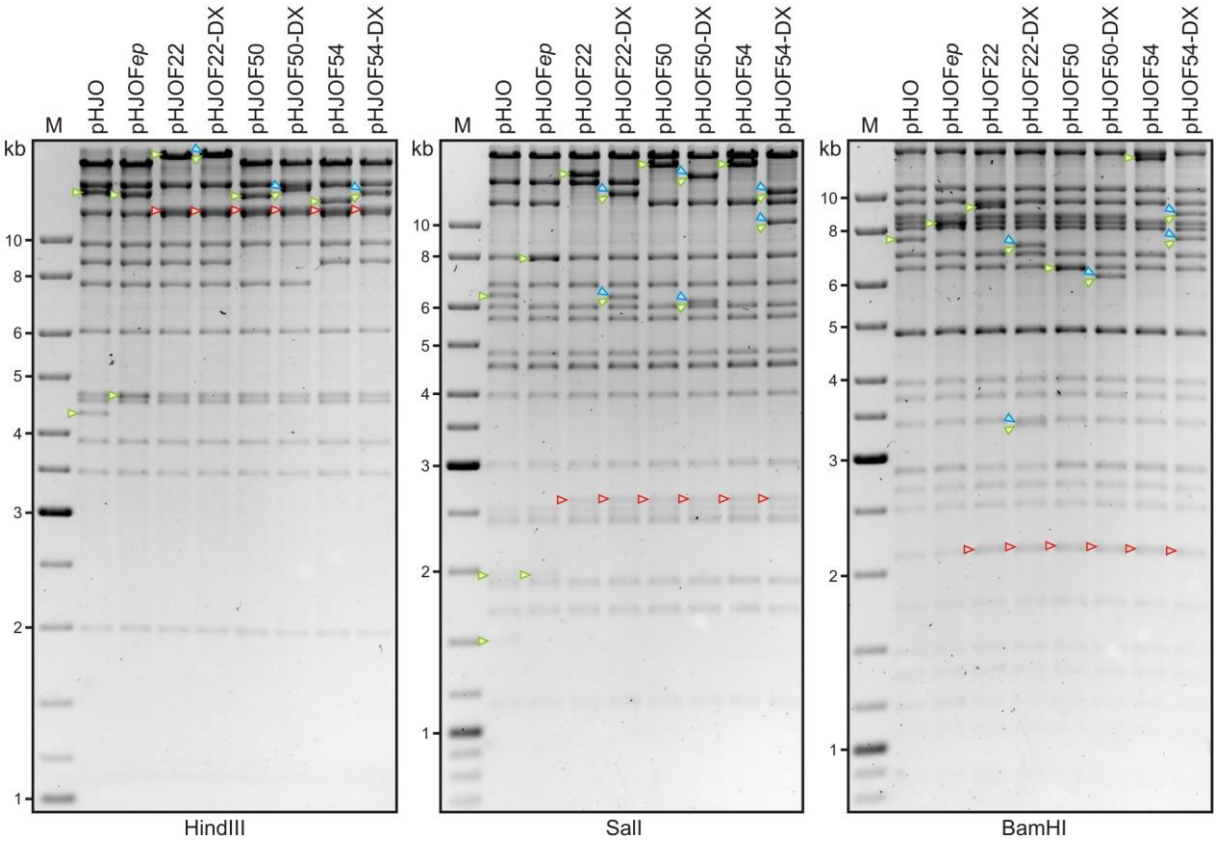

Figure 23. RFLP analysis of pHJOF22-DX, pHJOF50-DX, and pHJOF54-DX. Restriction fragment pattern of HindIII, SalI, or BamHI digested pHJO, pHJOF*ep*, pHJOF22, pHJOF22-DX, pHJOF50, pHJOF50-DX, pHJOF54, or pHJOF54-DX BAC DNA. Fragments that comprise the pBeloBAC11 elements (green arrows), the restored unique AvrII site of the US region (red arrows), or sequences of the reverse genomic duplications (blue arrows) are marked. All fragment rearrangements of the engineered pHJO-DX constructs in comparison to the pHJO variants, and of the pHJO variants in comparison to pHJOF*ep* and pHJO were observed as expected.

For instance, the genomic 7.6 kb Hind III fragment that contains the *ORF54* appeared in pHJOF54 due to the insertion of the 6.4 kb pBeloSphI BAC vector, which lack a HindIII site in contrast to the vector elements of pHJO or pHJOF*ep*, as a 14 kb band, and an additional 12.5 kb band occurred that indicates the vector excision from the US AvrII site (Figure 23). The insertion of the reverse genomic duplication into the pBeloSphI elements within the *ORF54* fragment causes a shift of the 14 kb band of pHJOF54 into a 15.4 kb band in pHJOF54-DX. Furthermore, the seamless repair of the unique AvrII site in all three pHJO variants was confirmed by PCR and sequencing analysis (data not shown). The transposition of the mini-F sequences into *ORF22*, *ORF50*, or *ORF54* and the insertion of the corresponding reverse genomic duplications in the pBeloBAC11 sequences in the three pHJO-DX variants were confirmed via PCR (data not shown). These results demonstrated that the pBeloBAC11 sequences were seamlessly transposed within the HJO genome into *ORF22*, *ORF50,* or *ORF54* and that the integrity of the initially cloned viral DNA appeared to be conserved during the pBeloBAC11 insertion and excision reaction and subsequent integration of the reverse genomic duplications. In conclusion, a novel mini-F vector transposition reaction was established which enables the rapid, safe, and perfect restructuring of the infectious pHJO BAC in *E. coli*.

4.3.3 Efficient vector excision from essential genes following delayed virus reconstitution

In order to investigate the mini-F excision from the disrupted *ORF22*, *ORF50*, or *ORF54* upon virus reconstitution, I purified pHJOF22-DX, pHJOF50-DX, or pHJOF54-DX BAC DNA from *E. coli* and transfected the BACs into MeWo cells. In addition, to evaluate if the vector insertion into *ORF22*, *ORF50*, or *ORF54* abrogates virus propagation, I also used the corresponding BAC variants pHJOF22, pHJOF50, and pHJO54 without inserted duplication for the transfection of the VZV-permissive cells. In comparison to the virus reconstitution from the original pHJO BAC, the formation of the VZV-typic CPEs in MeWo cultures transfected with the different pHJO-DX variants was detected only after one additional cell passage. As expected, CPEs were not detected in MeWo cultures transfected with the BAC variants pHJOF22 or pHJOF54 used as controls. In contrast, virus reconstitution from the control BAC pHJOF50 was detected directly after transfection of the MeWo cells without further passage of the MeWo cells. However, the plaques generated by the pHJOF50-derived progeny appeared to be smaller with VZV-atypical and indistinct syncytia formation in comparison to that provoked by HJO wild-type virus or all the other reconstituted viruses (data not shown). These resulted indicated that the insertion of the pBeloBAC11 sequences

into *ORF22* or *ORF54* apparently fully abrogated the virus propagation, whereas not completely when introduced into *ORF50* and that the genomic duplication can reverse these detrimental effects.

Finally, to determine the mini-F excision from the disrupted ORFs by the expected events of homologous recombination between the genomic duplications (Figure 22), the viruses reconstituted from the three pHJO-DX variants were propagated as described and DNA from the MeWo cells infected with the progenies of the different virus passages was prepared for PCR analysis. The primers P9 and P10, or P11 and P12, or P13 and P14 (Table 1) that annealed within the viral DNA exterior of the corresponding genomic duplication and up- or downstream of the mini-F insertion site of *ORF22*, *ORF50*, or *ORF54* were used to determine the complete excision of the pBeloBAC11 elements in pHJOF22-DX-, pHJOF50-DX-, or pHJOF54-DX-derived progeny (Figure 22). To differentially analyze the retention or loss of the two pBeloBAC11 vector parts divided by the genomic duplications, I applied the introduced *sopA* and *cat* specific primers in the PCR (Figure 12). In all three recombinant progenies, the complete excision of the vector elements from the respective disrupted ORF was detected right upon virus reconstitution and not in the corresponding BACs used for the transfection of the MeWo cells (Figure 24). Remaining *sopA* or *cat* sequences were usually present until virus passage 4 after transfection of the MeWo cells (Figure 24). Thus, the duplication-mediated BAC self-excision from *ORF22, ORF50,* or *ORF54* was more efficient than from the unique AvrII site. However, the vector sequences were, despite their highly impairing or abrogating effect on the virus replication, not immediately eliminated upon reconstitution of the viral progeny. In addition, the virus reconstitution from all three pHJO-DX variants occurred with delayed kinetics.

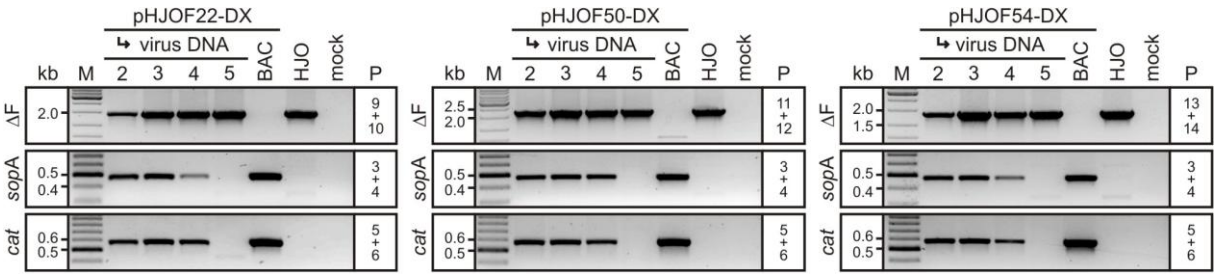

Figure 24. PCR analysis of the vector excision upon virus recovery from pHJOF22-DX, pHJOF50-DX, or pHJOF54-DX. PCR analysis of the pBeloBAC11 vector excision (ΔF) or the retention of *sopA* or *cat* sequences in DNA from MeWo cells infected with pHJOF22-DX-, pHJOF50-DX-, or pHJOF54-DX-derived progeny of virus passage 2-5 using the indicated primers (P). Total DNA from MeWo cells infected with wild-type HJO or uninfected cells as well as BAC DNA of the three pHJO-DX variants were analyzed as controls.

4.4 Genome-intrinsic mini-F vector release

Since the novel mini-F vector transposition reaction was based on Red recombination in *E. coli*, it allowed the rapid generation of BAC variants of the original pHJO clone independently from the viral DNA replication or genome maturation process. This initiated the possibility to develop pHJO variants comprising the mini-F vector sequences in specific genome positions that can be repaired by intrinsic VZV DNA replication mechanisms. We assumed that the mini-F elements of such engineered BACs can be efficiently and seamlessly released after virus reconstitution even without a genomic duplication. Moreover, the absence of a genomic duplication would additionally avoid the potential for illegitimate events of homologous recombination during the F-factor-mediated replication in bacteria or the viral DNA replication in eukaryotic cells.

It was described that single deletion of the duplicated *ORF62/71* that is located within the large S repeats and encodes the immediate-early transactivator IE62, leads to efficient repair of the disrupted repeat region by inherent homologous recombination events with the intact repeated region (Sato et al., 2003). Furthermore, it was surmised for the herpesvirus genome maturation process that the formation of the genomic termini is to some degree governed independently by two precise cleavages of a terminase complex coordinated from the two packaging signals (Figure 4) (Hodge and Stow, 2001; McVoy et al., 2000; Schynts et al., 2003; Umene, 1999; Varmuza and Smiley, 1985; Wang et al., 2008). In addition, sequences at the genomic termini were believed to be recombinational hot-spots due to the induction of an additional double-strand break mechanism or due to the high GC content at the DNA ends (McVoy and Ramnarain, 2000; Mocarski et al., 1980; Severini et al., 1996; Slobedman et al., 1999; Thiry et al., 2005; Umene, 1999). Therefore, we assumed that mini-F sequences inserted into one of the coding domains of the immediate-early transactivator IE62 or into the predominantly cleaved genomic terminal junction between the S and L component at the *ORF0* end of the VZV UL region (S/L0), can be rapidly released by intrinsic DNA replication or genome maturation processes. Consequently, I planned to engineer pHJO variants comprising pBeloBAC11 elements in *ORF62*, *ORF71*, or the genomic terminal S/L0 junction.

4.4.1 Mini-F transposition into duplicated genes or the terminal genome junction

For the insertion of the pBeloBAC11 sequences into *ORF62* of the TRS region, or into *ORF71* of the IRS region, I developed the mini-F vector transfer plasmids pBelo-HJO62-in and pBelo-HJO71-in in the following cloning procedure. First, 1.4 kb HJO sequences of 0.7

kb regions that are found on either side of a BamHI site in *ORF62/71*, were amplified from pHJO by PCR using the primers S and T, digested with SpeI and inserted into the XbaI site of the *MCS* between the I-CeuI sites of the pCeu2 vector (Tischer et al., 2007). Subsequently, the BAC vector pBeloBamHI was linearized with BamHI and introduced into the BamHI site of the pCeu2-cloned fragment of *ORF62/71* in reverse or in forward orientation, to generate pBelo-HJO62-in and pBelo-HJO71-in, respectively (Figure 25).

For the introduction of the pBeloBAC11 elements into the terminal S/L0 junction, I constructed the transfer plasmid pBelo-HJO*pac*-in as follows. To generate a BamHI site directly between the DNA ends of the S and L component for the subsequent incorporation of the mini-F plasmid pBeloBamHI, 0.7 kb viral sequences of the S and the L0 terminus were amplified separately from pHJO via PCR with the primers U and V or primers W and X (Table 1), whereby primer W provides a BamHI site, treated with SalI or SpeI, and successively cloned into the XhoI or XbaI site between the I-CeuI sites of pCeu2. Then, the pBeloBamHI BAC vector was cleaved with BamHI and introduced in forward orientation into the engineered BamHI site directly between the DNA ends of the pCeu2 vector-cloned terminal S/L0 transition, resulting in pBelo-HJO*pac*-in (Figure 25).

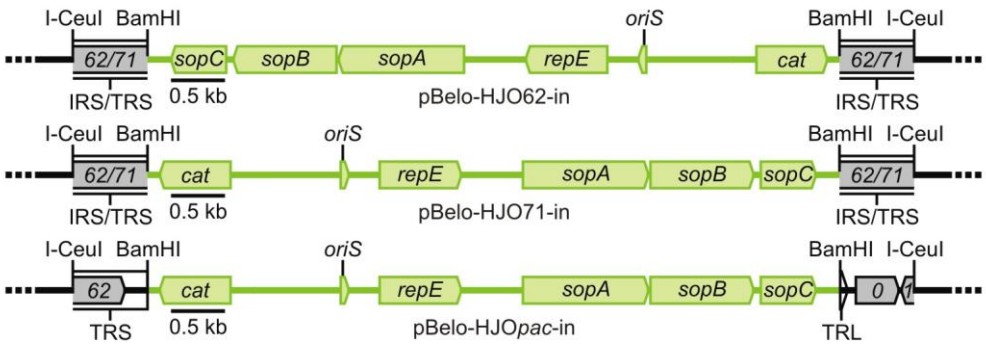

Figure 25. Mini-F vector transfer plasmids pBelo-HJO62-in, pBelo-HJO71-in, and pBelo-HJO*pac*-in. To construct pBelo-HJO62-in, pBelo-HJO71-in, or pBelo-HJO*pac*-in, the pBeloBAC11 sequences were inserted into the BamHI site of the pCeu2-cloned fragments of *ORF62/71* in forward or reverse orientation or into the cloned the terminal S/L0 transition.

The generated plasmids were used for the transposition reaction to move the mini-F sequences into *ORF62*, *ORF71*, or the terminal genomic junction of the BAC-cloned HJO genome. For this procedure, the plasmids pBelo-HJO62-in, pBelo-HJO71-in, or pBelo-HJO*pac*-in were digested with I-CeuI and the released fragments were used to insert the pBeloBamHI vector into *ORF62*, *ORF71*, or the S/L junction of the *en passant* mini-F excision-ready BAC pHJOF*ep* via Red recombination in *E. coli* GS1783 in inverse orientation with respect to the

pre-existing *aphAI*-I-SceI-associated pBeloBAC11 fragment in the US AvrII site (Figure 20). As described before, the pre-existing *aphAI*-I-SceI linked mini-F replicon at the unique AvrII site of the VZV US region was subsequently excised after *I-sceI*- and *red*-expression during the second *en passant* step (Figure 20). The resulting BAC constructs with pBeloBamHI vector in the *ORF62* of the TRS region, in *ORF71* of the IRS region, or in the S/L0 terminal junction between the two packaging signals at the *ORF0* end of the UL region, were termed pHJOF62, pHJOF71, or pHJOF*pac* (Figure 26).

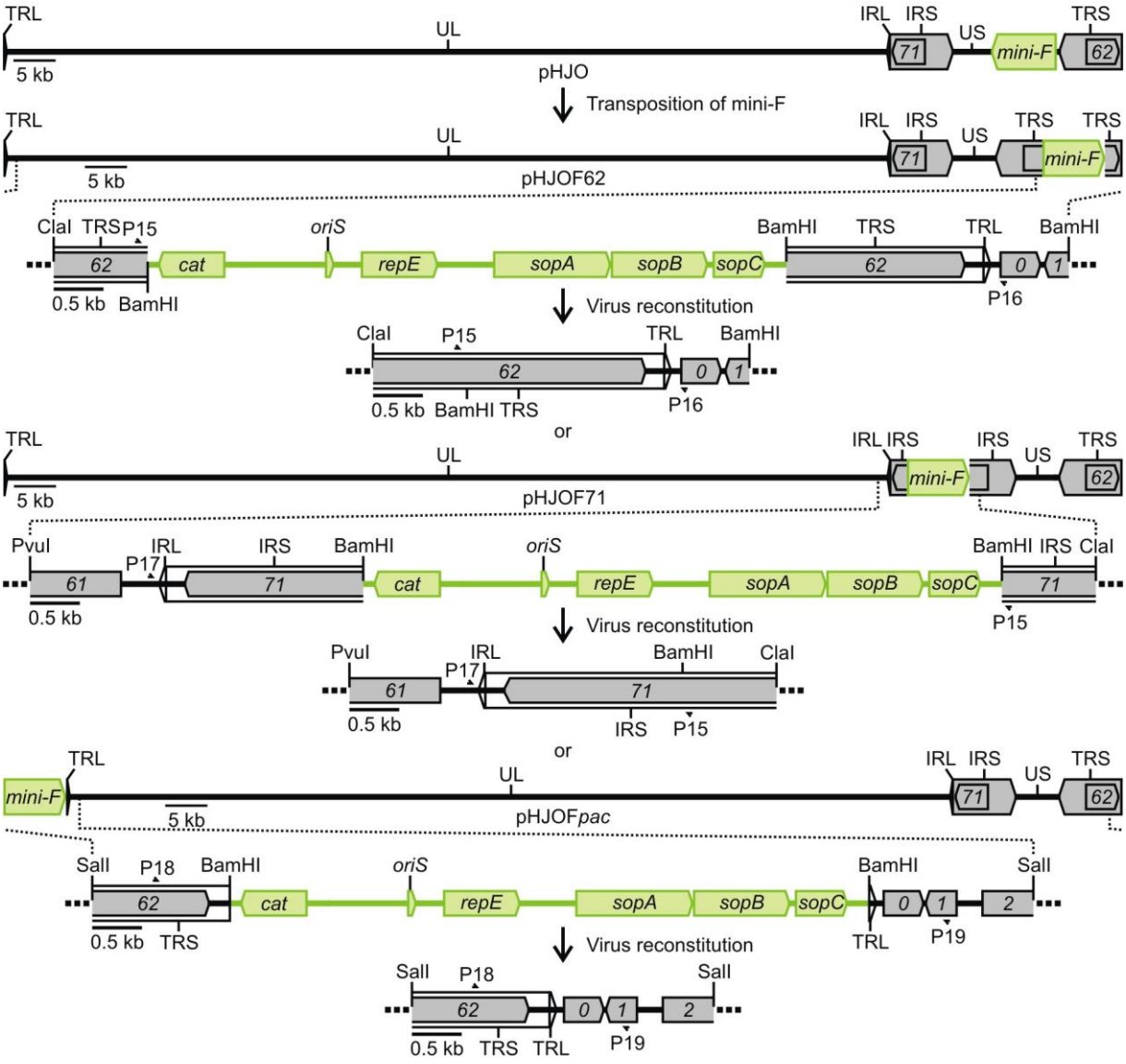

Figure 26. Generation of pHJOF62, pHJOF71, and pHJOF*pac*. Upon mini-F sequence transposition, the pBeloBAC11 elements (green) were removed from the pHJO-cloned VZV genome and inserted into *ORF62*, *ORF71*, or the terminal genomic junction at the *ORF0* end or the UL region, resulting in pHJOF62, pHJOF71 or pHJOF*pac*. After transfection of the BACs into VZV-permissive cells and virus reconstitution, the pBeloBAC11 elements were released by inherent genome replication mechanisms. Primers P15 and P16, P15 and P17, or P18 and P19 were used to verify the vector excision from *ORF62*, *ORF71*, or the terminal genomic junction.

4.4.2 Preservation of the VZV DNA after BAC transposition into repeated regions

To confirm the integrity of the originally cloned HJO DNA as well as the transposition of the mini-F sequences into *ORF62*, *ORF71*, or the S/L0 terminal transition, I compared the SalI, PvuII, SphI, or BamHI RFLPs of the engineered pHJO variants with that of the original pHJO BAC and pHJOF*ep*. The restriction fragment patterns of pHJOF62, pHJOF71, and pHJOF*pac* BAC DNA in relation to pHJO and pHJOF*ep* were confirmed to correlate with the band shifts that were expected by the insertion of the pBeloBAC11 sequences into *ORF62* of the TRS region, into *ORF71* of the IRS region, or into the S/L0 terminal localization, and by the removal of the vector elements from the US unique AvrII site (Figure 27). For example, the 3 kb SalI fragment of pHJO and pHJO*ep* that represents the terminal S/L0 transition appears in pHJOF*pac* as a 9.4 kb band by the integration of the 6.4 kb pBeloBamHI vector, which did not contain an additional SalI site in contrast to the vector sequences of pHJO and pHJOF*ep*. Furthermore, the expected 2.6 kb HJO genomic SalI fragment encompassing the restored unique US AvrII site was detected in pHJOF*pac* BAC DNA (Figure 27).

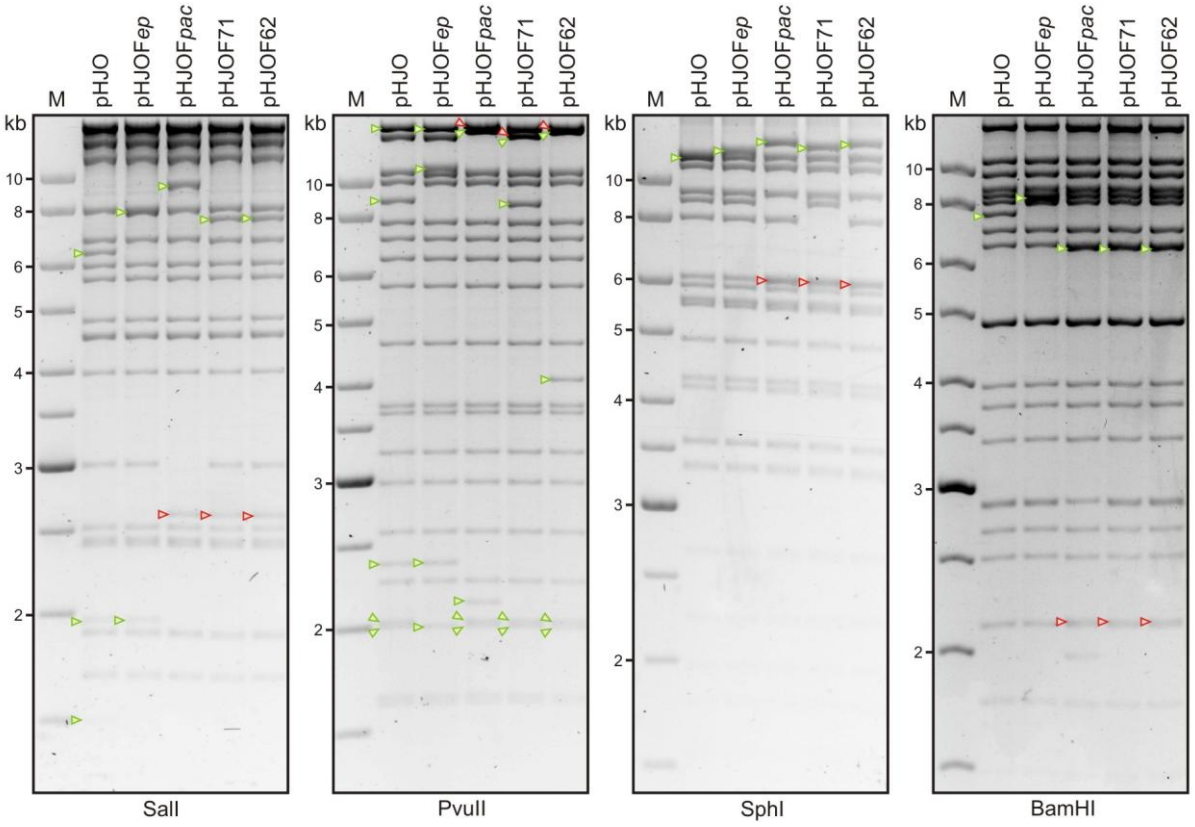

Figure 27. RFLP analysis of pHJOF*pac* pHJOF71, and pHJOF62. Restriction fragment patterns of SalI, PvuII, SphI, or BamHI digested pHJO, pHJOF*ep*, pHJOF*pac*, pHJOF71, or pHJOF62 BAC DNA. Fragments containing vector sequences (green arrows) or the restored unique AvrII site of the VZV US region (red arrows) are indicated. All fragment rearrangements in the three pHJO variants in comparison to pHJO and pHJOF*ep* were observed as expected.

These results and, thus, the stability of the pHJOF*pac* clone during the mini-F replicon mediated BAC replication in *E. coli* could also be confirmed by Southern-blot hybridization (see section 4.4.6). In addition, the scarless repair of the unique AvrII site as well as the pBeloBAC11 insertion into *ORF62*, *ORF71*, or the S/L0 transition in pHJOF62, pHJOF71, or pHJOF*pac* was confirmed via PCR and sequencing analysis (data not shown). Thus, the cloned HJO genome was fully maintained during the mini-F sequence transposition reaction to generate the pHJOF62, pHJOF71, or the pHJOF*pac* BAC construct. These results demonstrated that the mini-F transposition reaction also allows the movement of the pBeloBAC11 sequences into repeated domains of the cloned HJO genome in *E. coli*.

4.4.3 Efficient intrinsic BAC vector release from the genomic junction

In order to determine the proposed intrinsic vector release from *ORF62*, *ORF71*, or the terminal S/L0 transition upon recovery of recombinant progeny, I isolated pHJOF62, pHJOF71, or pHJOF*pac* BAC DNA from the *E. coli* GS1783 cells and transfected the BACs into MeWo cells. VZV-characteristic focal CPEs were detected in the MeWo monolayers four to five days after transfection of the cells with the three different pHJO variants. The reconstituted viruses were propagated as described before and DNA of MeWo cells infected with the passaged progeny was investigated via PCR. To specifically determine the complete excision of the pBeloBAC11 elements from *ORF62* of the TRS region, from *ORF71* of the IRS region, or from the terminal S/L transition at the *ORF0* end of the UL region, I used the primers P15 and P16, P15 and P17, or P18 and P19 (Table 1) in the PCR, that annealed on either side of the mini-F insertion position and of which one primer bound within the S repeats and the other in the UL region (Figure 26). Since the vector was not divided into two parts by a genomic duplication, the persistence of the pBeloBAC11 sequences in the viral DNA was only analyzed by the primers specific for the *cat* gene (Figure 12).

In the recombinant progenies derived from pHJOF62 or pHJOF71, the *cat* sequences were detected via PCR until virus passage five or four (Figure 28). During propagation of virus progenies derived from two different clones of pHJOF62 or pHJOF71, the vector elements were present until virus passage seven and beyond or six (data not shown). In contrast, in the DNA of pHJOF*pac*-derived progeny the *cat* gene was always traceable only until virus passage two (Figure 28). However, PCR fragments that indicate the complete pBeloBAC11 excision from the viral genomes were not only obtained from the viral DNA, but also in minor quantities from the pHJOF*pac* clone and in significant amounts from the pHJOF71 or the

pHJOF62 BAC DNA used for the transfection of the MeWo cells (Figure 28). This might indicate that the BAC sequences of the three pHJO variants were already excised in a portion of viral genomes during the F-factor mediated replication in *E. coli*. In contrast, corresponding fragments that reflect the vector excision were not detected in the BAC DNA isolated from the GS1783 cells by RFLP analysis (Figure 27) and specifically for the pHJOF*pac* clone also not by Southern-blot hybridization (see section 4.4.6). For example, the 3 kb SalI fragment that would correspond with the mini-F excision from the unique AvrII site was not detectable in the restriction fragment pattern of pHJOF*pac* (Figure 27 and section 4.4.6). In addition, it was described for the investigation of the VZV repeat regions of infectious cosmid clones that false positive signals can be generated during PCR amplification, even if one primer anneals within the unique region (Figure 26) (Sato et al., 2003). Therefore, we concluded that the pBeloBAC11 sequences were efficiently released from the viral DNA only after the virus reconstitution from the three pHJO variants. Since the pBeloBAC11 sequences in virus derived from the pHJOF*pac* clone were much more efficiently released in comparison to that of all the other generated progenies, this viral BAC appeared to be the ideal candidate to rapidly generate vector-free VZV mutants.

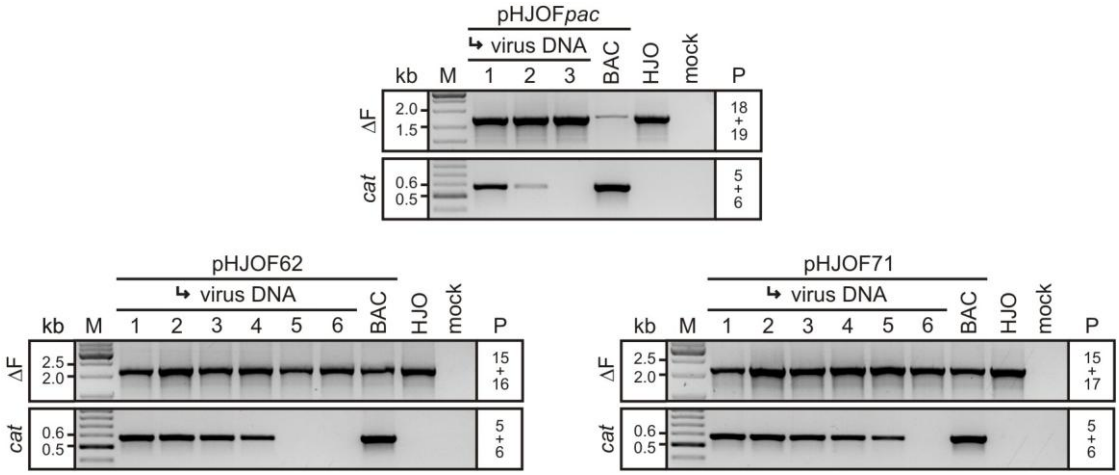

Figure 28. PCR analysis of the vector release in virus progeny derived from pHJOF*pac*, pHJOF71, or pHJOF62. PCR analysis of total DNA from MeWo cells infected with pHJOF71-, pHJOF62-, or pHJOF*pac*-derived virus progeny of virus passage 1-6 or 1-3 for determination of the pBeloBAC11 vector release or the persistence of *cat* sequences using the designated primers (P). Total DNA of MeWo cells infected with HJO wild-type virus or uninfected cells as well as BAC DNA of the pHJO variants were analyzed as controls.

4.4.4 Sequence inversions after insertion of the BAC vector into the terminal junction

The PCR fragments from pHJOF*pac* which were generated with the primers P18 and P19 (Figure 26) may indicate the excision of the pBeloBAC11 elements already during the DNA replication in *E. coli* (Figure 28). However, they could also result from the inversion of the

UL region by homologous recombination of the small inverted L repeats. Therefore, I tried to determine if the mini-F sequences were also present at the *ORF61* end of the L component, which would result from the inversion of the UL region in pHJOF*pac* (Figure 29A). For this purpose, the purified pHJOF*pac* BAC DNA used for the transfection of MeWo cells to reconstitute recombinant progeny, as well as BAC DNA of the original pHJO clone as a negative control, were analyzed via PCR using the following primer pairs. To confirm the existence of the mini-F sequences at the *ORF0* end of the L component (F-L0), I used the primer P20, which anneals in sense orientation on the pBeloBAC11 end at the TRL region, and the primer P19, which binds in antisense direction in *ORF1* of the UL region (Figure 29A). To detect the mini-F sequences at the *ORF61* end of the L component (F-L61), I applied primers P19 and P21, which bound in sense orientation in *ORF61* of the UL region (Figure 29A). The expected fragments of 1 kb (1020 bp or 1028 bp) were derived in significant amounts from pHJOF*pac* BAC when using the primers P19 and P20 for the detection of the F-L0 transition and in minor quantities also when using the primers P20 and P21 for the detection of the F-L62 transition (Figure 29B).

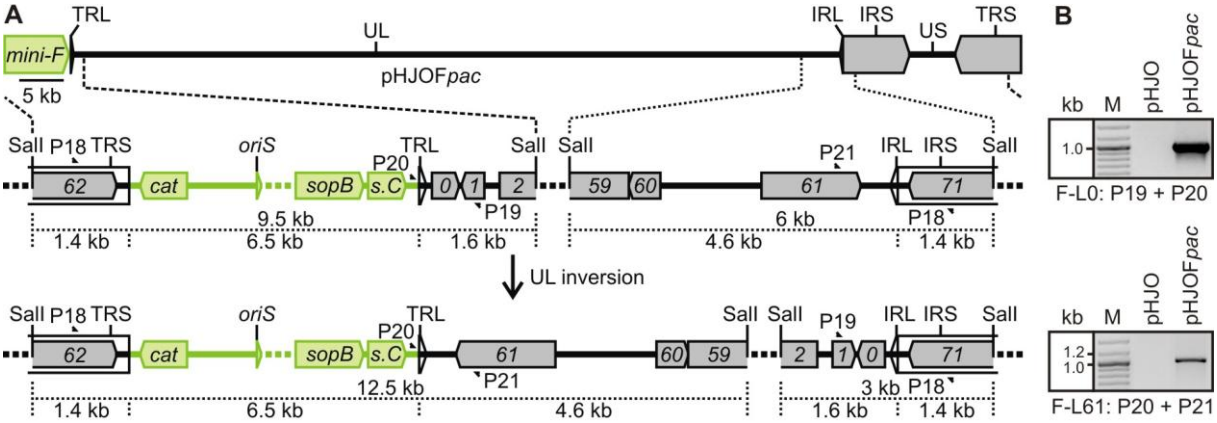

Figure 29. PCR analysis of a putative UL inversion in pHJOF*pac*. A) Inversion of the UL region in BAC DNA of pHJOF*pac* in an overview of both S/L transitional SalI fragments. Fragment lengths and the ranges from the SalI sites to the S/L junctions (dotted line) are indicated. Also the binding positions of primers P18-P21 are given. Primers P18 and P19 were used to analyze pBeloBAC11 excision from the S/L0 junction in pHJOF-*pac*-derived virus. Primers P19 and P20 were used to verify the presence of the mini-F vector at the *ORF0* end of the UL region (F-L0). Primers P20 and P21 were used to detect the existence of the mini-F vector at the *ORF61* end of the UL region (F-L61), which would be the result from the inversion of the UL region. **B)** PCR analysis of pHJOF*pac* DNA for confirmation of the F-L0 or the putative F-L61 transition as outlined in A using the given primes. BAC DNA of original pHJO was analyzed as control.

These PCR results could indicate that the UL region rarely undergoes inversion by homologous recombination of the small inverted repeats during the low-copy mini-F replication in *E. coli* GS1783. As for the mini-F excision, the inversion of the UL region was not detectable in

the restriction fragment patterns of pHJOF*pac* BAC DNA prepared from *E. coli*. For example, the 12.5 kb and 3 kb SalI fragments that would result from the inversion of the UL region (Figure 29A), were neither detected via RFLP analysis (Figure 27), nor by Southern-blot hybridization (see section 4.4.6). Therefore, we concluded that the PCR results which may indicate UL inversion were also false positive signals possibly generated by annealing of the amplified repeat regions, as suggested before for the analysis of the mini-F excision (section 4.4.3 and Figure 28) (Sato et al., 2003).

4.4.5 Seamless intrinsic BAC vector release from the VZV DNA termini

To confirm the seamless vector excision from the VZV DNA ends after virus reconstitution from pHJOF*pac*, I analyzed the terminal S/L0 junction of the derived mini-F vector-free progeny, termed rHJO*pac*-F⁻, as follows. Due to nucleotide polymorphisms at the VZV DNA ends, it was not possible to define the sequence of the 1.6 kb fragments that were generated from the terminal S/L0 transition of rHJO*pac*-F⁻ by PCR amplification of the DNA from infected MeWo cells with the primers P18 and P19 (Figure 26 and 28). Therefore, the 1.6 kb PCR products of the terminal junction from the MeWo cells infected with rHJO*pac*-F⁻ or with HJO wild-type virus as positive control were first cloned into the pCR2.1-TOPO vector and subsequently analyzed via sequencing. The repair of the S/L0 transition was confirmed in 16 cloned PCR fragments derived from rHJO*pac*-F⁻ (Figure 30).

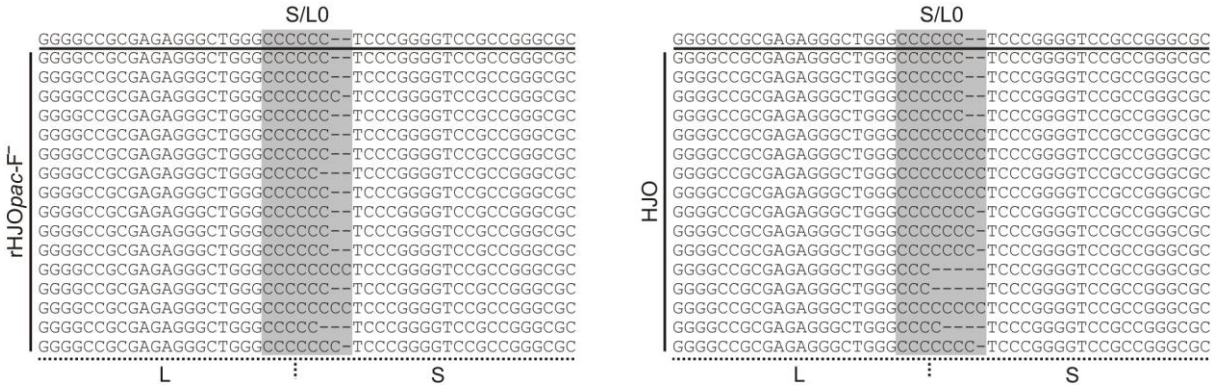

Figure 30. Sequence analysis of the terminal genomic junction of rHJO*pac*-F⁻. Sequence analysis of 16 cloned PCR fragments that were generated with the primers P18 and P19 (Figure 26) of the S/L0 transition of rHJO*pac*-F⁻ or wild-type HJO DNA from infected MeWo cells. The derived sequences were aligned to the sequence of the terminal S/L0 transition of the original pHJO clone (first line). The GC tract of the S/L0 junction (highlighted in gray) as well as L and S component sequences (dotted lines) are marked.

A variability of the number of the GC base pairs (ranging from 3 to 8 GC bp) directly at the junction was detected in DNA of the recombinant progeny and HJO wild-type virus (Figure

30). The sequence variability at the S/L0 junction of rHJO*pac*-F⁻ appeared to be less pronounced as in the case of wild-type HJO. In addition, the number of AT base pairs of the *pac2* signal in DNA of rHJO*pac*-F⁻ appeared more conserved than in DNA of wild-type HJO (data not shown). Short deletions directly at the S/L0 junctions were found in DNA of rHJO*pac*-F⁻ and of HJO, which was additionally verified by screening of further cloned DNA fragments via PCR (data not shown). Thus, the vector sequences were seamlessly released from the genomic termini upon virus reconstitution from pHJOF*pac*, whereby the nucleotide polymorphisms directly at the junction and the *pac2* signal in the vector free progeny was not as variable as in the case of the wild-type virus.

4.4.6 Repair of the VZV genome upon vector release from the DNA termini

To define the genome organization after the release of the vector elements from the DNA termini, I determined the restriction fragment patterns of the pHJOF*pac*-derived mini-F sequence-free progeny rHJO*pac*-F⁻ via Southern-blot hybridization (Figure 31). For this purpose, I digested total DNA from MeWo cells infected with HJO wild-type virus or rHJO*pac*-F⁻, and pHJO, pHJOF*ep*, and pHJOF*pac* BAC DNA from *E. coli* GS1783 with SalI and PvuII and hybridized the resulting DNA-fragment to a probe specific for the S/L0 transition (Figure 31A), for pHJO sequences, or for the pBeloBAC11 vector. All obtained restriction fragment pattern of the rHJO*pac*-F⁻ genome were comparable to that of the HJO wild-type virus (Figure 31B). For example, the 3 kb SalI fragments that correlate with the repair of the genomic S/L0 transition and the 1.6 kb or 1.4 kb SalI fragments that correspond to free L0 and S termini of linearized VZV genomes were specifically detected with the S/L0 probe in the DNA of rHJO*pac*-F⁻, whereas not in pHJOF*pac* BAC DNA (Figure 31B). Moreover, pBeloBAC11 sequences were only detected in the RFLP pattern of the digested BAC DNAs and not in the virus DNA (Figure 31B). These results demonstrated that rHJO*pac*-F⁻ generated from pHJOF*pac* exhibited genome properties that were indistinguishable to that of the wild-type HJO virus. These result also confirmed that the mini-F sequences were efficiently released from the HJO genomic termini by intrinsic mechanisms during the VZV DNA replication upon virus reconstitution in eukaryotic cells and not during the F-factor mediated replication in *E. coli* GS1783 cells (Figures 28 and 29). In overall conclusion, the HJO genome organization was preserved during the entire BAC cloning and mini-F vector transposition procedure in *E. coli* and upon virus reconstitution from the pHJOF*pac* construct in eukaryotic cells.

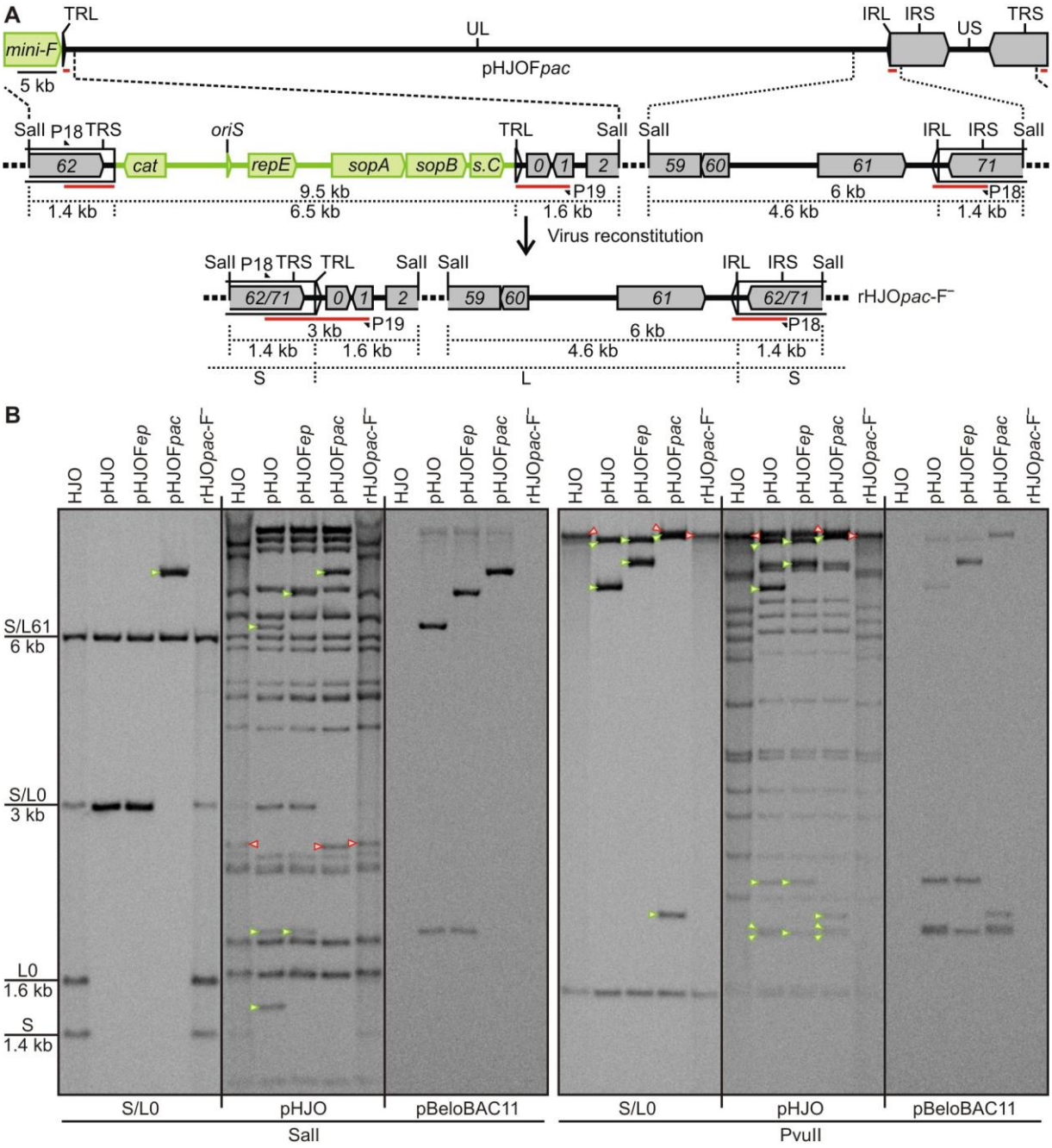

Figure 31. Southern-blot analysis of pHJOF*pac*-derived progeny rHJO*pac*-F⁻. A) Scheme of both S/L transitional SalI fragments of pHJOF*pac* and rHJO*pac*-F⁻. Upon virus reconstitution from pHJOF*pac*, the pBeloBAC11 sequences (green) were released from the viral genome, resulting in the vector-free progeny rHJO*pac*-F⁻ with restored terminal S/L0 junction. Fragment lengths and the distances from the SalI sites to the S/L junctions as well as indicators for L and S component sequences are given (dotted lines). Also the binding sites of the probe (red bars) used for Southern-blot analysis of the S/L0 transition are indicated. The probe was derived from PCR products generated with the primers P18 and P19. **B)** Southern-blot analysis for detection of S/L0 transitional (red bar in A), pHJO-, or pBeloBAC11-specific fragments in SalI or PvuII digested DNA from MeWo cells infected with HJO or rHJO*pac*-F⁻, or in digested pHJO, pHJOF*ep*, or pHJOF*pac* BAC DNA. The 3 kb and 6 kb Sal fragments that correlate to the genomic S/L61 or S/L0 transition, and the 1.6 kb and 1.4 kb Sal fragments that correspond to free L0 and S termini in viral DNA as given in A are marked. Also the fragments comprising the unique AvrII site of the VZV US region or pBeloBAC11 sequences are indicated (red or green arrows).

4.4.7 Wild-type virus-like replication kinetics after vector release from the DNA termini

Finally, to exclude any detrimental effects on the viral propagation after release of the vector sequences from the DNA ends, I investigated the replication kinetics of the vector-free pHJOF*pac*-derived progeny rHJO*pac*-F⁻. Therefore, in parallel and quantitatively synchronized experiments, I inoculated MeWo cells with cell-associated HJO wild-type virus or rHJO*pac*-F⁻, and determined by titration the amount of plaque forming units (PFU) generated at 1-5 days post infection (d.p.i.). The obtained growth curves of rHJO*pac*-F⁻ were comparable to that of the wild-type virus HJO (Figure 32). These results revealed that pHJOF*pac* allowed the rapid generation of recombinant progeny that exhibited indistinguishable replication kinetics to that of the wild-type virus.

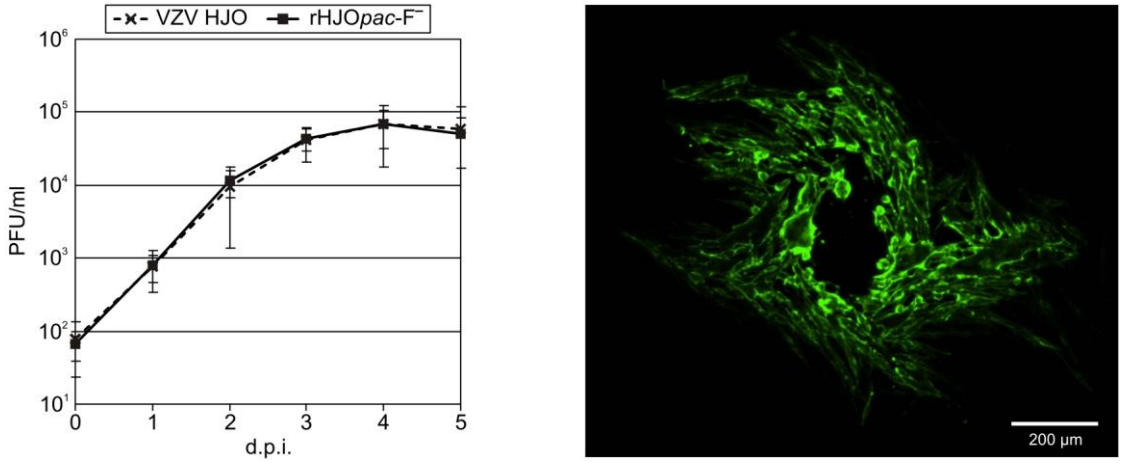

Figure 32. Growth kinetics of rHJO*pac*-F⁻. Multistep growth kinetics of recombinant rHJO*pac*-F⁻ in comparison to wild-type HJO upon propagation in MeWo cells. The plaque forming units per ml (PFU/ml) generated 1-5 days post infection (d.p.i.) are indicated. Means and standard deviations of two independent experiments are depicted. A picture of a virus plaque is shown on the right after staining by immunofluorescence for VZV glycoprotein I 3 d.p.i. of subconfluent MeWo cells with the titrated inoculum.

5. Discussion

Herpesvirus genomes engineered as infectious BACs are well-established and widely-used plasmid constructs to facilitate the generation of mutant virus progeny for functional investigations. The large viral genomes can be maintained by the low-copy mini-F replicon as a "sleeping beauty" in *E coli*, seamlessly manipulated by versatile bacterial recombination techniques and subsequently shuttled into virus-permissive cells, where consistent viral populations are reconstituted in a reliable and safe manner (Brune et al., 2000; Messerle et al., 1997; Wagner et al., 2002). However, whenever bacterial sequences are used to manipulate viral genomes, the overall effect on virus replication of introduced, foreign sequence scars, such as the mini-F cassette itself, is unpredictable. In this project, I introduced novel procedures that allow the efficient and seamless excision of the bacterial vector sequences after virus reconstitution from two independently established infectious VZV BACs. These novel techniques, in addition to the recently developed markerless Red-recombination-based mutagenesis methods in *E. coli* (Sawitzke et al., 2007; Sharan et al., 2009; Tischer et al., 2009; Tischer et al., 2006; Warming et al., 2005), resolve the last major problem for the rapid generation of mutant herpesvirus progeny without leaving behind any unwanted operational sequences in the manipulated viral genomes.

5.1 Mini-F vector self-excision by stabilized genomic duplication

In the first part of my thesis, I established a novel strategy for the seamless removal of the bacterial sequences from the BAC-cloned VZV genomes during the virus reconstitution in eukaryotic cells by homologous recombination of genomic duplications. This newly developed system applying duplicated viral sequences from both sides of the mini-F integration site between the origin of replication and the selection marker allowed the stable maintenance of the cloned herpesvirus genomes in Red-recombination-competent *E. coli*, such as GS1783 (Figure 10). These herpesvirus BACs can therefore be manipulated by virtually every mutagenesis technique that is based on Red-recombination or ET cloning.

Previous strategies to completely remove the mini-F sequences after virus reconstitution from herpesvirus BACs by homologous recombination were based on genomic duplications engineered in direct orientation at either site of the bacterial vector elements (Strive et al., 2007; Wagner et al., 1999). However, these BACs can apparently not be stably propagated in *E. coli* harbouring the temperature-inducible expression cassette for the Red recombination system on a defective λ prophage integrated into host chromosome (Lee et al., 2001). Although the

expression of the Red proteins is tightly controlled by a temperature-inducible promoter, rare recombination events of the duplicated viral sequences leading to the complete deletion of the BAC sequences can also occur in an uninduced state during the replication cycle of the bacteria. Therefore, to manipulate these BACs by Red-recombination or ET cloning, the required recombination proteins had to be temporarily provided on an additionally introduced plasmid, which also had to be easily curable from the bacteria after the mutagenesis procedure (Strive et al., 2007; Wagner et al., 1999). However, recombineering by expressing the Red functions from a plasmid appears to be 50 to 100-fold less efficient than the λ prophage system (Lee et al., 2001; Muyrers et al., 1999; Narayanan et al., 1999; Yu et al., 2000). In addition, the temperature-controlled expression of the Red proteins from the plasmid confers a higher leakiness than the expression of the recombination functions from the λ prophage system, leading to higher instability rates of the BACs during the manipulation process. Another problem during the Red manipulation procedure using plasmids is formed by the fact, that they are frequently lost from the bacteria, which can entail the complete failure of the intended recombination. Moreover, the steady selection for the expression plasmid or their incompatibility with other plasmids limits their use for specific recombineering strategies (Lee et al., 2001; Yu et al., 2000; Zhang et al., 1998).

All these limitations appear not to be valid for the novel duplication-mediated self-excision system, since this strategy tolerates rare recombination events induced by the λ prophage system during the replication cycle of the *E. coli*. Even 3 kb genomic duplications of 1.5 kb viral sequences adjoining the mini-F integration site that contained sequences of the large S repeats did not provoke any detectable instability on the propagation of the VZV BACs in *E. coli* GS1783 (Figures 16 and 17). Consequently, this novel self-excision strategy can presumably be applied in general for established infectious herpesvirus BACs independently of the organization and the complexity of the cloned viral genome. In addition, using the universal transfer plasmid pBelo*MCS*-in-Belo, respective genomic duplications can be easily engineered within the vector sequences of all herpesvirus BACs that have been constructed by usage of the pBeloBAC11 mini-F sequences (Figure 11) (Tischer et al., 2007).

Dependent on the mini-F vector integration site within the cloned VZV genomes and the orientation of the genomic duplication within the vector, the novel self-excision strategy allowed the efficient release of the BAC sequences during four virus passages, as demonstrated for the pP-Oka-DX construct (Figures 12 and 14). However, even 3 kb genomic duplications of 1.5 kb regions adjoining the vector integration site did not provide the efficient elimination

of the mini-F sequences from the VZV US unique AvrII site of the BAC-cloned HJO genome, independently of the orientation of the duplication (Figures 12, 14, 16, and 17).

For the previous vector self-excision system, it was demonstrated that 0.5 kb genomic duplications flanking the bacterial vector elements in direct orientation on both sides, can efficiently induce the elimination of the vector sequences after the virus reconstitution from an infectious cytomegalovirus BAC in also four virus passages, only (Wagner et al., 1999). In addition, it had been shown for a canine herpesvirus BAC that 2.7 kb direct genomic duplications flanking the vector insertion site can induce the complete removal from the viral progeny during one round of replication (Strive et al., 2007). Therefore, the previous duplication-mediated vector self-excision system appeared to be more efficient than the newly established one.

However, the slow replication kinetics and the highly cell-associated growth of VZV allows the polyclonal propagation of virus particles within the same infected cell and from cell to cell in culture, which could significantly impair the separation of non-repaired genomes and vector-free genomes and, thus, the elimination of the BAC sequences from the reconstituted VZV populations. In addition, the relatively small herpesvirus genome of VZV may better tolerate the large mini-F cassette due to less limited packaging constraints in comparison for example to the large cytomegalovirus genome (Wagner et al., 1999). It might therefore be possible that the novel self-excision system is much more efficient for BACs of cell-free viruses, faster replicating viruses, or viruses with larger genomes. To compare the efficacies of the novel duplication-mediated vector self-excision system with the previous one, these systems had to be applied for the same herpesvirus BAC using identically sized duplicated sequences and tested in parallel and synchronized experiments *in vitro*. Even though the developed novel duplication-mediated vector-removal strategy can be easily applied to virtually every established herpesvirus BAC using the appropriate transfer plasmids, its efficacy has to be determined specifically for each of these engineered infectious clones separately, since it obviously depends heavily on the BAC vector integration site within the viral genome. However, this is presumably due for every other deletion strategy that is based on homologous recombination of engineered genomic duplications.

Although larger forward or reverse genomic duplications were engineered within the vector elements of pHJO (Figures 12 and 16), the BAC sequences of pP-Oka were much more efficiently released by a corresponding reverse genomic duplication during the replication of the reconstituted progeny than in the HJO system (Figure 14). The main difference between these two BACs is the position of the bacterial mini-F replicon. In pP-Oka, the mini-F

element is located within the S repeats in approximately 200 bp distance from the US region, whereas that of pHJO is situated in the US region (Figure 9). Regarding the self-repair potential of the S repeats during VZV DNA replication (Sato et al., 2003), it might therefore be possible after virus recovery that the vector sequences are also released from pP-Oka in significant portions *per se* from the viral DNA even without the addition of a genomic duplication, and, thus, explain the rapid vector elimination after virus reconstitution from pP-Oka-DX (Figures 12 and 14).

It can also be assumed that regions of the S repeats promote homologous recombination more efficiently due to their high GC content, and the greater the GC content is within the genomic duplication, the more efficiently the vector sequences are released. However, these assumptions cannot explain why the removal of the resistance gene *cat* from the unique AvrII site of the US region after virus reconstitution from the corresponding pHJO-DX variants appeared to be significantly impaired in contrast to that of the *sopA* element (Figure 14). Since the vector resistance gene within the pHJO-DX variants is flanked by the duplicated S repeat sequences, but not the mini-F replicon, the *cat* sequences should be eliminated from the virus populations, in theory, with higher efficacy than the *sopA* sequences (Figure 12). Perhaps the duplicated sequences of the S repeats within the different pHJO variants mediate frequent inversion events of recombination that did not promote the vector excision and that also did not have a detrimental effect on the viral replication (Figure 12).

This in turn does not explain why a reversely inserted duplication in comparison to directly oriented duplication within the BAC vector elements seemed to support the vector excision more efficiently after virus recovery from the different pHJO-DX constructs (Figures 12 and 14). Regarding the required recombination events (Figure 10), the independent excision of the mini-F replicon and the resistance gene can be expected to be rather promoted by a directly inserted duplication than by a reversely introduced duplicated sequence within the BAC vector of pHJO (Figure 12). Therefore, it is surprising that the two vector parts separated by the genomic duplication were apparently non-detectable at different time points after virus reconstitution from pHJO-DX, whereas not from pHJO-DXfw (Figure 14). However, which parallel and/or antiparallel intra- and/or intermolecular recombination events eventually mediate the vector excision during the complex herpesvirus replication processes is difficult to determine, especially when regarding the duplicated S repeats, which are then present as triplicates, totally (Figure 12). Nevertheless, a directly or reversely inserted duplication within the vector of an established VZV BAC can promote the seamless release of bacterial sequences, providing the reconstitution of VZV mutants with vector-free genomes. Plaque purifica-

tion of virus progeny can be one option to enhance the vector removal from the viral DNA. However, this approach can be associated with the separation of illegitimately recombined genomes and, thus, entails laborious investigation experiments, which would render the pHJO-DX variants inappropriate for rapid mutant generation.

In conclusion, pP-Oka-DX appeared to be a valuable tool to rapidly generate P-Oka mutant progeny without vector remainders and with correct genome structure (Figures 14 and 15). The pP-Oka-DX construct might be a valuable tool to precisely define the nucleotide variations that are responsible for the phenotype of the vaccine strain V-Oka, and, therefore, facilitate the development of a second generation strategy for varicella and zoster prevention.

5.2 Duplication-mediated mini-F vector self-excision from essential genes

In order to significantly enhance the duplication-mediated vector self-excision, I engineered variants of the original pHJO BAC comprising self-excisable mini-F elements with corresponding inverse genomic duplications in genes putatively essential for the virus propagation *in vitro* (Figure 22). To achieve this aim, I established a novel synchronous Red-mediated mini-F vector insertion and excision reaction which allowed the rapid, targeted, and seamless restructuring of the BAC-cloned herpesvirus genome in *E. coli* (Figure 20). Since the mini-F vector transposition reaction is target-sequence independent and based on Red-recombination, it appears to enable the rapid generation of virtually every rearranged variant of a BAC in *E. coli* under perfect preservation of the integrity of the cloned DNA. In the context of the recently introduced highly versatile and markerless recombineering techniques (Sawitzke et al., 2007; Sharan et al., 2009; Tischer et al., 2009; Tischer et al., 2006; Warming et al., 2005), this novel mini-F vector transposition reaction eliminates the last hurdle to rapidly perform any kinds of imaginable targeted seamless BAC modifications in *E. coli*. The mini-F transposition reaction can be therefore generally a valuable tool to optimize, reorganize, or repair other established BACs as well, which may have an immediate impact on the development of gene therapy or vaccine vectors (Adler et al., 2003; Brune et al., 2000; McGregor and Schleiss, 2001; Sparwasser and Eberl, 2007; Wagner et al., 2002). In addition, this may be also useful to facilitate the generation and optimization of specific targeting vectors for mutant animals, such as conditional knock-out mice (Copeland et al., 2001; Ristevski, 2005; Shizuya and Kouros-Mehr, 2001; Yang and Gong, 2005).

The essential features of the two-step *en passant* mutagenesis (Tischer et al., 2009; Tischer et al., 2006) allowed the targeted insertion of a second mini-F vector into the putative essential

gene and the markerless removal of the pre-existing mini-F vector of the viral genome via two simultaneously induced Red recombinations combined with an intermediary I-SceI-induced double-strand break (Figure 20). However, it is not clear when actually the second mini-F vector recombines with the cloned VZV genome and when the present vector is excised from the viral DNA. Eventually, it can also be surmised that the replication of intermediate molecules with two mini-F replicons is completely suppressed in *E. coli*, regarding that maximally two BAC copies can exist per bacterial cell (Shizuya et al., 1992; Shizuya and Kouros-Mehr, 2001). However, the existence of non-replicating intermediates with two mini-F units seemed to be unlikely, since replication forks for sites of homologous recombination would not be originated and, consequently, there would be no potential for the excision of the present mini-F vector. Alternatively, it might be possible that the insertion and excision events of the pBeloBAC11 sequences are conducted in parallel during the second Red recombination of the transposition reaction after inducing a double-strand break at the pre-existing vector (Figure 20). A stable maintenance of putative intermediates with two F-factor replicons can neither be confirmed nor excluded, since recombinants after insertion of the second mini-F vector via the first Red recombination of the transposition reaction were not further investigated. However, the versatility and efficiency of the developed transposition technique was finally proved by shifting the mini-F vector into different unique and repeated regions distributed over a cloned herpesvirus genome, finally resulting in six rearranged and infectious BAC variants (Figures 22 and 26).

The observation that viral progenies were reconstituted from pHJOF22-DX and pHJOF54-DX after further passaging the transfected cells and not from the BACs pHJOF22 and pHJOF54, indicates that the vector insertion into *ORF22* or *ORF54* completely abrogated virus replication and that this highly detrimental effect was neutralized after a short decay upon repair of the gene by homologous recombination of the genomic duplication (Figures 22 and 24). Consequently, the VZV large tegument protein and the capsid portal protein encoded by *ORF22* or *ORF54* might be indeed essential for the virus replication *in vitro*, which corresponds to their HSV-1 and PRV homologs. The absence of the large tegument protein of HSV-1 and PRV results in accumulation of DNA-filled non-enveloped capsids in the cytoplasm and the nucleus; these capsids appear unable to traffic to the site of secondary envelopment and to acquire tegument (Desai, 2000; Fuchs et al., 2004; Luxton et al., 2006). In addition, the VZV *ORF54* homolog of HSV-1 forms a portal for entry of DNA into preformed capsids and is dispensable for the capsid assembly, but essential for the genome maturation and packaging process (Lamberti and Weller, 1996; Newcomb et al., 2001; Patel et al., 1996). In analogy to

these findings, it can be surmised that the viral particles reconstituted from pHJOF22-DX and pHJOF54-DX BAC DNA are only enveloped and tegumented, or filled with genomes after repair of the disrupted ORF by the recombination of the genomic duplications, and the infectivity can spread form cell to cell. The delayed virus reconstitution from pHJOF22-DX or pHJOF54-DX may then correspond to the time period required for the recombination events of the vector self-excision to restore *ORF22* or *ORF54*. However, despite of the evident complete disruption of *ORF22* or *ORF54*, it was interesting that remaining pBelo-BAC11 sequences were detected in three further passages after virus reconstitution from pHJOF22-DX and pHJOF54-DX (Figure 24). This phenomenon may be explained by the highly cell-associated growth of VZV, which may cause an intimate polyclonal virus spread from cell to cell and, thus, allow the propagation of remaining pBeloBAC11 sequences upon *trans*-complementation (Grose et al., 1979; Harson and Grose, 1995; Weller, 1953).

The result that virus was reconstituted from pHJOF50-DX and that small CPEs were detected also in cultures transfected with pHJOF50 indicated that the vector insertion into *ORF50* is only slightly detrimental for the virus propagation and that the gene repair by homologous recombination is required for efficient replication of the virus. This conclusion corresponds to a recently introduced detailed study that VZV gM encoded by *ORF50* is important for efficient virus cell-to-cell spread in culture, but not essential for virus growth *in vitro* (Yamagishi et al., 2008). Although the vector insertion into *ORF50* is apparently not completely abrogating virus propagation, it was conflictive that the virus reconstitution from pHJOF50-DX was only detected after one further cell passage of the transfetced MeWo cells. Perhaps, the presence or an initial anti-parallel recombination event of the reverse duplication had an additional impairing effect on the virus propagation and that a second recombination event might be required to overcome this detrimental impact on the virus replication.

In theory, just one recombination event should lead to the repair of *ORF50* or *ORF54* in pHJOF50-DX or pHJOF54-DX-derived progeny (between the duplicated fragments c or e, Figure 22), whereas two recombinations should be necessary to restore *ORF22* in virus reconstituted from pHJOF22-DX (Figure 22). With regard of this different requirement for recombination to restore the gene function, in addition to the discussed conclusions that *ORF22* and *ORF54* maybe essential for the virus propagation *in vitro*, it is surprising that the virus reconstitution from all three pHJO-DX variants was observed after one further passage of the transfected MeWo cells. It is also astonishing that an efficacy difference for the elimination of the pBeloBAC11 sequences was not detected in the three different recombinant progenies (Figure 24). More detailed, quantitative experiments would be needed to confirm these obser-

vations and to define more profoundly the recombination mechanisms matching the findings. In summary, the three BACs pHJOF22-DX, pHJOF50-DX, and pHJOF54-DX allow the efficient vector release upon virus reconstitution, but appear to be suboptimal for further mutant generation, because the virus reconstitution occurs at delayed kinetics.

5.3 Genome-intrinsic mini-F vector release

Herpesvirus BAC construction via conventional or cosmid-based strategies includes recombination during the virus propagation in eukaryotic cells and transfer of circular replication intermediates into *E. coli* (Figure 7) (Messerle et al., 1997; Tischer et al., 2007). It is therefore presumably difficult to integrate the mini-F vector into repeated regions with self-repair potential or into sites involved in the viral genome replication or maturation process. Using the novel mini-F vector transposition method, which is completely independent from virus DNA replication, I developed the first herpesvirus BACs, of which the vector sequences were efficiently released by genome-intrinsic features during the genome maturation process, thus, without the need of additional sequences, such as *loxP* sites or genomic duplications (Figure 26) (Smith and Enquist, 2000; Tischer et al., 2007; Wagner et al., 1999). This strategy to generate mutant herpesvirus progeny does not only avoid any remaining vector sequences in the viral genome, it also reduces the risk of illegitimate events of homologous recombination of the chimeric DNA during the bacterial or viral DNA replication. Finally, I identified the herpesviral terminal genomic junction as an optimal mini-F vector integration site for the construction of an infectious BAC that provides the rapid and spontaneous generation of recombinant progeny completely devoid of any bacterial vector elements (Figures 28, 30, 31, and 32). The terminal genomic junction might, therefore, be in general an optimal integration site of the mini-F sequences to construct other herpesvirus genomes or even other large linear viral DNA genomes as infectious BACs.

The efficient vector release in virus recovered from pHJOF71 or pHJOF62 may indicate that *ORF71* or *ORF62* of the large S repeats was seamlessly repaired by inherent homologous recombination events during the viral DNA replication (Figures 26 and 28). This may support the previous detailed investigation of cosmid vector-generated VZV mutants that the single deletion of the S-repeated *ORF62*/*71* encoding the major immediate early-transactivator IE62 results in rapid repair of the disrupted region by recombination with the intact repeat (Sato et al., 2003). In addition, the observation that the vector sequences in viral progeny reconstituted from pHJOF62 were more rapidly released than in virus derived from pHJOF71, may

correspond to the former results that the *ORF62/71* within the TRS regions can be more rapidly repaired than in the IRS region (Figure 28) (Sato et al., 2003). For this conclusion, it should be considered that the US region of the pHJO clones occurs in inverse orientation with respect to the UL segment regarding the defined VZV prototype arrangement (Figures 4 and 9). However, to clearly confirm the repair of both repeats after virus reconstitution from pHJOF71 or pHJOF62, the viral genomes had to be analyzed in detail, for instance by Southern-blot hybridization. In addition, the seamless repair of the genomic sequence at the former mini-F vector insertion site within the *ORF62/71* must be confirmed in both S repeats, to exclude any minor illegitimate homologous recombination events.

The observation that the mini-F sequences in progeny reconstituted from pHJOF*pac* were much more efficiently released in comparison to that of all other generated recombinant viruses may support the proposal that the vector sequences can be actively excised by a terminase complex from the genomic termini (Figures 26 and 28). This conclusion would then greatly support the general assumption that the formation of the herpesvirus genomic termini is to some degree governed independently from the two packaging signals (Hodge and Stow, 2001; McVoy et al., 2000; Schynts et al., 2003; Umene, 1999; Varmuza and Smiley, 1985; Wang et al., 2008). However, besides such an active cleavage mechanism, the mini-F vector excision from the genomic terminal S/L0 junction may also be achieved by highly frequent homologous recombination, supported by a different double-strand break mechanism or by a high GC content (Thiry et al., 2005; Umene, 1999). Serially repetitive sequences that contain the packaging signals and that connect the S and L component at both junctions after circularization of the HSV-1 genome are considered as recombinational hot-spots, but analogous elements are not present in VZV DNA (Dutch et al., 1995; Dutch et al., 1994; Mocarski et al., 1980). The S and L repeats flanking the mini-F sequences at the disrupted S/L0 junction may recombine with the repeats at the intact S/L61 junction to release the vector sequences from the DNA of pHJOF*pac*-derived virus (Figures 29A and 31A). Both VZV repeats have a high GC content, but the L repeats are just 88 bp in length, making a highly efficient vector release by a non-induced homologous recombination process from the genomic termini rather unlikely (Davison, 1984; Davison and Scott, 1986). The maintenance of non-repaired genomes within the first two passages of progeny generated from pHJOF*pac* (Figure 28) may be explained by rare genome maturation and packaging initiated from the S/L61 junction, encapsidating non-excised mini-F vector sequences within the S/L0 transition (Figures 5 and 31A). In assumption that the vector excision is not a frequent incident during viral DNA replication, it may also be possible that the cleavage/packaging machinery prefers restored

S/L0 transitions within concatemeric DNA, actively promoting the propagation of repaired genomes via a different mechanism (Figures 5 and 31A).

In the performed experiments, I observed a genetic variability at the genomic junction upon VZV propagation in MeWo cells (Figure 30), reflecting mainly the situation in concatemeric DNA, which may correspond to the observation that VZV strains can express S/L proteins of varying length *in vitro* (Kemble et al., 2000). The slightly less pronounced variation of the GC base pairs tract directly at the S/L0 junction (Figure 30) or of the AT stretch of the *pac2* signal in DNA of rHJO*pac*-F$^-$ in comparison to HJO may be explained by its clonal origin from the BAC template. Considering that DNA of rHJO*pac*-F$^-$ shows already after two virus passages nucleotide polymorphisms at the S/L0 transition, it can be assumed that the genetic constitution of the recombinant virus is upon further propagation adapted to the situation in DNA of wild-type HJO. The fact that virus reconstitution from pHJOF*pac* was not impaired in comparison to that from original pHJO may support the previous observation that the VZV S/L protein has a non-essential function *in vitro* (Kemble et al., 2000), and/or also indicate the immediate excision of the vector elements from the genomic termini.

Although the stability of the two pHJOF62/71 variants and especially that of the pHJOF*pac* clone has been extensively confirmed by RFLP analysis, it appeared that rare mini-F excision or UL inversion within these BACs during their propagation in *E. coli* can be detected via PCR (Figures 28 and 29). Regarding the BAC arrangements of these three pHJO variants, inversion of the UL region seemed to be more likely than excision of the mini-F vector by homologous recombination of the inverted repeat elements (Figures 26, 29A and 31A). In fact, it appeared that inversion of the UL region in DNA of pHJOF*pac* can be confirmed via PCR (Figure 29). However, in context of the low-copy F-plasmid replication (Shizuya et al., 1992; Shizuya and Kouros-Mehr, 2001), inversion of the UL region by recombination of the small L repeats seemed to be unlikely in BAC DNA of pHJOF*pac*, although the small L repeats have a high GC content. In addition, neither UL inversion, nor mini-F excision was specifically detectable via RFLP analysis in pHJOF*pac* (Figures 27 and 31B) or the pHJOF62/71 variants (Figure 27), even not during further manipulation of the pHJOF*pac* clone using Red recombination (data not shown). In conclusion, the PCR products that should prove the UL inversion (Figure 29) or mini-F excision (Figure 28) in the BACs are most likely be explained by super-primer formation (“mega priming”) during PCR amplification generating false-positive signals, a phenomenon already described in a similar way for the analysis of infectious VZV cosmid clones (Figure 33) (Sato et al., 2003).

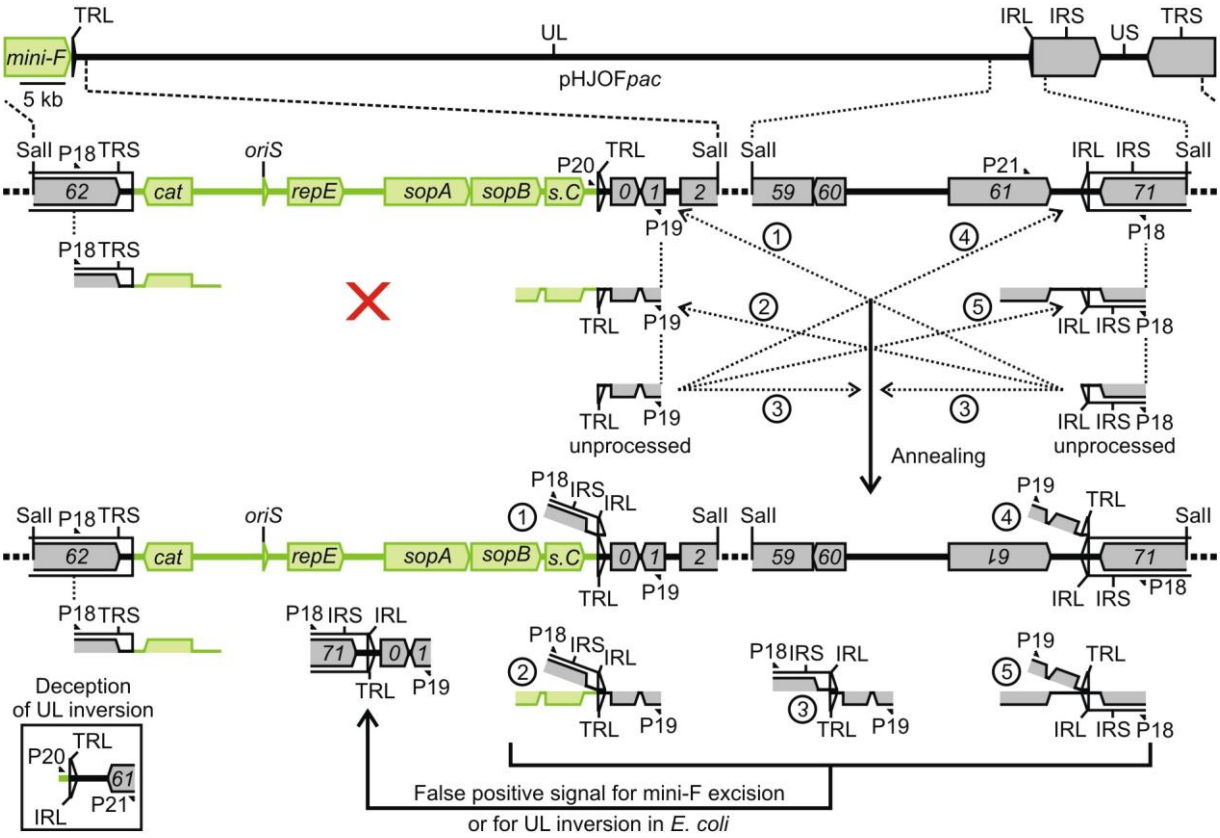

Figure 33. Mega-priming hypothesis. Schematic depiction of super primer formation during PCR amplification of pHJOF*pac* exemplified for primers P18 and P19 in a detailed overview of both S/L transitional SalI fragments. As primer P18 binds within the S repeats, its extension in a PCR adjusted for 2 kb polymerizations leads to two different oligonucleotides comprising TRS and pBeloBAC11 sequences (*cat*), or IRS, IRL, and sequences of the *ORF61* end of the UL region. Primer P19 binds reversely within the *ORF0* end of the UL region and its extension leads to the generation of oligomeres with *ORF0-1* sequences, TRL and elements of the pBeloBAC11 vector. Unprocessed oligonucleotides derived by extension of primers P18 or P19, containing reverse complementary IRL and TRL sequences at its 3'-ends, may anneal with the BAC template (dotted arrows 1 and 4), with processed amplificates (dotted arrows 2 and 5), or even with one another (dotted arrow 3) to act as super primer during PCR amplification (mega-priming). Independently of the annealing reaction, further PCR amplification leads to the generation of DNA fragments of exactly the same size and sequence of the DNA fragments resulting from possible mini-F excision or UL inversion within pHJOF*pac*. Also the PCR product that can be generated by mega-priming using the primers P20 and P21 and deceive UL inversion are shown (framed box).

Nevertheless, it may also be possible that a minor proportion of UL segments were indeed inverted, or that even the mini-F sequences were excised from the viral DNA already upon BAC propagation in *E. coli* and that these small amounts were only detectable via PCR and not by RFLP analysis. Inversion of the UL region in the two pHJOF62/71 variants should theoretically not have a detrimental effect on the virus reconstitution, since the genome organization of the viral DNA is retained after such an event (Figure 26). In addition, minor proportions of BAC-vector sequences that have lost the viral insert DNA can be neglected in transfection experiments. This is also the case for the pHJOF*pac* clone, but UL inversion during propagation of this BAC should result in the positioning of the mini-F sequences at the occasionally cleaved S/L61 junction (Figures 29 and 31A) (Davison, 1984; Ecker and Hyman,

1982; Kinchington et al., 1985), which may have an influence on the efficiency of the vector excision after virus reconstitution.

Regarding that both unique region regions can invert frequently during VZV DNA replication (Davison, 1984; Schynts et al., 2003; Slobedman and Simmons, 1997), in addition to the super-primer formation hypothesis (Figure 33) (Sato et al., 2003), it is presumably impossible to determine unambiguously via PCR in infected cells the mini-F vector excision and the repair of the interrupted repeat after virus reconstitution from the three pHJO variants (Figure 26). The obtained PCR fragments that should prove the vector excision after virus reconstitution could therefore not be accepted as the only indication for the repair of the investigated VZV region (Figure 28). In this context, only conventional Southern-blot analysis allowed the clarification of the integrity of the effected repeat region (Figure 31B).

All three engineered pHJO variants (Figure 26) could stably be propagated in *E. coli* and enable the efficient intrinsic vector excision after virus reconstitution (Figure 28), accepting them as valuable tools to generate VZV mutants without leaving behind any operational sequences. The pHJOF*pac* clone proved to be the infectious BAC which is most efficiently for the spontaneous generation of recombinant VZV that is virtually identical to HJO wild-type virus (Figures 28, 30, 31, and 32). Moreover, the versatility of pHJOF*pac* has already been proven by the generation of different vector-free GFP-fusion VZV mutants and by the development of a BAC chimera with a recombinant HJO/V-Oka VZV genome (Tanja Krater and Anne-Kathrin Brunnemann, data not shown). Thus, pHJOF*pac* is a novel and highly efficient tool for the rapid and targeted generation of VZV mutants without any secondary genome alterations. In conclusion, this BAC should facilitate the precise investigation of the nucleotide variations that might be responsible for the pain induction during herpes zoster.

6. Materials and Methods

6.1 Molecular biology techniques and bacterial strains

6.1.1 DNA preparation

For analysis and cloning procedures, plasmids and BACs were isolated from *E. coli* by alkaline lysis (Birnboim and Doly, 1979). Bacteria harbouring the constructs were grown overnight in 5 ml Luria Bertani broth (LB) medium (5 g/l yeast extract, 10 g/l tryptone, 10 g/l NaCl) with appropriate antibiotics 30 µg/ml Cm, 35 µg/ml kanamycin (Kan), and/or 100 µg/ml ampicillin (Amp) at 32°C (GS1783) or 37°C (XL-1 Blue, Stratagene, Amsterdam, The Netherlands; DH5α, Invitrogen, Karlsruhe, Germany) until the static phase was reached and then pelleted by centrifugation at 3,000 x g. The pellet was resuspended in 300 µl of solution I (50 mM Tris-hydroxymethyl-aminomethan (Tris)-HCl (pH 8.0), 10 mM ethylenediaminetetraacetic acid (EDTA), and 100 µg/ml ribonuclease A; stored at 2-8°C). For bacterial lysis, 300 µl of solution II (200 mM NaOH, 1% (w/v) sodium dodecyl sulfate (SDS)) were added to the suspension and the mixture was incubated for 4 min at room temperature. Immediately, 300 µl of solution III (3 M potassium acetate, pH 5.5) were added to the mixture and the derived solution was incubated on ice for 10 min. Cell debris and genomic DNA were sedimented by centrifugation of the mixture at 16,000 x g and the supernatant was vigorously mixed with 600 µl isopropanol. The DNA was pelleted at 16,000 x g, washed with 500 µl 70% ethanol, pelleted again, and finally resuspended in 50 µl H_2O.

BAC DNA for transfection or electroporation was prepared with the Plasmid Maxi Kit (Qiagen, Hilden, Germany) according to the manufacturer's instructions. The purified DNA was gently dissolved in 100-300 µl H_2O and stored at at 4°C.

For PCR analysis of viral DNA, approximately 1 x 10^6 infected MeWo cells were resuspended in 100 µl of lysis buffer (500 mM KCl; 100 mM Tris-HCl, pH 8.3; 15 mM $MgCl_2$; 0.01% (w/v) gelatin; 0.5% (v/v) Tween20; 0.7% (v/v) proteinase K). The suspension was incubated for 1.5-2 h at 56°C and finally for 10 min at 95°C for proteinase K inactivation.

Total DNA from MeWo cells for Southern-blot analysis was purified with the DNeasy Blood & Tissue Kit (Qiagen). Approximately 5 x 10^6 infected MeWo cells were prepared according to the manufacturer's instructions. The aqueous DNA solution was vigorously mixed with 1/10 volumes of sodium acetate (pH 5.5) and 2 volumes of 100% ethanol. The mixture was placed for 30 min at -80°C and subsequently centrifuged at 16,000 x g. Finally, the DNA pellet was washed twice with 70% ethanol, centrifuged again, and dissolved in 20 µl H_2O.

6.1.2 Polymerase chain reaction

PCR was performed with *Taq* DNA polymerase (Fermentas, St. Leon-Rot, Germany) or Phusion polymerase (New England Biolabs, Frankfurt, Germany). Usually, 100-200 ng of purified DNA or 1 µl of the MeWo cell lysate were used for PCR in 50 µl volumes. The reaction mixes were adjusted to the final concentration of 0.02 U/µl enzyme, 200 µM of each deoxynucleotide triphosphate, 0.6 µM of both primer oligonucleotides, and 2 µM $MgCl_2$ in 1 x *Taq* buffer with $(NH_4)_2SO_4$ or Phusion GC-reaction buffer when using Phusion-polymerase for the amplification of GC-rich regions; DMSO (5%) was added optionally. In reactions with *Taq* polymerase, DNA was amplified by the initial denaturation at 95°C for 10 min, 35 cycles of DNA denaturation at 95°C for 30 s, primer annealing at 50-70°C (standard at 55°C) for 30 s and primer extension at 72°C for 60 s per 1 kb, and a final extension time for 10 min at 72°C. When Phusion polymerase was used to amplify GC-rich regions, the PCR was performed by denaturation at 98°C for 30 s, 35 cycles of denaturation at 98°C for 10 s, annealing at 50-70°C for 30 s, and extension at 72°C for 15-30 s per 1 kb, and a final extension time at 98°C for 10 min.

3.1.3 Oligonucleotides

Table 1: Construction (A-X) and Detection (P1-P21) Primers

Primer	Sequence (5'- 3')	Primer	Sequence (5'- 3')
A	ACTAGTGCTTCTGCGCACAATGCCACAG	**P1**	ATTGGAAGCGACGTCGACAC
B	ACTAGTGAACGGTACTTCGCCGCCGCGC	**P2**	TGTAACGCGCGTAATACAGATCG
C	ACTAGTATAAATCTGTTCGGTAACGTGG	**P3**	TGGGGTTTCTTCTCAGGCTATC
D	ACTAGTTTAATTAAAACATACACCGGATAAAAGC	**P4**	TTAACTCAGTTTCAATACGGTGCAG
E	GACTAGTATTGGAAGCGACGTCGACAC	**P5**	TGCCACTCATCGCAGTACTG
F	GACTAGTTGTAATGGGGCGTGACTCTG	**P6**	AGGCATTTCAGTCAGTTGCTC
G	TACGCTCGAGGATCCTACTCGAGGTCA	**P7**	TGTAACGCGCGTAATACAGATCG
H	TGACCTCGAGTAGGATCCTCGAGCGTA	**P8**	ACCTACGAGAGATCCTGACACCC
I	TACGCTCGAGCATGCTACTCGAGGTC	**P9**	TCAATTTGACGGTGCCCTG
J	GACCTCGAGTAGCATGCTCGAGCGTA	**P10**	TTCACGCATATAGCGTGTCTCC
K	ACTAGTTATGTGTGCTCTTGTTGATCTCCC	**P11**	TAGCCGTAGCCTTGTGATG
L	ACTAGTAACTTGTAACGCGTATAAGTTCCG	**P12**	ACGCCCTAATGACTGGTAG
M	ACTAGTATTAACACGTGTATATAATGCGCC	**P13**	CGGTTTCGGTAATATCTCCAAC
N	ACTAGTATTGTGGGGGAGTATAATTGTCC	**P14**	CGGACATTGAGCCTGTAGG
O	ACTAGTTATCGTTCTCGCCCATTATACG	**P15**	TGGTTTCCAAGGCCAAGAG
P	ACTAGTTTTCCGCTAATTAAATAAACGGAG	**P16**	CCATCCGAGCAGTAAACGAG
Q	ATAAATACCTGTGACGGAAGATCACTTCGCAGAATAAATA	**P17**	AGGAAGTCGGGTGTATTGG
	AATCCCGATTTATTCAACAAAGCCACGT	**P18**	CTTCGACCCGTCTTCCTTCC
	TTACGTTATTATTAAATAAAACATGTAGACATTATTAATA	**P19**	AGGTGTTCGGGAATCTGATAGC
R	ATCCTAGGAACAATCAAATCCATATTTGTAAGTTATGTTT	**P20**	TGCTGCTGTGTCCTGCTTATC
	AACCCCTCCCTAGGGATAACAGGGTAATGCCAG	**P21**	TTGGCTGTTGGATGGACTC
S	GACTAGTTACACGTGATACTGAGACAAAGCG		
T	GACTAGTGGGAGGATGAGGCTGTGAGA		
U	CGCGTCGACCCTGCCGCAGAACCACTCGTGC		
V	CGCGTCGACCCTAGGGGGCCCCCCTCCCGGGGT		
W	GACTAGTGGATCCAGGGGGGCCCAGCCCTCTC		
X	GACTAGTCGTCCGCGCAACTGAAAATG		

6.1.4 Restriction enzyme digestion

Independently of the template, 0.5 U/µl conventional endonuclease (Fermentas) or 0.25 U/µl of the homing endocuclease I-CeuI (New England Biolabs) were used in corresponding 1 x buffer conditions for DNA digestion at 37°C. For analytical approaches, approximately 200 µg DNA of plasmids were cleaved in 10 µl volumes for 1-2 h, and 1 µg VZV BAC DNA or 10 µg DNA purified from VZV infected cells were incubated in 20 µl digestion solutions for 6-8 h. To prepare fragments or linearized vectors, up to 4 µg DNA were digested in 50 µl volumes for 3.5-6 h.

6.1.5 Agarose-gel electrophoresis

For RFLP analysis, length determination, and isolation of DNA fragments, the digested DNA or PCR products were separated by agarose gel-electrophoresis and visualized by ethidium-bromide staining. Usually, the aqueous DNA solutions resulting from restriction enzyme digestion or PCR were loaded with 1/10 volumes of loading dye (50% v/v glycerol, 10 mM EDTA, and 2.5 mg/ml brome phenol blue) onto 0.8-1.2% agarose gels with 0.008% (v/v) ethidium bromide, and the DNA fragments were separated for 1 h at 120 V in TBE-buffer (89 mM Tris-HCl, 2 mM EDTA, 89 mM Boric acid) and visualized under ultraviolet light using the LAS 3000 imaging system (Fuji, Tokyo, Japan). For RFLP analysis of digested VZV BAC DNA, fragments were electrophoretically separated at 30 V in 0.5-1% agarose gels with ethidium bromide for at least 16 h. For sequencing or subsequent cloning reactions, the desired DNA fragments were purified using the Nucleospin Extract Kit II (Macherey-Nagel, Düren, Germany) according to the manufacturer's instructions.

6.1.6 Nucleotide sequencing

DNA sequences were determined with the Sanger dideoxynucleotide chain termination reaction using BigDye version 1.1 (Applied Biosystems, Darmstadt, Germany). Nucleotide sequences of VZV BACs or DNA from MeWo cell lysates were determined by using 5-50 ng PCR products amplified from the region of interest and plasmid sequences were verified by using 150-300 ng DNA, to set up reactions in 10 µl volumes; plasmids were optionally linearized to facilitate sequencing of GC-rich regions. Reactions were adjusted to the final concentrations of 0.5 µM oligonucleotide, 0.5 x sequencing buffer, and 1/10 diluted BigDye v1.1. Polymerization reactions were performed by initial denaturation at 96°C for 1 min and 25 cycles of denaturation at 96°C for 10 s, annealing at 50°C for 5 s, and extension at 60°C

for 4 min. Fragments were purified, separated, and analyzed by fluorescence detection according to the manufacturer's recommendations.

6.1.7 DNA cloning

PCR fragments were either cloned directly via endonuclease recognition sites into the target vector or first via the TOPO TA Cloning Kit (Invitrogen) according to the manufacturer's instructions. For direct cloning, insert and vector DNA were mixed in a molar ratio of 3:1 (50-400 ng of dephosphorylated vector DNA) in 20 µl volumes with 0.25 U/µl T4 DNA Ligase (Fermentas) and 1 x Rapid Ligation Buffer conditions, and ligated by incubation for 5-30 min at room temperature. To generate vector chimeras, the linearized plasmid and pBeloBAC11 vector were ligated in a molar ratio of 1:1 (approximately 400 ng of dephosphorylated BAC vector) as described above. For dephosphorylation of linearized DNA (2-4 µg), pBeloBAC11 vector fragments were incubated overnight and plasmids were treated for 1 h in 50 µl volumes adjusted to 0.02 U/µl calf-intestinal alkaline phosphatase (Fermentas) and 1 x appropriate reaction buffer.

6.1.8 Transformation of bacteria

For plasmid cloning, chemically competent *E. coli* DH5α or XL-1 Blue bacteria (Invitrogen) were transformed via the heat-shock method. Portions (25 µl) of the bacteria suspension were gently mixed with 2-4 µl of the ligation reaction or 50-100 ng plasmid DNA, placed on ice for 20 min, heat-shocked for 45 s at 42°C in a water bath, immediately placed on ice and resuspended in 250 µl LB medium. Bacteria were grown for 1 h at 37°C and 10-100 µl volumes of the suspensions were streaked onto agar plates with antibiotics (30 µg/ml Cm, 35 µg/ml Kan, and/or 100 µg/ml Amp) to select for transformants by incubation at 37°C.

To clone BAC DNA, electrocompetent *E. coli* GeneHogs (Invitrogen) or GS1783 (Tischer et al., 2009) were transformed via electroporation. The non-commercial *E. coli* cells GS1783 were made competent as follows. Bacteria were grown overnight in 5 ml LB medium with antibiotics until static phase, diluted 1:20 in LB medium with antibiotics, grown until A_{600} of 0.5-0.6, placed on ice for 20 min, washed three times by centrifugation at 4,500 x g for 5 min and resuspension in 10% glycerol in H_2O, again sedimented and finally resuspended in 10% glycerol in H_2O of 1/100 volume of the original culture. A 50 µl portion of the bacteria suspension was either used immediately for electroporation or after storage at -80°C.

Then, the DNA was transformed into GS1783 or GeneHogs *E. coli* by a short electric shock. For this purpose, electrocompetent 50 µl bacteria were gently mixed with 1 µl ligation mix or 200-400 ng purified BAC DNA in H_2O, electroporated at 15 kV per cm, 25 µF, and 200 Ω, immediately placed on ice, and resuspended in 1 ml LB medium. Suspensions were grown at 37°C for 1 h when transforming GeneHogs or at 32°C for 2 h when using GS1783, and 50-200 µl volumes were streaked onto agar plates with corresponding antibiotics for transformant selection by incubation at 37°C or 32°C, respectively.

6.1.9 Southern-blot hybridization

Southern-blot hybridization was performed using the DIG High Prime DNA Labelling and Detection Starter Kit II (Roche, Mannheim, Germany). First, the digoxigenin-labelled DNA probes were generated as follows. Approximately 1-2 µg of eluted PCR fragments or sonicated BAC DNA was resuspended in 16 µl H_2O, denatured at 95°C in a water bath for 10 min, and immediately placed on ice. After denaturation, 4 µl DIG High Prime was added to the solution and labelled DNA fragments were generated overnight (16 h) by incubation of the mixture at 37°C. To stop the reaction, 2 µl 0.2 M EDTA (pH 8.0) were added and the solution was incubated for 10 min at 65°C. Subsequently, 2.5 µl of 4 M LiCl and 75 of absolute ethanol were added to the solution. The mixture was incubated for 30 min at -80°C and then centrifuged for 1 h at 16,000 x g. The DNA pellet was washed twice with 70% ethanol, sedimented again, and finally resuspended in 50 µl TE buffer (10 mM; Tris-HCl, pH 7.5; 1 mM EDTA). The probe was titrated by serially diluting the dissolved labelled DNA 1/10 until reaching 10^{-6} and 1 µl of each dilution was transferred onto a positively charged nylon membrane (Roche).

The labelled DNA was detected as follows. The probed membrane was gently shaken for 5 min in washing buffer (0.1 M maleic acid, 0.15 M NaCl; pH 7.5; 0.3% (v/v) Tween20), 45 min incubated in maleic acid buffer (0.1 M maleic acid, 0.15 M NaCl; adjusted with NaOH to pH 7.5), 30 min incubated in maleic acid buffer with 1/10,000 diluted anti-digoxigenin antibody conjugated to alkaline phosphatase (anti-digoxigenin-AP), shaken twice for 15 min in washing buffer, equilibrated for 5 min in detection buffer (0.1 M Tris-HCl, 0.1 M NaCl; pH 9.5), incubated in detection buffer with 1/100 diluted chemiluminescence substrate for alkaline phosphatase solution and finally incubated after removal of the substrate for 10 min in day light. The labelled DNA was then visualized by chemiluminescence detection using the LAS 3000 imaging system. Based on experimental experience, 5 µl of the original probe

solution was used for the following hybridization reactions if a clear signal was still visual at the 10^{-4} dilution or accordingly 10-fold volume more or less if the last clear signal was emitted from a dilution higher or lower.

Having adjusted the probe concentration, the Southern-blot hybridization was performed as follows. Approximately 1 µg BAC DNA or 10 µg total DNA from infected MeWo cells were digested and electrophoretically separated in a 1% agarose gel without ethidiumbromide as described above. To prepare the DNA for capillary transfer, the gel was irradiated for 3 min with ultraviolet light using the LAS 3000 imaging system, shaken for 30 min in H_2O and for 10 min in 0.25 N HCl (until the brome-phenol blue turned into yellow) and rinsed shortly in H_2O. Then, the DNA was blotted from the agarose gel onto a positively charged nylon membrane by upward capillary DNA transfer overnight using alkaline transfer buffer (0.4 N NaOH with 1 M NaCl). After that, the membrane was dried, irradiated for 2.5 min with ultraviolet light to cross-link the DNA and prepared for hybridization by rinsing in DIG Easy Hyb at 45°C for 30 min. The digoxigenin-labelled probe was denatured for 10 min at 95°C in a waterbath, immediately transferred in pre-warmed 10 ml DIG Easy Hyb onto the membrane and hybridized to the blotted DNA fragments overnight by 45°C. For hybrid detection, the membrane was rinsed 2 x 10 min in 2 x SSC buffer (0.3 NaCl, 30 mM sodium citrate, pH 7.0) with 0.1% SDS at room temperature, washed 2 x 15 min in 0.1 x SSC with 0.1% SDS at 68°C and further treated for chemiluminescence visualization as described above for estimating the probe concentration.

3.1.10 *En passant* mutagenesis

Red-recombination-based *en passant* mutagenesis was performed as described before (Lee et al., 2001; Tischer et al., 2009; Tischer et al., 2006). Primers that provide sequences for homologous recombination were purified by polyacrylamide gel electrophoresis (Biomers, Ulm, Germany). Reactions were applied in *E. coli* GS1783, since they harbour an expression cassette for the phage λ Red proteins under a temperature-inducible promoter and an L-(+)-arabinose-inducible *I-sceI* gene on a defective prophage integrated into the host genome (Tischer et al., 2009).

To insert a genomic duplication into the mini-F vector of the VZV BAC (pP-Oka, pHJO or the pHJO variants; Figure 12 and 22), the *en passant* protocol was accomplished as follows. First, the duplication was introduced into the VZV BAC via the transfer construct (Figure 11 and 21) by Red recombination (Figure 12). Therefore, *E. coli* GS1783 harboring the VZV

BAC were grown in LB with 30 µg/ml Cm overnight until static phase was reached, then 1/20 diluted in LB with 30 µg/ml Cm and grown to A_{600} of 0.5 to 0.6. Then, the bacteria were shaken in a 42°C water bath for 15 min to induce the *Red*-genes and immediately chilled on ice for 20 min. Afterwards, the bacteria were washed three times by centrifugation at 4,500 x g for 5 min at 0°C and resuspension in 10% glycerol, sedimented again and finally resuspended in 1/100 volume 10% glycerol of the original culture. Bacteria suspensions were adjusted to 50 µl portions, which were either used directly for the recombination reaction or after storage at -80°C. Then, a 50 µl portion of the electro- and recombination competent GS1783 was mixed with 100-300 ng of the *en passant* construct, electroporated at 15 kV/cm, 25 µF, and 200 Ω and resuspended in 1 ml pre-warmed LB without antibiotics. Bacteria were grown for 2 h at 32°C and streaked out in 50-200 µl volumes onto agar plates containing 35 µg/ml Kan and 30 µg/ml Cm to select for recombinants with both resistance markers by incubation at 32°C.

Having confirmed the correct insertion BAC mutants, the *en passant* reaction for the excision of the introduced selection marker was conducted by an I-SceI double-strand break-mediated second Red recombination (Figure 12). Bacteria clones from a fresh colony or 100 µl from a static phase overnight LB culture with 30 µg/ml Cm and 35 µg/ml Kan were transferred into 2 ml LB with 30 µg/ml Cm and grown for 4 h at 32°C. Then, 2 ml LB with 30 µg/ml Cm and 1% arabinose was added for *I-sceI* expression and the bacteria suspension was grown for 1 h at 32°C, incubated at 42°C in a shaken water bath for 30 min to express the Red proteins. Afterwards, the bacteria were grown at 32°C for 4 h and finally streaked out in 1-50 µl volumes on agar plates with 30 µg/ml Cm and 1% arabinose to favor the growth of clones with excised I-SceI site at 32°C.

For the BAC vector transposition reaction (Figure 20), a novel *en passant*-based protocol was developed as follows. First, the vector resistance gene *cat* of the pHJO clone was substituted by the kanamycin resistance gene *aphAI*, an I-SceI site, and the 50 bp duplication of viral sequences by Red recombination using the prepared PCR construct as described above (see also Figure 20), but bacteria clones harboring recombinants (pHJOF*ep*, Figure 20) were selected on agar plates with 35 µl/ml Kan, only.

The vector insertion and excision reaction of the transposition procedure was performed via the following novel protocol, which includes two immediately following events of Red recombination and an I-SceI induced double-strand break (Figure 20). Therefore, *E. coli* GS1783 harboring pHJOF*ep* (Figure 20) were prepared for Red recombination as outlined,

except that the used LB cultures contained 35 µg/ml Kan. Electro- and recombination-competent bacteria (50 µl portions) were mixed with 100-300 ng of the mini-F transfer construct, electroporated with 15 kV per cm, 25 µF, and 200 Ω, resuspended in 1 ml LB without antibiotics and grown for 2 h at 32°C as usual. Then, the excision of the previous mini-F vector was promoted immediately. Therefore, 1 ml of pre-warmed (32°C) LB with 60 µg/ml Cm and 1% arabinose was added to the *E. coli* culture to induce the expression of *I-sceI* and to enable simultaneously the maintenance of recombinants with the newly inserted mini-F vector. Subsequently, bacteria were grown for 1 h at 32°C, incubated at 42°C for 30 min in a waterbath shaker to express the Red-proteins again to enable the recombination of the short 50 bp genomic duplication flanking the BAC vector (Figure 20), grown for further 2 h at 32°C and 50-200 µl volumes of the suspension were finally streaked onto agar plates with 30 µg/ml Cm and 1% arabinose to select clones harboring recombinant DNA with novel mini-F sequences by incubation at 32°C.

6.2 Cell biology techniques and virus culture

6.2.1 Virus and cell culture

VZV-permissive melanoma cells (MeWo cells) were cultivated in *Dulbecco's Modified Eagle Essential Medium* (DMEM; PAA, Cölbe, Germany) with 10% fetal bovine serum (FBS; PAA) and 1x penicillin/streptomycin (PAA) (D10 medium), at 37°C, 90% relative humidity, and 5% CO_2, and splitted in a ratio of 1:4 to 1:5 when grown to confluent monolayers in 6-8 day periods. Viruses were propagated in cultivated MeWo cells and passaged by cocultivation of infected cells in different ratios with 1:4 diluted uninfected cells of confluent monolayers to yield cultures with CPEs of 70-80% after 6-8 days. Infected cells of the different virus passages for PCR or Southern-blot analysis were harvested by trypsinization or scraping, respectively, resuspended in phosphate-buffered saline (PBS), sedimented at 350 x g and prepared as described above.

6.2.2 Virus reconstitution

Reconstitution of viruses was enabled by the transfection of MeWo cells with BAC DNA using Lipofectamine2000 (Invitrogen) according to the manufacturer's instructions. Transfection was performed in 6 well format with 4 µg of affinity chromatography purified BAC DNA. DNA-lipofectamine complexes were added to the cells in DMEM without L-glutamine.

Transfection medium was replaced after 24 h with D10 medium. The following day, cells from three wells were collected and dispersed onto a 6-fold larger culture area.

6.2.3 Immunofluorescence

VZV-infected cells (in 24-well format) were detected by indirect immunofluorescence staining. After medium removal, the cells were fixed for 20 min using 2% paraformaldehyde in PBS, permeabilized with 1% saponin in PBS for 5 min and blocked for 1 h with 10% FBS in PBS at RT. Following that, cells were incubated for 1 h in 100 µl PBS with 10% FBS, 0.02% sodium azide, and 1/500 diluted VZV-specific primary antibody (mouse monoclonal anti-VZV glycoprotein I, anti-VZV gI, Millipore, Schwalbach, Deutschland) and incubated for 1 h in 100 µl of PBS with 10% FBS and 1/1000 diluted fluorescent coupled secondary antibody (Alexa 488-conjugated goat anti-mouse, Invitrogen). The cells were rinsed three times with PBS following each step. Fluorescence was visualized using the inverse microscope OLYMPUS IX81 (Olympus, Tokyo, Japan).

6.2.4 Multi-step growth kinetics

Growth curves of recombinant rHJO*pac*-F^{-} in comparison to wild-type virus HJO were generated by titration of the amount of infectious progeny generated at defined time points after inoculating the same number of cells with equal quantity of plaque forming units (PFU). Since VZV replicates highly cell-associated, usually whole cells are used for PFU determination, whereby high standard deviations are common. First, inoculi were adjusted to 100 PFU of cell-associated virus. Therefore, MeWo cells (from cultures with ~70 to 80% CPE) infected with wild-type virus or the mutant virus were trypsinized, resuspended in D10 medium, pelleted at 350 x g, washed in PBS, and finally vigorously resuspended in FBS with 10% DMSO. At minimum, 10 x 1 ml portions were frozen at -80°C and kept there for at least 2 days. A portion of each virus type was titrated in quadruplicate by generating accurately mixed serially 1/10 dilutions adjusted in D10 medium to 1 ml volumes, and 100 µl of each derived dilution was added to 2 x 10^5 MeWo cells seeded one day before in 24-well formats. After three days of cultivation, plaques were counted by indirect immune fluorescence staining using anti-VZV gI primary antibody and Alexa 488-conjugated secondary antibody. Titers from three portions of each virus-type were determined to calculate the PFU per ml for the whole frozen virus charge by the geometric median in total of 3 x 4 counts.

Having elucidated the titers, the growth kinetics of the recombinant virus was analyzed in direct comparison to the wild-type virus. Therefore, one frozen portion of every virus type was used to accomplish six parallel inoculations using 100 PFU of cell-associated virus to infect 1 x 10^6 MeWo cells, which have been seeded 24 h before in 6-well formats. Virus concentration of the used frozen portion was confirmed by adjusting four times 100 PFU with D10 medium to 1 ml volumes, which were then titrated as described above to calculate the actual amount of PFU for the used inoculum volumina. At days 1-5, infected cells of each well were washed gently with PBS, dispersed with 1 ml trypsin and resuspended in additional 9 ml D10 medium, and 4 x 1 ml of the resulting 10 ml cell suspension were used for titer determination as outlined above. Three portions of each virus were used to generate a growth curve. In total, the average amount of PFU yielded at the defined time-points after inoculation was determined by 3 x 4 counts per day. The entire experiment was repeated using different charges of the same virus type and the final growth curve was averaged by 24 (2 x 3 x 4) counts for each day.

7. References

Adler, H., Messerle, M., Koszinowski, U.H., 2001. Virus reconstituted from infectious bacterial artificial chromosome (BAC)-cloned murine gammaherpesvirus 68 acquires wild-type properties in vivo only after excision of BAC vector sequences. J. Virol. 75, 5692-5696.

Adler, H., Messerle, M., Koszinowski, U.H., 2003. Cloning of herpesviral genomes as bacterial artificial chromosomes. Rev. Med. Virol. 13, 111-121.

Almazan, F., DeDiego, M.L., Galan, C., Escors, D., Alvarez, E., Ortego, J., Sola, I., Zuniga, S., Alonso, S., Moreno, J.L., Nogales, A., Capiscol, C., Enjuanes, L., 2006. Construction of a severe acute respiratory syndrome coronavirus infectious cDNA clone and a replicon to study coronavirus RNA synthesis. J. Virol. 80, 10900-10906.

Almazan, F., Gonzalez, J.M., Penzes, Z., Izeta, A., Calvo, E., Plana-Duran, J., Enjuanes, L., 2000. Engineering the largest RNA virus genome as an infectious bacterial artificial chromosome. Proc. Natl. Acad. Sci. U S A 97, 5516-5521.

Almeida, J.D., Howatson, A.F., Williams, M.G., 1962. Morphology of varicella (chicken pox) virus. Virology 16, 353-355.

Annunziato, P.W., Lungu, O., Panagiotidis, C., Zhang, J.H., Silvers, D.N., Gershon, A.A., Silverstein, S.J., 2000. Varicella-zoster virus proteins in skin lesions: implications for a novel role of ORF29p in chickenpox. J. Virol. 74, 2005-2010.

Baines, J.D., Roizman, B., 1993. The UL10 gene of herpes simplex virus 1 encodes a novel viral glycoprotein, gM, which is present in the virion and in the plasma membrane of infected cells. J. Virol. 67, 1441-1452.

Batterson, W., Furlong, D., Roizman, B., 1983. Molecular genetics of herpes simplex virus. VIII. further characterization of a temperature-sensitive mutant defective in release of viral DNA and in other stages of the viral reproductive cycle. J. Virol. 45, 397-407.

Ben-Porat, T., Tokazewski, S.A., 1977. Replication of herpesvirus DNA. II. Sedimentation characteristics of newly synthesized DNA. Virology 79, 292-301.

Birnboim, H.C., Doly, J., 1979. A rapid alkaline extraction procedure for screening recombinant plasmid DNA. Nucleic Acids Res. 7, 1513-1523.

Boehmer, P.E., Lehman, I.R., 1997. Herpes simplex virus DNA replication. Annu. Rev. Biochem. 66, 347-384.

Boehmer, P.E., Nimonkar, A.V., 2003. Herpes virus replication. IUBMB. Life 55, 13-22.

Boehmer, P.E., Villani, G., 2003. Herpes simplex virus type-1: a model for genome transactions. Prog. Nucleic Acid Res. Mol. Biol. 75, 139-171.

Borst, E.M., Hahn, G., Koszinowski, U.H., Messerle, M., 1999. Cloning of the human cytomegalovirus (HCMV) genome as an infectious bacterial artificial chromosome in Escherichia coli: a new approach for construction of HCMV mutants. J. Virol. 73, 8320-8329.

Browne, H., Bell, S., Minson, T., 2004. Analysis of the requirement for glycoprotein M in herpes simplex virus type 1 morphogenesis. J. Virol. 78, 1039-1041.

Brune, W., Messerle, M., Koszinowski, U.H., 2000. Forward with BACs: new tools for herpesvirus genomics. Trends Genet. 16, 254-259.

Carpenter, J.E., Henderson, E.P., Grose, C., 2009. Enumeration of an extremely high particle-to-PFU ratio for Varicella-zoster virus. J. Virol. 83, 6917-6921.

Carter, D.M., Radding, C.M., 1971. The role of exonuclease and beta protein of phage lambda in genetic recombination. II. Substrate specificity and the mode of action of lambda exonuclease. J. Biol. Chem. 246, 2502-2512.

Caunt, A.E., Taylor-Robinson, D., 1964. Cell-free varicella-zoster virus in tissue culture. J. Hyg. (Lond) 62, 413-424.

Chang, W.L., Barry, P.A., 2003. Cloning of the full-length rhesus cytomegalovirus genome as an infectious and self-excisable bacterial artificial chromosome for analysis of viral pathogenesis. J. Virol. 77, 5073-5083.

Chen, J.J., Zhu, Z., Gershon, A.A., Gershon, M.D., 2004. Mannose 6-phosphate receptor dependence of varicella zoster virus infection in vitro and in the epidermis during varicella and zoster. Cell 119, 915-926.

Cohen, J.I., Seidel, K.E., 1993. Generation of varicella-zoster virus (VZV) and viral mutants from cosmid DNAs: VZV thymidylate synthetase is not essential for replication in vitro. Proc. Natl. Acad. Sci. U S A 90, 7376-7380.

Cohen, J.I., Straus, S.E., Arvin, A.M., 2007. Varicella-Zoster virus replication, pathogenesis, and management. In: Fields, B., Virology. Fifth Edition, pp. 2773-2818.

Cook, M.L., Stevens, J.G., 1968. Labile coat: reason for noninfectious cell-free varicella-zoster virus in culture. J. Virol. 2, 1458-1464.

Copeland, N.G., Jenkins, N.A., Court DL, 2001. Recombineering: a powerful new tool for mouse functional genomics. Nat. Rev. Genet. 2, 769-779.

Cottingham, M.G., Andersen, R.F., Spencer, A.J., Saurya, S., Furze, J., Hill, A.V., Gilbert, S.C., 2008. Recombination-mediated genetic engineering of a bacterial artificial chromosome clone of modified vaccinia virus Ankara (MVA). PLoS One 3, e1638.

Croen, K.D., Ostrove, J.M., Dragovic, L.J., Straus, S.E., 1988. Patterns of gene expression and sites of latency in human nerve ganglia are different for varicella-zoster and herpes simplex viruses. Proc. Natl. Acad. Sci. U S A 85, 9773-9777.

Davison, A.J., 1984. Structure of the genome termini of varicella-zoster virus. J. Gen. Virol. 65, 1969-1977.

Davison, A.J., 2002. Evolution of the herpesviruses. Vet. Microbiol. 86, 69-88.

Davison, A.J., Dargan, D.J., Stow, N.D., 2002. Fundamental and accessory systems in herpesviruses. Antiviral Res. 56, 1-11.

Davison, A.J., Scott, J.E., 1986. The complete DNA sequence of varicella-zoster virus. J. Gen. Virol. 67, 1759-1816.

Davison, A.J., Wilkie, N.M., 1983. Location and orientation of homologous sequences in the genomes of five herpesviruses. J. Gen. Virol. 64, 1927-1942.

Defechereux, P., Debrus, S., Baudoux, L., Rentier, B., Piette, J., 1997. Varicella-zoster virus open reading frame 4 encodes an immediate-early protein with posttranscriptional regulatory properties. J. Virol. 71, 7073-7079.

Deiss, L.P., Chou, J., Frenkel, N., 1986. Functional domains within the a sequence involved in the cleavage-packaging of herpes simplex virus DNA. J. Virol. 59, 605-618.

Delecluse, H.J., Hilsendegen, T., Pich, D., Zeidler, R., Hammerschmidt, W., 1998. Propagation and recovery of intact, infectious Epstein-Barr virus from prokaryotic to human cells. Proc. Natl. Acad. Sci. U S A 95, 8245-8250.

Desai, P.J., 2000. A null mutation in the UL36 gene of herpes simplex virus type 1 results in accumulation of unenveloped DNA-filled capsids in the cytoplasm of infected cells. J. Virol. 74, 11608-11618.

Dohner, K., Wolfstein, A., Prank, U., Echeverri, C., Dujardin, D., Vallee, R., Sodeik, B., 2002. Function of dynein and dynactin in herpes simplex virus capsid transport. Mol. Biol. Cell 13, 2795-2809.

Domi, A., Moss, B., 2002. Cloning the vaccinia virus genome as a bacterial artificial chromosome in Escherichia coli and recovery of infectious virus in mammalian cells. Proc. Natl. Acad. Sci. U S A 99, 12415-12420.

Dutch, R.E., Bianchi, V., Lehman, I.R., 1995. Herpes simplex virus type 1 DNA replication is specifically required for high-frequency homologous recombination between repeated sequences. J. Virol. 69, 3084-3089.

Dutch, R.E., Zemelman, B.V., Lehman, I.R., 1994. Herpes simplex virus type 1 recombination: the Uc-DR1 region is required for high-level a-sequence-mediated recombination. J. Virol. 68, 3733-3741.

Ecker, J.R., Hyman, R.W., 1982. Varicella zoster virus DNA exists as two isomers. Proc. Natl. Acad. Sci. U S A 79, 156-160.

Forghani, B., Mahalingam, R., Vafai, A., Hurst, J.W., Dupuis, K.W., 1990. Monoclonal antibody to immediate early protein encoded by varicella-zoster virus gene 62. Virus Res. 16, 195-210.

Fuchs, W., Klupp, B.G., Granzow, H., Mettenleiter, T.C., 2004. Essential function of the pseudorabies virus UL36 gene product is independent of its interaction with the UL37 protein. J. Virol. 78, 11879-11889.

Furlong, D., Swift, H., Roizman, B., 1972. Arrangement of herpesvirus deoxyribonucleic acid in the core. J. Virol. 10, 1071-1074.

Gabel, C.A., Dubey, L., Steinberg, S.P., Sherman, D., Gershon, M.D., Gershon, A.A., 1989. Varicella-zoster virus glycoprotein oligosaccharides are phosphorylated during posttranslational maturation. J. Virol. 63, 4264-4276.

Garber, D.A., Beverley, S.M., Coen, D.M., 1993. Demonstration of circularization of herpes simplex virus DNA following infection using pulsed field gel electrophoresis. Virology 197, 459-462.

Garland, J., 1943. Varicella following exposure to herpes zoster. N. Engl. J. Med 228, 336-337.

Gershon, A., Cosio, L., Brunell, P.A., 1973. Observations on the growth of varicella-zoster virus in human diploid cells. J. Gen. Virol. 18, 21-31.

Gershon, A.A., Sherman, D.L., Zhu, Z., Gabel, C.A., Ambron, R.T., Gershon, M.D., 1994. Intracellular transport of newly synthesized varicella-zoster virus: final envelopment in the trans-Golgi network. J. Virol. 68, 6372-6390.

Gomi, Y., Sunamachi, H., Mori, Y., Nagaike, K., Takahashi, M., Yamanishi, K., 2002. Comparison of the complete DNA sequences of the Oka varicella vaccine and its parental virus. J. Virol. 76, 11447-11459.

Grose, C., 1981. Variation on a theme by Fenner: the pathogenesis of chickenpox. Pediatrics 68, 735-737.

Grose, C., 1990. Glycoproteins encoded by varicella-zoster virus: biosynthesis, phosphorylation, and intracellular trafficking. Annu. Rev. Microbiol. 44, 59-80.

Grose, C., Perrotta, D.M., Brunell, P.A., Smith, G.C., 1979. Cell-free varicella-zoster virus in cultured human melanoma cells. J. Gen. Virol. 43, 15-27.

Hambleton, S., Gershon, A.A., 2005. Preventing varicella-zoster disease. Clin. Microbiol. Rev. 18, 70-80.

Harper, D.R., Mathieu, N., Mullarkey, J., 1998. High-titre, cryostable cell-free varicella zoster virus. Arch. Virol. 143, 1163-1170.

Harson, R., Grose, C., 1995. Egress of varicella-zoster virus from the melanoma cell: a tropism for the melanocyte. J. Virol. 69, 4994-5010.

Hayward, G.S., Jacob, R.J., Wadsworth, S.C., Roizman, B., 1975. Anatomy of herpes simplex virus DNA: evidence for four populations of molecules that differ in the relative orientations of their long and short components. Proc. Natl. Acad. Sci. U S A 72, 4243-4247.

Head, H., Campbell, A.W., Kennedy, P.G., 1997. The pathology of Herpes Zoster and its bearing on sensory localisation. Rev. Med Virol. 7, 131-143.

Hodge, P.D., Stow, N.D., 2001. Effects of mutations within the herpes simplex virus type 1 DNA encapsidation signal on packaging efficiency. J. Virol. 75, 8977-8986.

Hope-Simpson, R.E., 1954. Studies on shingles: is the virus the ordinary chickenpox virus? Lancet 2, 1299-1302.

Hope-Simpson, R.E., 1965. The nature of herpes zoster: A long-term study and a new hypothesis. Proc. R. Soc. Med. 58, 9-20.

Horsburgh, B.C., Hubinette, M.M., Tufaro, F., 1999. Genetic manipulation of herpes simplex virus using bacterial artificial chromosomes. Methods Enzymol. 306, 337-352.

Ioannou, P.A., Amemiya, C.T., Garnes, J., Kroisel, P.M., Shizuya, H., Chen, C., Batzer, M.A., de Jong, P.J., 1994. A new bacteriophage P1-derived vector for the propagation of large human DNA fragments. Nat. Genet. 6, 84-89.

Jacob, R.J., Morse, L.S., Roizman, B., 1979. Anatomy of herpes simplex virus DNA. XII. Accumulation of head-to-tail concatemers in nuclei of infected cells and their role in the generation of the four isomeric arrangements of viral DNA. J. Virol. 29, 448-457.

Jacquet, A., Haumont, M., Chellun, D., Massaer, M., Tufaro, F., Bollen, A., Jacobs, P., 1998. The varicella zoster virus glycoprotein B (gB) plays a role in virus binding to cell surface heparan sulfate proteoglycans. Virus Res. 53, 197-207.

Jamsai, D., Orford, M., Nefedov, M., Fucharoen, S., Williamson, R., Ioannou, P.A., 2003. Targeted modification of a human beta-globin locus BAC clone using GET Recombination and an I-Scei counterselection cassette. Genomics 82, 68-77.

Jones, F., Grose, C., 1988. Role of cytoplasmic vacuoles in varicella-zoster virus glycoprotein trafficking and virion envelopment. J. Virol. 62, 2701-2711.

Jones, J.O., Arvin, A.M., 2006. Inhibition of the NF-kappaB pathway by varicella-zoster virus in vitro and in human epidermal cells in vivo. J. Virol. 80, 5113-5124.

Karu, A.E., Sakaki, Y., Echols, H., Linn, S., 1975. The gamma protein specified by bacteriophage gamma. Structure and inhibitory activity for the recBC enzyme of Escherichia coli. J. Biol. Chem. 250, 7377-7387.

Kemble, G.W., Annunziato, P., Lungu, O., Winter, R.E., Cha, T.A., Silverstein, S.J., Spaete, R.R., 2000. Open reading frame S/L of varicella-zoster virus encodes a cytoplasmic protein expressed in infected cells. J. Virol. 74, 11311-11321.

Kennedy, P.G., Grinfeld, E., Gow, J.W., 1998. Latent varicella-zoster virus is located predominantly in neurons in human trigeminal ganglia. Proc. Natl. Acad. Sci. U S A 95, 4658-4662.

Kim, U.J., Shizuya, H., de Jong, P.J., Birren, B., Simon, M.I., 1992. Stable propagation of cosmid sized human DNA inserts in an F factor based vector. Nucleic Acids Res. 20, 1083-1085.

Kinchington, P.R., Bookey, D., Turse, S.E., 1995. The transcriptional regulatory proteins encoded by varicella-zoster virus open reading frames (ORFs) 4 and 63, but not ORF 61, are associated with purified virus particles. J. Virol. 69, 4274-4282.

Kinchington, P.R., Hougland, J.K., Arvin, A.M., Ruyechan, W.T., Hay, J., 1992. The varicella-zoster virus immediate-early protein IE62 is a major component of virus particles. J. Virol. 66, 359-366.

Kinchington, P.R., Reinhold, W.C., Casey, T.A., Straus, S.E., Hay, J., Ruyechan, W.T., 1985. Inversion and circularization of the varicella-zoster virus genome. J. Virol. 56, 194-200.

Kmiec, E., Holloman, W.K., 1981. Beta protein of bacteriophage lambda promotes renaturation of DNA. J. Biol. Chem. 256, 12636-12639.

Knipe, D.M., Batterson, W., Nosal, C., Roizman, B., Buchan, A., 1981. Molecular genetics of herpes simplex virus. VI. Characterization of a temperature-sensitive mutant defective in the expression of all early viral gene products. J. Virol. 38, 539-547.

Krause, P.R., Croen, K.D., Straus, S.E., Ostrove, J.M., 1988. Detection and preliminary characterization of herpes simplex virus type 1 transcripts in latently infected human trigeminal ganglia. J. Virol. 62, 4819-4823.

Krause, P.R., Klinman, D.M., 1995. Efficacy, immunogenicity, safety, and use of live attenuated chickenpox vaccine. J. Pediatr. 127, 518-525.

Krause, P.R., Klinman, D.M., 2000. Reply to "Varicella vaccine revisited". Nat. Med. 6, 1300.

Kress, M., Fickenscher, H., 2001. Infection by human varicella-zoster virus confers norepinephrine sensitivity to sensory neurons from rat dorsal root ganglia. FASEB J. 15, 1037-1043.

Ku, C.C., Besser, J., Abendroth, A., Grose, C., Arvin, A.M., 2005. Varicella-Zoster virus pathogenesis and immunobiology: new concepts emerging from investigations with the SCIDhu mouse model. J. Virol. 79, 2651-2658.

Ku, C.C., Zerboni, L., Ito, H., Graham, B.S., Wallace, M., Arvin, A.M., 2004. Varicella-zoster virus transfer to skin by T Cells and modulation of viral replication by epidermal cell interferon-alpha. J. Exp. Med. 200, 917-925.

Laguardia, J.J., Cohrs, R.J., Gilden, D.H., 1999. Prevalence of varicella-zoster virus DNA in dissociated human trigeminal ganglion neurons and nonneuronal cells. J. Virol. 73, 8571-8577.

Lamberti, C., Weller, S.K., 1996. The herpes simplex virus type 1 UL6 protein is essential for cleavage and packaging but not for genomic inversion. Virology 226, 403-407.

Lee, E.C., Yu, D., Martinez de Velasco, J., Tessarollo, L., Swing, D.A., Court DL, Jenkins, N.A., Copeland, N.G., 2001. A highly efficient Escherichia coli-based chromosome engineering system adapted for recombinogenic targeting and subcloning of BAC DNA. Genomics 73, 56-65.

Li, Q., Ali, M.A., Cohen, J.I., 2006. Insulin degrading enzyme is a cellular receptor mediating varicella-zoster virus infection and cell-to-cell spread. Cell 127, 305-316.

Little, J.W., 1967. An exonuclease induced by bacteriophage lambda. II. Nature of the enzymatic reaction. J. Biol. Chem. 242, 679-686.

Luxton, G.W., Lee, J.I., Haverlock-Moyns, S., Schober, J.M., Smith, G.A., 2006. The pseudorabies virus VP1/2 tegument protein is required for intracellular capsid transport. J. Virol. 80, 201-209.

MacLean, C.A., Robertson, L.M., Jamieson, F.E., 1993. Characterization of the UL10 gene product of herpes simplex virus type 1 and investigation of its role in vivo. J. Gen. Virol. 74, 975-983.

Mahalingam, R., Wellish, M., Lederer, D., Forghani, B., Cohrs, R., Gilden, D., 1993. Quantitation of latent varicella-zoster virus DNA in human trigeminal ganglia by polymerase chain reaction. J. Virol. 67, 2381-2384.

Mahalingam, R., Wellish, M., Wolf, W., Dueland, A.N., Cohrs, R., Vafai, A., Gilden, D., 1990. Latent varicella-zoster viral DNA in human trigeminal and thoracic ganglia. N. Engl. J. Med 323, 627-631.

Mallory, S., Sommer, M., Arvin, A.M., 1997. Mutational analysis of the role of glycoprotein I in varicella-zoster virus replication and its effects on glycoprotein E conformation and trafficking. J. Virol. 71, 8279-8288.

Manning, W.C., Mocarski, E.S., 1988. Insertional mutagenesis of the murine cytomegalovirus genome: one prominent alpha gene (ie2) is dispensable for growth. Virology 167, 477-484.

McGeoch, D.J., Dalrymple, M.A., Davison, A.J., Dolan, A., Frame, M.C., McNab, D., Perry, L.J., Scott, J.E., Taylor, P., 1988. The complete DNA sequence of the long unique region in the genome of herpes simplex virus type 1. J. Gen. Virol. 69, 1531-1574.

McGeoch, D.J., Dolan, A., Donald, S., Rixon, F.J., 1985. Sequence determination and genetic content of the short unique region in the genome of herpes simplex virus type 1. J. Mol. Biol. 181, 1-13.

McGeoch, D.J., Rixon, F.J., Davison, A.J., 2006. Topics in herpesvirus genomics and evolution. Virus Res. 117, 90-104.

McGregor, A., Schleiss, M.R., 2001. Recent advances in herpesvirus genetics using bacterial artificial chromosomes. Mol. Genet. Metab. 72, 8-14.

McVoy, M.A., Nixon, D.E., Hur, J.K., Adler, S.P., 2000. The ends on herpesvirus DNA replicative concatemers contain pac2 cis cleavage/packaging elements and their formation is controlled by terminal cis sequences. J. Virol. 74, 1587-1592.

McVoy, M.A., Ramnarain, D., 2000. Machinery to support genome segment inversion exists in a herpesvirus which does not naturally contain invertible elements. J. Virol. 74, 4882-4887.

Messerle, M., Crnkovic, I., Hammerschmidt, W., Ziegler, H., Koszinowski, U.H., 1997. Cloning and mutagenesis of a herpesvirus genome as an infectious bacterial artificial chromosome. Proc. Natl. Acad. Sci. U S A 94, 14759-14763.

Mocarski, E.S., Post, L.E., Roizman, B., 1980. Molecular engineering of the herpes simplex virus genome: insertion of a second L-S junction into the genome causes additional genome inversions. Cell 22, 243-255.

Mocarski, E.S., Roizman, B., 1982. Structure and role of the herpes simplex virus DNA termini in inversion, circularization and generation of virion DNA. Cell 31, 89-97.

Muniyappa, K., Radding, C.M., 1986. The homologous recombination system of phage lambda. Pairing activities of beta protein. J. Biol. Chem. 261, 7472-7478.

Murphy, K.C., 1991. Lambda Gam protein inhibits the helicase and chi-stimulated recombination activities of Escherichia coli RecBCD enzyme. J. Bacteriol. 173, 5808-5821.

Murphy, K.C., 1998. Use of bacteriophage lambda recombination functions to promote gene replacement in Escherichia coli. J. Bacteriol. 180, 2063-2071.

Murphy, K.C., 2007. The lambda Gam protein inhibits RecBCD binding to dsDNA ends. J. Mol. Biol. 371, 19-24.

Muyrers, J.P., Zhang, Y., Benes, V., Testa, G., Rientjes, J.M., Stewart, A.F., 2004. ET recombination: DNA engineering using homologous recombination in E. coli. Methods Mol. Biol. 256, 107-121.

Muyrers, J.P., Zhang, Y., Stewart, A.F., 2000. ET-cloning: think recombination first. Genet. Eng (N. Y.) 22, 77-98.

Muyrers, J.P., Zhang, Y., Stewart, A.F., 2001. Techniques: Recombinogenic engineering--new options for cloning and manipulating DNA. Trend. Biochem. Sci. 26, 325-331.

Muyrers, J.P., Zhang, Y., Testa, G., Stewart, A.F., 1999. Rapid modification of bacterial artificial chromosomes by ET-recombination. Nucleic Acids Res. 27, 1555-1557.

Nagaike, K., Mori, Y., Gomi, Y., Yoshii, H., Takahashi, M., Wagner, M., Koszinowski, U., Yamanishi, K., 2004. Cloning of the varicella-zoster virus genome as an infectious bacterial artificial chromosome in Escherichia coli. Vaccine 22, 4069-4074.

Narayanan, K., Williamson, R., Zhang, Y., Stewart, A.F., Ioannou, P.A., 1999. Efficient and precise engineering of a 200 kb beta-globin human/bacterial artificial chromosome in E. coli DH10B using an inducible homologous recombination system. Gene. Ther. 6, 442-447.

Newcomb, W.W., Juhas, R.M., Thomsen, D.R., Homa, F.L., Burch, A.D., Weller, S.K., Brown, J.C., 2001. The UL6 gene product forms the portal for entry of DNA into the herpes simplex virus capsid. J. Virol. 75, 10923-10932.

Ojala, P.M., Sodeik, B., Ebersold, M.W., Kutay, U., Helenius, A., 2000. Herpes simplex virus type 1 entry into host cells: reconstitution of capsid binding and uncoating at the nuclear pore complex in vitro. Mol. Cell Biol. 20, 4922-4931.

Oppenheim, A.B., Rattray, A.J., Bubunenko, M., Thomason, L.C., Court DL, 2004. In vivo recombineering of bacteriophage lambda by PCR fragments and single-strand oligonucleotides. Virology 319, 185-189.

Oxman, M.N., Levin, M.J., 2008. Vaccination against Herpes Zoster and Postherpetic Neuralgia. J. Infect. Dis. 197 Suppl 2, S228-S236.

Oxman, M.N., Levin, M.J., Johnson, G.R., Schmader, K.E., Straus, S.E., Gelb, L.D., Arbeit, R.D., Simberkoff, M.S., Gershon, A.A., Davis, L.E., Weinberg, A., Boardman, K.D., Williams, H.M., Zhang, J.H., Peduzzi, P.N., Beisel, C.E., Morrison, V.A., Guatelli, J.C., Brooks, P.A., Kauffman, C.A., Pachucki, C.T., Neuzil, K.M., Betts, R.F., Wright, P.F., Griffin, M.R., Brunell, P., Soto, N.E., Marques, A.R., Keay, S.K., Goodman, R.P., Cotton, D.J., Gnann, J.W., Jr., Loutit, J., Holodniy, M., Keitel, W.A., Crawford, G.E., Yeh, S.S., Lobo, Z., Toney, J.F., Greenberg, R.N., Keller, P.M., Harbecke, R., Hayward, A.R., Irwin, M.R., Kyriakides, T.C., Chan, C.Y., Chan, I.S., Wang, W.W., Annunziato, P.W., Silber, J.L., 2005. A vaccine to prevent herpes zoster and postherpetic neuralgia in older adults. N. Engl. J. Med. 352, 2271-2284.

Patel, A.H., Rixon, F.J., Cunningham, C., Davison, A.J., 1996. Isolation and characterization of herpes simplex virus type 1 mutants defective in the UL6 gene. Virology 217, 111-123.

Pfeffer, S., Sewer, A., Lagos-Quintana, M., Sheridan, R., Sander, C., Grasser, F.A., van Dyk, L.F., Ho, C.K., Shuman, S., Chien, M., Russo, J.J., Ju, J., Randall, G., Lindenbach, B.D., Rice, C.M., Simon, V., Ho, D.D., Zavolan, M., Tuschl, T., 2005. Identification of microRNAs of the herpesvirus family. Nat. Methods 2, 269-276.

Pfeffer, S., Zavolan, M., Grasser, F.A., Chien, M., Russo, J.J., Ju, J., John, B., Enright, A.J., Marks, D., Sander, C., Tuschl, T., 2004. Identification of virus-encoded microRNAs. Science 304, 734-736.

Pickering, L.K., 2008. Antimicrobial resistance among enteric pathogens. Adv. Exp. Med. Biol. 609, 154-163.

Pickering, L.K., Orenstein, W.A., 2002. Development of pediatric vaccine recommendations and policies. Semin. Pediatr. Infect. Dis. 13, 148-154.

Post, L.E., Roizman, B., 1981. A generalized technique for deletion of specific genes in large genomes: alpha gene 22 of herpes simplex virus 1 is not essential for growth. Cell 25, 227-232.

Puvion-Dutilleul, F., Pichard, E., Laithier, M., Leduc, E.H., 1987. Effect of dehydrating agents on DNA organization in herpes viruses. J. Histochem. Cytochem. 35, 635-645.

Ramsay, M., 1994. Yeast artificial chromosome cloning. Mol. Biotechnol. 1, 181-201.

Ristevski, S., 2005. Making better transgenic models: conditional, temporal, and spatial approaches. Mol. Biotechnol. 29, 153-163.

Roizman, B., Kristie, T., McKnight, J.L., Michael, N., Mavromara-Nazos, P., Spector, D., 1988. The trans-activation of herpes simplex virus gene expression: comparison of two factors and their cis sites. Biochimie 70, 1031-1043.

Sato, B., Ito, H., Hinchliffe, S., Sommer, M.H., Zerboni, L., Arvin, A.M., 2003. Mutational analysis of open reading frames 62 and 71, encoding the varicella-zoster virus immediate-early transactivating protein, IE62, and effects on replication in vitro and in skin xenografts in the SCID-hu mouse in vivo. J. Virol. 77, 5607-5620.

Sawitzke, J.A., Thomason, L.C., Costantino, N., Bubunenko, M., Datta, S., Court DL, 2007. Recombineering: in vivo genetic engineering in E. coli, S. enterica, and beyond. Methods Enzymol. 421, 171-199.

Sawyer, M.H., Chamberlin, C.J., Wu, Y.N., Aintablian, N., Wallace, M.R., 1994. Detection of varicella-zoster virus DNA in air samples from hospital rooms. J. Infect. Dis. 169, 91-94.

Schaffer, P.A., 1975a. Genetics of herpesviruses - a review. IARC Sci. Publ., 195-217.

Schaffer, P.A., 1975b. Temperature-sensitive mutants of herpesviruses. Curr. Top. Microbiol. Immunol. 70, 51-100.

Schaffer, P.A., Weller, S.K., Pancake, B.A., Coen, D.M., 1984. Genetics of herpes simplex virus. J. Invest. Dermatol 83, 42s-47s.

Schalkwyk, L.C., Francis, F., Lehrach, H., 1995. Techniques in mammalian genome mapping. Curr. Opin. Biotechnol. 6, 37-43.

Schmidt, M., Fickenscher, H., 2009. Manuscript in preparation.

Schmidt, M., Kress, M., Heinemann, S., Fickenscher, H., 2003. Varicella-zoster virus isolates, but not the vaccine strain OKA, induce sensitivity to alpha-1 and beta-1 adrenergic stimulation of sensory neurones in culture. J. Med. Virol. 70 Suppl 1, S82-S89.

Schumacher, D., Tischer, B.K., Fuchs, W., Osterrieder, N., 2000. Reconstitution of Marek's disease virus serotype 1 (MDV-1) from DNA cloned as a bacterial artificial chromosome and characterization of a glycoprotein B-negative MDV-1 mutant. J. Virol. 74, 11088-11098.

Schynts, F., McVoy, M.A., Meurens, F., Detry, B., Epstein, A.L., Thiry, E., 2003. The structures of bovine herpesvirus 1 virion and concatemeric DNA: implications for cleavage and packaging of herpesvirus genomes. Virology 314, 326-335.

Severini, A., Scraba, D.G., Tyrrell, D.L., 1996. Branched structures in the intracellular DNA of herpes simplex virus type 1. J. Virol. 70, 3169-3175.

Sharan, S.K., Thomason, L.C., Kuznetsov, S.G., Court DL, 2009. Recombineering: a homologous recombination-based method of genetic engineering. Nat. Protoc. 4, 206-223.

Shizuya, H., Birren, B., Kim, U.J., Mancino, V., Slepak, T., Tachiiri, Y., Simon, M., 1992. Cloning and stable maintenance of 300-kilobase-pair fragments of human DNA in Escherichia coli using an F-factor-based vector. Proc. Natl. Acad. Sci. U S A 89, 8794-8797.

Shizuya, H., Kouros-Mehr, H., 2001. The development and applications of the bacterial artificial chromosome cloning system. Keio J. Med. 50, 26-30.

Slobedman, B., Simmons, A., 1997. Concatemeric intermediates of equine herpesvirus type 1 DNA replication contain frequent inversions of adjacent long segments of the viral genome. Virology 229, 415-420.

Slobedman, B., Zhang, X., Simmons, A., 1999. Herpes simplex virus genome isomerization: origins of adjacent long segments in concatemeric viral DNA. J. Virol. 73, 810-813.

Smiley, J.R., 1980. Construction in vitro and rescue of a thymidine kinase-deficient deletion mutation of herpes simplex virus. Nature 285, 333-335.

Smith, G.A., Enquist, L.W., 2000. A self-recombining bacterial artificial chromosome and its application for analysis of herpesvirus pathogenesis. Proc. Natl. Acad. Sci. U S A 97, 4873-4878.

Spaete, R.R., Mocarski, E.S., 1987. Insertion and deletion mutagenesis of the human cytomegalovirus genome. Proc. Natl. Acad. Sci. U S A 84, 7213-7217.

Sparwasser, T., Eberl, G., 2007. BAC to immunology--bacterial artificial chromosome-mediated transgenesis for targeting of immune cells. Immunology 121, 308-313.

Sperber, S.J., Smith, B.V., Hayden, F.G., 1992. Serologic response and reactogenicity to booster immunization of healthy seropositive adults with live or inactivated varicella vaccine. Antiviral Res. 17, 213-222.

Stavropoulos, T.A., Strathdee, C.A., 1998. An enhanced packaging system for helper-dependent herpes simplex virus vectors. J. Virol. 72, 7137-7143.

Steiner, G., 1875. Zur Inokulation der Varizellen. Wien. Med. Wochenschr. 25, 306.

Stevenson, D., Colman, K.L., Davison, A.J., 1994. Characterization of the putative protein kinases specified by varicella-zoster virus genes 47 and 66. J. Gen. Virol. 75, 317-326.

Stow, N.D., Davison, A.J., 1986. Identification of a varicella-zoster virus origin of DNA replication and its activation by herpes simplex virus type 1 gene products. J. Gen. Virol. 67, 1613-1623.

Stow, N.D., McMonagle, E.C., Davison, A.J., 1983. Fragments from both termini of the herpes simplex virus type 1 genome contain signals required for the encapsidation of viral DNA. Nucleic Acids Res. 11, 8205-8220.

Straus, S.E., Aulakh, H.S., Ruyechan, W.T., Hay, J., Casey, T.A., Vande Woude, G.F., Owens, J., Smith, H.A., 1981. Structure of varicella-zoster virus DNA. J. Virol. 40, 516-525.

Straus, S.E., Hay, J., Smith, H., Owens, J., 1983. Genome differences among varicella-zoster virus isolates. J. Gen. Virol. 64, 1031-1041.

Strive, T., Hardy, C.M., French, N., Wright, J.D., Nagaraja, N., Reubel, G.H., 2006. Development of canine herpesvirus based antifertility vaccines for foxes using bacterial artificial chromosomes. Vaccine 24, 980-988.

Strive, T., Hardy, C.M., Wright, J., Reubel, G.H., 2007. A virus vector based on Canine Herpesvirus for vaccine applications in canids. Vet. Microbiol. 119, 173-183.

Takahashi, M., Asano, Y., Kamiya, H., Baba, K., Ozaki, T., Otsuka, T., Yamanishi, K., 2008. Development of varicella vaccine. J. Infect. Dis. 197 Suppl 2, S41-S44.

Takahashi, M., Otsuka, T., Okuno, Y., Asano, Y., Yazaki, T., 1974. Live vaccine used to prevent the spread of varicella in children in hospital. Lancet 2, 1288-1290.

Tan, A.Y., Connett, C.J., Connett, G.J., Quek, S.C., Yap, H.K., Meurice, F., Lee, B.W., 1996. Use of a reformulated Oka strain varicella vaccine (SmithKline Beecham Biologicals/Oka) in healthy children. Eur. J. Pediatr. 155, 706-711.

Tanaka, M., Kagawa, H., Yamanashi, Y., Sata, T., Kawaguchi, Y., 2003. Construction of an excisable bacterial artificial chromosome containing a full-length infectious clone of herpes simplex virus type 1: viruses reconstituted from the clone exhibit wild-type properties in vitro and in vivo. J. Virol. 77, 1382-1391.

Taylor-Robinson, D., 1959. Chickenpox and herpes zoster. III. Tissue culture studies. Br. J. Exp. Pathol. 40, 521-532.

Thiry, E., Meurens, F., Muylkens, B., McVoy, M., Gogev, S., Thiry, J., Vanderplasschen, A., Epstein, A., Keil, G., Schynts, F., 2005. Recombination in alphaherpesviruses. Rev. Med. Virol. 15, 89-103.

Thomason, L., Court DL, Bubunenko, M., Costantino, N., Wilson, H., Datta, S., Oppenheim, A., 2007. Recombineering: genetic engineering in bacteria using homologous recombination. Curr. Protoc. Mol. Biol. Chapter 1, Unit 1.16.

Tischer, B.K., Kaufer, B.B., Sommer, M., Wussow, F., Arvin, A.M., Osterrieder, N., 2007. A self-excisable infectious bacterial artificial chromosome clone of varicella-zoster virus allows analysis of the essential tegument protein encoded by ORF9. J. Virol. 81, 13200-13208.

Tischer, B.K., Schumacher, D., Messerle, M., Wagner, M., Osterrieder, N., 2002. The products of the UL10 (gM) and the UL49.5 genes of Marek's disease virus serotype 1 are essential for virus growth in cultured cells. J. Gen. Virol. 83, 997-1003.

Tischer, B.K., Smith, G., Osterrieder, N., 2009. En passant Mutagenesis - A two step markerless Red recombination system. In: Braman, J., In Vitro Mutagenesis Protocols. Humana Press Inc., Tatowa. In press.

Tischer, B.K., von Einem, J., Kaufer, B., Osterrieder, N., 2006. Two-step red-mediated recombination for versatile high-efficiency markerless DNA manipulation in Escherichia coli. Biotechniques 40, 191-197.

Umene, K., 1999. Mechanism and application of genetic recombination in herpesviruses. Rev. Med. Virol. 9, 171-182.

Varmuza, S.L., Smiley, J.R., 1985. Signals for site-specific cleavage of HSV DNA: maturation involves two separate cleavage events at sites distal to the recognition sequences. Cell 41, 793-802.

Visalli, R.J., Nicolosi, D.M., Irven, K.L., Goshorn, B., Khan, T., Visalli, M.A., 2007. The Varicella-zoster virus DNA encapsidation genes: Identification and characterization of the putative terminase subunits. Virus Res. 129, 200-211.

von Bokay, J., 1909. Über den ätiologischen Zusammenhang der Varizellen mit gewissen Fällen von Herpes Zoster. Wien. Klin. Wochenschr. 22, 1323-1326.

Wagner, M., Jonjic, S., Koszinowski, U.H., Messerle, M., 1999. Systematic excision of vector sequences from the BAC-cloned herpesvirus genome during virus reconstitution. J. Virol. 73, 7056-7060.

Wagner, M., Ruzsics, Z., Koszinowski, U.H., 2002. Herpesvirus genetics has come of age. Trends Microbiol. 10, 318-324.

Wang, J.B., Nixon, D.E., McVoy, M.A., 2008. Definition of the minimal cis-acting sequences necessary for genome maturation of the herpesvirus murine cytomegalovirus. J. Virol. 82, 2394-2404.

Wang, N., Baldi, P.F., Gaut, B.S., 2007. Phylogenetic analysis, genome evolution and the rate of gene gain in the Herpesviridae. Mol. Phylogenet. Evol. 43, 1066-1075.

Warming, S., Costantino, N., Court DL, Jenkins, N.A., Copeland, N.G., 2005. Simple and highly efficient BAC recombineering using galK selection. Nucleic Acids Res. 33, e36.

Weller, T.H., 1953. Serial propagation in vitro of agents producing inclusion bodies derived from varicella and herpes zoster. Proc. Soc. Exp. Biol. Med. 83, 340-346.

Weller, T.H., Witton, H.M., Bell, E.J., 1958. The etiologic agents of varicella and herpes zoster; isolation, propagation, and cultural characteristics in vitro. J. Exp. Med. 108, 843-868.

Whitley, R.J., 1999. Approaches to the treatment of varicella-zoster virus infections. Contrib. Microbiol. 3, 158-172.

Whitley, R.J., 2008. Therapy of herpes virus infections in children. Adv. Exp. Med. Biol. 609, 216-232.

Yamagishi, Y., Sadaoka, T., Yoshii, H., Somboonthum, P., Imazawa, T., Nagaike, K., Ozono, K., Yamanishi, K., Mori, Y., 2008. Varicella-zoster virus glycoprotein M homolog is glycosylated, is expressed on the viral envelope, and functions in virus cell-to-cell spread. J. Virol. 82, 795-804.

Yamanishi, K., 2008. Molecular analysis of the Oka vaccine strain of varicella-zoster virus. J Infect. Dis. 197 Suppl 2, S45-S48.

Yang, X.W., Gong, S., 2005. An overview on the generation of BAC transgenic mice for neuroscience research. Curr. Protoc. Neurosci. Chapter 5.

Yoshii, H., Somboonthum, P., Takahashi, M., Yamanishi, K., Mori, Y., 2007. Cloning of full length genome of varicella-zoster virus vaccine strain into a bacterial artificial chromosome and reconstitution of infectious virus. Vaccine 25, 5006-5012.

Yu, D., Ellis, H.M., Lee, E.C., Jenkins, N.A., Copeland, N.G., Court DL, 2000. An efficient recombination system for chromosome engineering in Escherichia coli. Proc. Natl. Acad. Sci. U S A 97, 5978-5983.

Zhang, Y., Buchholz, F., Muyrers, J.P., Stewart, A.F., 1998. A new logic for DNA engineering using recombination in Escherichia coli. Nat. Genet. 20, 123-128.

Zhao, Y., Petherbridge, L., Smith, L.P., Baigent, S., Nair, V., 2008. Self-excision of the BAC sequences from the recombinant Marek's disease virus genome increases replication and pathogenicity. Virol. J. 5, 19.

Zhou, F.C., Zhang, Y.J., Deng, J.H., Wang, X.P., Pan, H.Y., Hettler, E., Gao, S.J., 2002. Efficient infection by a recombinant Kaposi's sarcoma-associated herpesvirus cloned in a bacterial artificial chromosome: application for genetic analysis. J. Virol. 76, 6185-6196.

Zhu, Z., Gershon, M.D., Ambron, R., Gabel, C., Gershon, A.A., 1995. Infection of cells by varicella zoster virus: inhibition of viral entry by mannose 6-phosphate and heparin. Proc. Natl. Acad. Sci. U S A 92, 3546-3550.

Zijl, M., Quint, W., Briaire, J., de, R.T., Gielkens, A., Berns, A., 1988. Regeneration of herpesviruses from molecularly cloned subgenomic fragments. J. Virol. 62, 2191-2195.

8. Abbreviations

Amp	ampicillin
BAC	bacterial artificial chromosome
BoHV	bovine herpesvirus
bp	base pairs
Cm	chloramphenicol
DMEM	*Dulbecco's Modified Eagle Medium*
CPE	cytopathic effect
DNA	deoxyribonucleic acid
dsDNA	double-stranded deoxyribonucleic acid
E. coli	*Escherichia coli*
EDTA	ethylenediaminetetraacetic acid
EHV	equine herpesvirus
FBS	fetal bovine serum
HSV	herpes simplex virus
IRL	internal repeat long
IRS	internal repeat short
Kan	kanamycin
L	long component
LB	Luria Bertani broth
kb	kilo base pairs
M	marker, DNA ladder
MCS	multiple cloning site
MPR^{ci}	cation-independent mannose 6-phosphate receptor
mRNA	messenger ribonucleic acid
ORF	open reading frame
P	primer
pac	packaging signal
PBS	phosphate-buffered saline
PCR	polymerase chain reaction
PFU	plaque-forming unit
P-Oka	parental Oka
PRV	pseudorabies virus
RFLP	restriction fragment length polymorphism

RT	room temperature
S	short component
S/L0	transition/junction of the short and long component at the open reading frame 0 of the unique region long
S/L61	transition/junction of the short and long component at the open reading frame 61 of the unique region long
SDS	sodium dodecyl sulfate
TGN	*trans*-Golgi network
Tris	Tris-(hydroxymethyl)-aminomethan
TRL	terminal repeat long
TRS	terminal repeat short
U	unit
UL	unique region long
US	unique region short
V-Oka	vaccine strain Oka
VZV	varicella-zoster virus

9. Publications and Presentations

Publications

Tischer, B.K., Kaufer, B.B., Sommer, M., Wussow, F., Arvin A.M., Osterrieder, N., 2007. A self-excisable infectious bacterial artificial chromosome clone of varicella-zoster virus allows analysis of the essential tegument protein encoded by ORF9. J. Virol. 81, 13200-13208.

Wussow, F., Fickenscher, H., Tischer, B.K., 2009. Red-mediated transposition and final release of the mini-F vector of a cloned infectious herpesvirus genome. PLoS One, in revision.

Presentations

Wussow, F., Kaufer, B.B., Osterrieder, N., Fickenscher, H., Tischer B.K., 2007. Bacterial artificial chromosome engineering for markerless reconstitution of varicella-zoster virus. Oral presentation, Second Mini-Herpesvirus Workshop, 22 June 2007, Berlin.

Wussow, F., Kaufer, B.B., Osterrieder, N., Fickenscher, H., Tischer, B.K., 2007. Bacterial artificial chromosome engineering for markerless reconstitution of varicella-zoster virus. Poster presentation, Third European Congress of Virology, 1-5 September 2007, Nuremberg.

Wussow, F., Fickenscher, H., Tischer, B.K., 2009. Red-mediated mini-F vector transposition into the terminal herpesviral genome junction in Escherichia coli generating an intrinsically releasing infectious bacterial artificial chromosome of varicella-zoster virus. Oral and poster presentation, 19. Annual Meeting of the German Society of Virology, 18-21 March 2009, Leipzig.

10. Acknowledgements

For his support in diverse ways and that he permitted me to work on the very attractive and progressive research topic and allowed me to develop my ideas and experimental operations freely, I would like to thank Prof. Dr. Helmut Fickenscher.

Many thanks go to Dr. Karsten Tischer, the "master of recombineering" and inventor of the *en passant* mutagenesis, who unfortunately left us in 2007. Without the fruitful discussions with him, it would not be possible to develop such elegant BAC engineering strategies.

For the enjoyable teamwork, I thank Tuna Toptan, Tanja Spiekermann, Gregor Maschkowitz, Oliver Braum, Anne-Kathrin Brunnemann, and Hanna Langenberger.

Thanks to Dr. Heike Hofmann for her support in some experimental details. I wish her and her family all the best for the future.

Especially, I would like to thank Tuna Toptan. Besides her personal support and motivation for me, I think she was a great enrichment for the whole research group not only in solving scientific problems and questions.

Again, I would like to thank my parents Ingrid and Erwin Wussow for supporting my funny idea to study biology. I am very grateful to them that they have tolerated my behaviour during the last three years.

Finally, I thank my sister Tatjana Wussow and Lutz Meyer for their mental support. I am very proud of them that they have made me to an uncle. Welcome on earth Mathilda!

11. Erklärung

Hiermit erkläre ich, dass die Abhandlung der vorliegenden Dissertation, abgesehen von der Beratung durch meine Betreuer Dr. Karsten Tischer und Prof. Dr. Helmut Fickenscher, nach Inhalt und Form die eigene Arbeit ist. Teile dieser Arbeit wurden bereits veröffentlicht oder zur Publikation eingereicht. Zudem entstand die vorliegende Arbeit unter Einhaltung der Regeln guter wissenschaftlicher Praxis der Deutschen Forschungsgemeinschaft.

Des Weiteren erkläre ich, dass ich noch keinen Promotionsversuch unternommen habe.

Kiel, den 20.10.2009

Felix Wussow